eman ta zabal zazu

Universidad del País Vasco
Euskal Herriko Unibertsitatea

NON-CODING VARIANTS AND EPITRANSCRIPTOMICS: A FUNCTIONAL STUDY OF A CELIAC DISEASE ASSOCIATED REGION

Doctoral Thesis

Ane Olazagoitia Garmendia

Leioa, 2022

Supervised by:

Ainara Castellanos Rubio

Jose Ramón Bilbao Catalá

This work was funded by a predoctoral fellowship from the Basque Department of Education, University and Research to Ane Olazagoitia Garmendia (PRE_2017_1_0306) and research project grants from the Spanish Ministry of Science, Universities and Innovation (PGC2018-097573-A-I00) and ISCIII Research project PI16/00258, cofinanced by the Spanish Ministry of Economy and Competitiveness and by the European Union ERDF/ESF ’A way to make Europe’.

ABBREVIATIONS

AGA	Anti-gliadin antibody
ALKBH5	AlkB homolog 5 RNA demethylase
APCs	Antigen presenting cells
CD	Celiac disease
CDS	Coding sequence
CT	Choleratoxin
CTR	Control individuals
DC	Dentritic cells
DMEM	Dulbecco's Modified Eagle's Medium
DTT	Dithiothreitol
EMA	Anti-endomysium antibody
EMSA	Electrophoretic Mobility Shift Assay
eQTL	Expression Quantitative Trait Loci
ESPGHAN	European Society of Pediatric Gastroenterology Hematology and Nutrition
FBS	Fetal Bovine Serum
FTO	Fat mass and obesity-associated protein
GEO	Gene Expression Omnibus
GFD	Gluten free diet
GWAS	Genome wide association study
HCMV	Human cytomegalovirus
HIV	Human immunodeficiency virus
HLA	Human leukocyte antigen
I	Inosine
IEC	Intestinal epithelial cell
IEL	Intraepithelial lymphocyte
IFN	Interferon
IκB-α	Inhibitor of kappa B alpha

IL	Interleukin
KO mice	Knockout mice
LD	Linkage disequilibrium
LMB	Leptomycin B
lncRNA	long non-coding RNA
LPS	Lipopolysaccharide
m^{1}A	N^1-methyladenosine
m^{5}C	^{5}-methylcytosine
m^{6}A	N^6-methyladenosine
m^{6}A-CLIP/ miCLIP	m^{6}A individual-nucleotide-resolution crosslinking and immunoprecipitation
m^{6}A-LAIC-seq	m^{6}A-level and isoform-characterization sequencing
m^{6}A-QTL	m^{6}A quantitative trait loci
m^{6}A-seq/ meRIP-seq	m^{6}A-specific methylated RNA immunoprecipitation (IP) with next-generation sequencing
m^{6}Am	N^6-2′-O-dimethyladenosine
m^{7}G cap	^{7}-methylguanosine cap
MAPK	mitogen-activated protein kinase
METTL3	Methyltransferase 3
MHC	Major histocompatibility complex
miRNA	microRNA
ncRNA	non-coding RNA
NF-κB	Nuclear factor kappa B
NGS	Next generation sequencing
NK	Natural killer
P/S	Penicillin and streptavidin
PA-m^{6}A-seq	Photo-crosslinking-assisted m^{6}A sequencing
PBS	Phosphate-buffered saline buffer
PI	Protease inhibitors
pQTL	Protein quantitative trait loci
PTG	Pepsin-Trypsin digested Gliadin

RBM15	RNA Binding Motif Protein 15
RIP	RNA immunoprecipitation
RPMI	Roswell Park Memorial Institute medium
RT-QPCR	Real-time quantitative reverse transcription polymerase chain reaction
SAM	S-adenosylmethionine
SCARLET	Site-specific cleavage and radioactive-labeling followed by ligation-assisted extraction and thin-layer chromatography
SNP	Single nucleotide polymorphism
SOCS	Suppressor of cytokine signaling
T1D	Type 1 diabetes
TG2	Tissue transglutaminase type 2
TGA	Anti-transglutaminase antibody
TLR	Toll-like receptor
UTR	Untranslated region
VIRMA	Vir Like m^6A Methyltransferase Associated
WT mice	Wild type mice
WTAP	Wilms' Tumor 1-Associating Protein
XPO1	Exportin 1
YTH domain	YT521-B homology domain
ZC3H13	Zinc Finger CCCH Domain-Containing Protein 13
ψ	Pseudouridine

LIST OF ORIGINAL PUBLICATIONS

This thesis is based on the following publication:

Olazagoitia-Garmendia A, Zhang L, Mera P, Godbout JK, Sebastian delaCruz M, Garcia-Santisteban I, Mendoza LM, Huerta A, Irastorza I, Bhagat G, Green PH, Herrero L, Serra D, Rodriguez JA, Verdu EF, He C, Bilbao JR, Castellanos-Rubio A., *Gluten-induced RNA methylation changes regulate intestinal inflammation via allele-specific XPO1 translation in epithelial cells*. **Gut (2021)** Feb, gutjnl-2020-322566.

During this thesis I have also participated in the following publications as first author:

Olazagoitia-Garmendia A, Castellanos-Rubio A., *Relative quantification of residue specific m^6A RNA methylation using m^6A-RT-QPCR.* ***Methods Mol Biol (2021)*** *Jun; 2298: 185-195.*

Olazagoitia-Garmendia A, Sebastian-delaCruz M, Castellanos-Rubio A., *Involvement of lncRNAs in celiac disease pathogenesis.* **IRCMB (2020)** Nov; 358: 241-264.

Olazagoitia-Garmendia A, Gonzalez-Moro I, Colli ML, Cobo-Vuilleumier N, Postler TS, Marselli L, Marchetti P, Ghosh S, Gauthier BR, Eizirik DL, Castellanos-Rubio A, Santin I., *The T1D-associated lncRNA Lnc13 modulates human pancreatic β cell inflammation by allele-specific stabilization of STAT1 mRNA*. **PNAS** (**2020**) Apr 21;117(16): 9022-9031.

Olazagoitia-Garmendia A, Santin I, Castellanos-Rubio A., *Functional implication of celiac disease associated lncRNAs in disease pathogenesis.* **Comput Biol Med.** (**2018**) Nov 1;102: 369-375.

And as co-author in the following publications:

Castellanos-Rubio I, Arriortua O, Marcano L, Rodrigo I, Iglesias-Rojas D, Barón A, **Olazagoitia-Garmendia A**, Olivi L, Plazaola F, Fdez-Gubieda ML, Castellanos-Rubio A, Garitaonandia JS, Orue I, Insausti M. *Shaping Up Zn-Doped Magnetite Nanoparticles from Mono- and Bimetallic Oleates: The Impact of Zn Content, Fe Vacancies, and Morphology on Magnetic Hyperthermia Performance.* **Chem Mater (2021)** Apr, 33, 9, 3139–3154

Sebastian-delaCruz M, **Olazagoitia-Garmendia A**, Huerta Madrigal A, Garcia-Etxebarria K, Mendoza LM, Fernandez-Jimenez N, Garcia Casales Z, de la Calle Navarro E, Calvo AE, Legarda M, Tutau C, Irastorza I, Bujanda L, Bilbao JR, Castellanos-Rubio A. *A Novel Noninvasive Method Based on Salivary Inflammatory Biomarkers for the Screening of Celiac Disease.* **CMGH (2021)** May

Sebastian-delaCruz M, Gonzalez-Moro I, **Olazagoitia-Garmendia A**, Castellanos-Rubio A, Santin I., *The role of lncrnas in gene expression regulation through mRNA stabilization.* ***Non-Coding RNA (2021)*** Jan 7, 3.

Sebastian-delaCruz M, **Olazagoitia-Garmendia A**, Gonzalez-Moro I, Santin I, Garcia-Etxebarria K, Castellanos-Rubio A., *Implication of m^6A mRNA methylation in the susceptibility to inflammatory bowel disease*. **Epigenomes** (**2020**) 4,16.

Castellanos-Rubio I, Rodrigo I, **Olazagoitia-Garmendia A**, Arriortua O, Gil de Muro I, Garitaonandia JS, Bilbao JR, Fdez-Gubieda ML, Plazaola F, Orue I, Castellanos-Rubio A, Insausti M., *Highly Reproducible Hyperthermia Response in Water, Agar and Cellular Environment by Discretely PEGylated Magnetite Nanoparticles*. **ACS Appl Mater Interfaces** (**2020**) Jun 24;12(25):27917-27929.

Aldaregia J, Errarte P, **Olazagoitia-Garmendia A**, Gimeno M, Uriz JJ, Gershon TR, Garcia I, Matheu A., *Erbb4 Is Required for Cerebellar Development and Malignant Phenotype of Medulloblastoma*. **Cancers** (**2020**) Apr 17;12(4):997.

Jauregi-Miguel A, Santin I, Garcia-Etxebarria K, **Olazagoitia-Garmendia A**, Romero-Garmendia I, Sebastian-delaCruz M, Irastorza I, Spanish Consortium for the Genetics of Celiac Disease, Castellanos-Rubio A, Bilbao JR., *MAGI2 Gene Region and Celiac Disease*. **Front Nutr** (**2019**) Dec 19; 6:187.

Castellanos-Rubio A, Santin I, **Olazagoitia-Garmendia A**, Romero-Garmendia I, Jauregi-Miguel A, Legarda M, Bilbao JR., *A novel RT-QPCR-based assay for the relative quantification of residue specific m6A RNA methylation*. **Sci Rep** (**2019**) Mar 12;9(1):4220.

Sousa dos Santos R, Marroqui L, Velayos T, **Olazagoitia-Garmendia A**, Jauregi-Miguel A, Castellanos-Rubio A, Eizirik DL, Castaño L, Santin I., *DEXI, a candidate gene for type 1 diabetes, modulates rat and human pancreatic beta cell inflammation via regulation of the type I IFN/STAT signalling pathway*. **Diabetologia** (**2019**) Mar;62(3):459-472.

PROJECT JUSTIFICATION AND SCOPE

Celiac disease (CD) is a chronic autoimmune disorder that develops upon gluten ingestion in genetically susceptible individuals. It is believed that prevention will be essential for the eradication of this disorder, and for that purpose, efficient mechanisms of prediction and early diagnosis are needed. Even if the major genetic risk factors have been known for a long time, they are not enough to explain the development of CD and the so called missing heritability remains a major goal in the field. In addition, the only available treatment so far is a life-long gluten-free diet which is difficult to comply to and doesn't work in all CD patients.

Therefore, it becomes essential to define which genes, pathways and regulatory mechanisms are involved in disease susceptibility. These studies will contribute to the understanding of the pathogenic mechanisms underlying CD development, pointing key genetic and epigenetic markers increasing risk of CD. Additionally, the identification of master regulators of complex pathways will help identify novel targets for intervention. Gluten-free diet will most probably remain the main treatment for celiac individuals, however, works like the present thesis open the door to novel therapeutic alternatives. Moreover, the new findings could be extrapolated to other complex and autoimmune diseases and postulate new points of view to the understanding of genetic diseases.

In order to dissect the genetics and epigenetics of CD, the current project has been focused on the search of functional determinants using genetic approaches and functional *in vitro* and *in vivo* validation of those candidates. More specifically, in the present doctoral thesis we have analyzed a new layer of gene regulation, i.e. m^6A RNA methylation, and we have scrutinized the involvement of gluten in the regulation of this epitranscriptomic mark and the downstream effects in the key inflammatory pathway NF-κB.

1.INTRODUCTION

1.1. CELIAC DISEASE

1.1.1. Celiac Disease

Celiac disease (CD) is a complex, chronic, immune-mediated inflammatory disorder. In genetically susceptible individuals gluten triggers a proinflammatory response that primarily affects the small intestine (presenting villous atrophy and crypt hyperplasia) (Caio et al., 2019; S. M. Kim et al., 2015). CD is characterized by the presence of proinflammatory gluten-specific T cells, cytotoxic transformation of intraepithelial lymphocytes, epithelial cell stress and the release of innate proinflammatory cytokines (Dieli-Crimi et al., 2015; Ricaño-Ponce et al., 2016).

Classical CD presents a wide range of symptoms and signs that can be divided into intestinal features (such as diarrhea, abdominal distension or vomiting) and those caused by malabsorption, like failure to thrive (low weight, lack of fat, hair thinning) or psychomotor impairment (muscle wasting) (Feighery, 1999). Other atypical symptoms also associated with CD include neurological events, dental enamel defects, infertility, osteoporosis, joint symptoms and elevated liver enzyme concentrations (Mäki & Collin, 1997).

As with other autoimmune diseases, CD has a strong hereditary component identified in studies performed in siblings (Greco et al., 2002; Nisticò et al., 2006). The main genetic predisposing factors locate in the major histocompatibility complex (MHC) region on 6p21, a region that contains many genes related to immune functions. HLA class II heterodimers, specifically DQ2 and DQ8, account for the main proportion of the heritability of CD (approximately 30%) and are responsible of presenting gluten peptides to CD4+ T cells (Dieli-Crimi et al., 2015).

Gluten, the main triggering factor in CD, is a mixture of monomeric alcohol soluble glutenins and polymeric gliadins found in cereals like wheat, barley and rye. Gliadins, the key components of gluten, are complex proteins which are not completely digested by intestinal enzymes (Silano et al., 2009). The final product of this partial

digestion is a mix of peptides that can trigger host responses (increased gut permeability and innate and adaptive immune responses) that closely resemble the exposure to other harmful microorganisms (Jelínková et al., 2004; Lammers et al., 2011; Picarelli et al., 1999; Shan et al., 2002). Gliadin fragments present in the gut lumen are good substrates for the enzyme tissue transglutaminase type 2 (TG2), which can deamidate gluten peptides increasing their ability to bind to HLA-DQ2 or HLA-DQ8 molecules, and provoke a gluten-specific CD4+ Th1 T-cell response. In addition, some *in vitro* studies also support the idea that some gliadin peptides are able to activate innate immune responses that are independent of MHC presentation (Jabri & Sollid, 2009; Schuppan et al., 2009).

To date, the only effective treatment for CD is a life-long, strict gluten-free diet (GFD), which improves most of symptoms typically within days or weeks (Murray et al., 2004). Insufficiently treated and untreated patients are predisposed to complications such as short stature, nutritional deficiencies, osteoporosis, secondary autoimmune disorders, malignancies, infertility and poor outcome of pregnancies (Y. Han et al., 2015; Lerner, 2010). Despite its effectiveness, compliance with a GFD is difficult and it is thought to decrease patients' quality of life (Samasca et al., 2014). Additionally, a small subgroup of patients shows non-responsive or refractory CD, and present persistent or recurrent symptoms, inflammation of the intestine and villous atrophy despite strict adherence to a GFD (Rubio-Tapia & Murray, 2010). In this sense, the development of a safe, effective and affordable alternative therapy is necessary.

1.1.2. Pathophysiology of CD

Besides the genetic predisposition and the exposure to gluten, the loss of intestinal barrier function, a pro-inflammatory innate immune response and inappropriate adaptive immune response are key to CD development.

1.1.2.1. Innate immunity

Studies performed in the last decade have stressed the role of the innate immune response in the pathogenesis of the disease. Gluten has shown a direct, toxic effect

on the epithelium, inducing the release of proinflammatory cytokines as *IL15* and *IL8*. Activation of *IL15* in intestinal epithelial cells can polarize immune cells and intraepithelial lymphocyte (IEL) function, the cells that mediate the destruction of enterocytes in active CD. In fact, CD patients present IELs expressing activating natural killer (NK) receptors endowing the ability to kill, secrete cytokines, and proliferate in response to damage and stress signals from epithelial cells (Meresse et al., 2006). Meanwhile, gliadin-induced production of *IL8* chemokine activates neutrophils (Barone et al., 2014; Jelínková et al., 2004), altogether creating the perfect environment to initiate CD enteropathy (Fig1).

Increasing evidence indicates that epithelial stress may be involved in the initiation steps of the small intestinal villous atrophy and active CD. Nevertheless, the molecular pathways involved in the recognition of gluten as a stress signal have not been identified yet.

1.1.2.2. Adaptive immunity

The most widely-accepted pathogenic model focuses on the adaptive immune mechanisms dependent on the stimulation of gluten-reactive CD4+ T cells, which are present in the intestinal mucosa of CD patients, but not in non-celiac individuals. Indeed, the erroneous adaptive immune response is a major consequence of the highly specific interplay between certain gluten peptides and HLA-DQ2 or HLA-DQ8 antigen presenting cells (APCs) (Ainara Castellanos-Rubio et al., 2009; Schuppan et al., 2009)(Ainara Castellanos-Rubio et al., 2009).

When genetically susceptible individuals are exposed to gluten, the gluten-derived peptides cross the intestinal epithelium and are deamidated by TG2. Deamidated peptides are presented by HLA-DQ2 and/or HLA-DQ8 APCs to pathogenic CD4+ T cells, triggering a Th1-mediated response, involving the production of proinflammatory cytokines as IFNγ and TNFα, anti-TG2 autoantibodies and anti-gluten antibodies (Fig1).

The role of CD4+ T cells in the pathophysiology of CD is not fully understood, as HLA-DQ2 and DQ8 molecules are necessary but not sufficient for CD development. There is evidence supporting that the expression of proinflammatory cytokines by enterocytes and IELs with activated NK receptors are also required, and it is believed that gluten-specific CD4+ T cells cooperate with those IELs to induce the infiltration of the epithelial *lamina propria* by inflammatory cells, together with crypt hyperplasia and villous atrophy (Jabri & Sollid, 2006; Schuppan et al., 2009).

Some aspects of the pathogenesis of CD still need to be clarified, especially the way in which gluten induces stress signals in enterocytes, the interaction between gluten-specific CD4+ T cells and IELs or the passage of gluten peptides into the *lamina propria* among others.

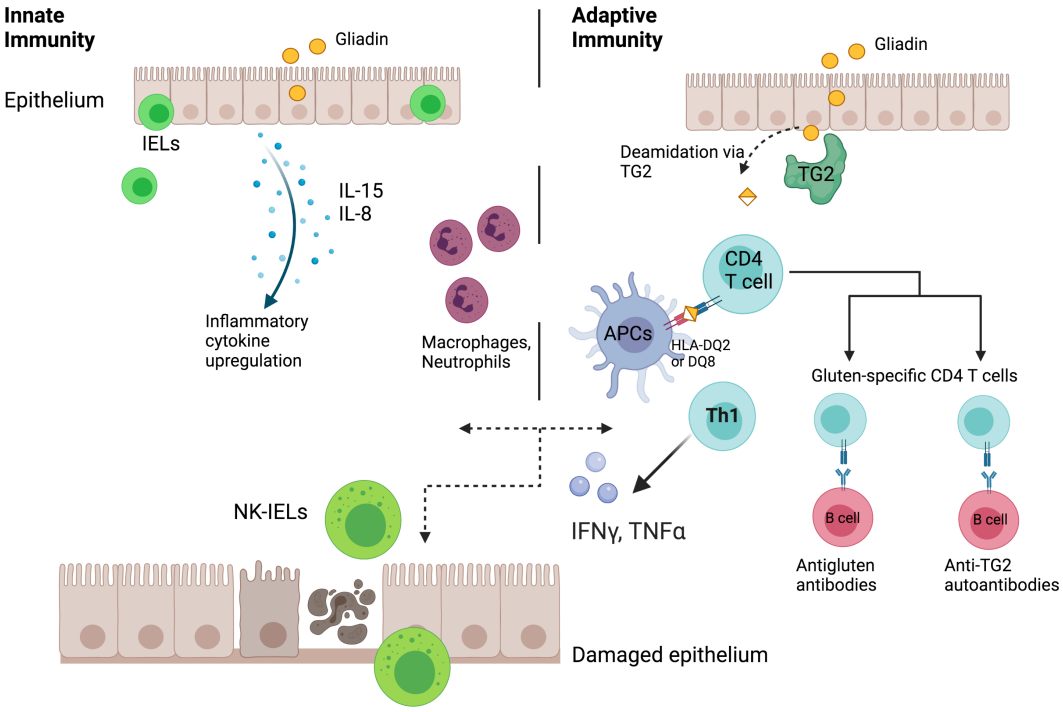

Figure 1. Model of CD pathogenesis. Gliadin peptides mediate innate and adaptive immune responses. The innate immune response results in the alteration of enterocytes, which up-regulate inflammatory cytokines, as *IL15* and *IL8,* with the consequent recruitment of immune

cells into the *lamina propria*. The adaptive immune response results in the activation of antigluten-specific CD4+ T cells and anti-TG2-specific B cells. Gliadin peptides are partially deamidated by TG2 and are recognized by HLA-DQ2/DQ8 APCs and then presented to T helper cells. T cells trigger the release of pro-inflammatory cytokines (IFNγ and TNFα) and the activation and maturation of B cells that produce antibodies against TG2. The crosstalk between the innate and adaptive immune responses activates and initiates CD enteropathy. Created with Biorender.

In addition, viral infections or microbiome composition are also thought to contribute to CD, increasing the complexity and heterogeneity of the pathophysiology of the disease.

Different studies have observed that gastrointestinal, but not respiratory, infections increase the risk of developing celiac autoimmunity. Moreover, the fact that viruses induce type-1 IFNs and that the *TLR7/TLR8* locus has been identified as a genetic risk factor for CD (Abadie et al., 2011; Silvester & Leffler, 2017; Stene et al., 2006), strengthens the potential role of viral infections in CD pathogenesis.

Recent advances in sequencing have enabled studies demonstrating that the dysregulation of the gut microbiota (dysbiosis) may also play a role in the pathogenesis of gastrointestinal diseases as well as autoimmune disorders (Maynard et al., 2012). Several studies have shown an association between CD and a change in the microbiome composition (Chander et al., 2018; Olivares et al., 2018) and many environmental factors that influence the composition of the intestinal microbiota are also thought to play a role in the development of CD (Lionetti et al., 2014; Vriezinga et al., 2014). One way in which dysbiosis could trigger CD is by driving the production of already known inducers of the disease. However, the evidence for this hypothesis is mostly indirect and studies analyzing how dysbiosis could drive dysregulated expression of these cytokines in the intestinal mucosa are further needed.

Indeed, to move from association to causation, large-scale, longitudinal studies are

necessary to define whether and how viral infections and the composition of gut microbiota may influence the loss of gluten tolerance and subsequent onset of CD in genetically susceptible subjects.

1.1.3. Genetics of CD

Even though the precise inheritance model of CD is still unknown, CD is considered to have a high heritability (Nisticò et al., 2006) and it is well characterized as a polygenic disease with a complex non-Mendelian pattern of inheritance, involving both MHC and non-MHC genes. Evidence of a strong genetic background in disease susceptibility comes from studies on the prevalence of CD in affected families, and especially those comparing twin pairs, in which the proportion of genetic and environmental risk factors in the disease prevalence can be estimated. According to these studies, genetics is a fundamental player both in the triggering and in the latter development of CD; with an estimated heritability (proportion of the risk of suffering from CD attributable to genetic factors, compared to environmental determinants) of around 87% (Greco et al., 2002).

Approximately 40% of the genetic risk to develop CD is conferred by the Human Leukocyte Antigen (HLA) genes and fine-mapping studies have revealed additional non–HLA regions that altogether account for an additional 7% of heritability (Caio et al., 2019).

1.1.3.1. MHC

HLA genes are located on the MHC, a region of chromosome 6p21 that carries many genes involved in the immune response and is characterized by strong linkage disequilibrium (LD) and extended, conserved haplotype blocks. HLA genes encode antigen presenting proteins that are expressed in most human cells and are essential for the ability of the organism to distinguish between self and foreign molecules (Ainara Castellanos-Rubio & Bilbao, 2018; de Haas et al., 2014). Genetic polymorphisms may alter the peptide-binding groove and affect the peptides that can be efficiently bound and presented.

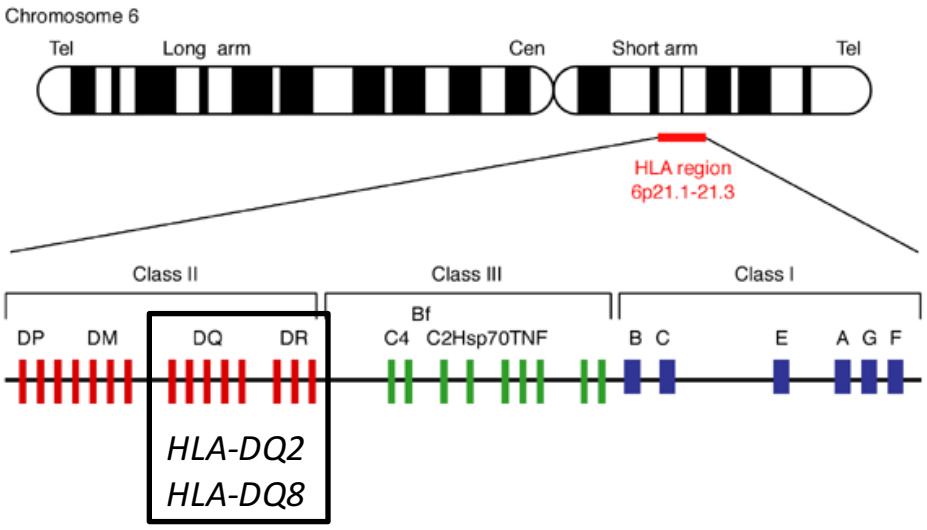

Figure 2. HLA genes.

The largest portion of the genetic risk to develop CD comes from the presence of HLA-DQ2 and HLA-DQ8 heterodimers encoded by the MHC class II genes (Fig2). It has been calculated that classical HLA class II variants alone explain 23% of CD heritability. HLA-DQ2 is more strongly associated with CD than HLA-DQ8 (Louka & Sollid, 2003), as HLA-DQ2 homozygosis confers a higher risk of developing early-onset CD due to a more efficient presentation of gluten peptides to CD4+ T (Vader et al., 2003). However, even if the role of these molecules is essential in the pathogenesis of the disease, their contribution to heredity is modest. In addition, HLA-DQ2/DQ8 is frequent among the general population (25–35%), and only a small proportion of those individuals will develop CD (Caio et al., 2019). Therefore, additional genes conferring genetic risk to CD may lead to the discovery of key pathways potentially involved in disease pathogenesis.

The complexity of the MHC region, mainly its numerous genes, high degree of polymorphism and broad linkage disequilibrium, have made it very difficult to identify additional risk variants in this region for many years. However, fine-mapping of the MHC region taking advantage of high-density imputation, was able to identify five new independent variants in this region. These five factors explain an additional 18%

of the disease heritability (Gutierrez-Achury et al., 2015). Taking together, MHC risk variants account for 40% of disease heritability, leaving a considerable fraction still unexplained.

1.1.3.2. Non-MHC

For a long time, only genetic variants located within the MHC region were firmly established as genetic factors contributing to CD risk. However, it was evident that CD-associated HLA-DQ molecules alone were not sufficient to cause CD development. Approaches based on linkage studies in affected families and association studies based on population screening have helped identify new non-MHC risk loci.

Linkage studies in families allow the identification of chromosomal regions which are repeatedly and consistently inherited by the affected members of a family through several generations (Gujral et al., 2012; van Heel et al., 2005). Nevertheless, with the exception of the MHC *locus*, the results of the linkage scans have been somewhat contradictory.

The real revolution in complex disease Genetics came with high-throughput genotyping platforms, which made Genome-Wide Association Studies (GWAS) feasible and changed the way we approach genetic studies of complex traits and diseases. GWAS have evolved into a powerful tool that enables researchers to scan a great number of genetic markers (polymorphisms) in large genomic DNA sample sets (case-control), with the aim of finding genetic variants associated with a particular disease. The two GWAS performed in CD analyzed approximately 5,000 patients and 10,000 controls, and revealed a total of 26 non-HLA associated regions (Dubois et al., 2010; Van Heel et al., 2007).

Other of the main findings of the GWAS was that part of this genetic component is shared with different immune disorders other than CD, suggesting that these

pathologies may be influenced by common molecular pathways (Fig3) (Cotsapas et al., 2011; Kumar et al., 2014).

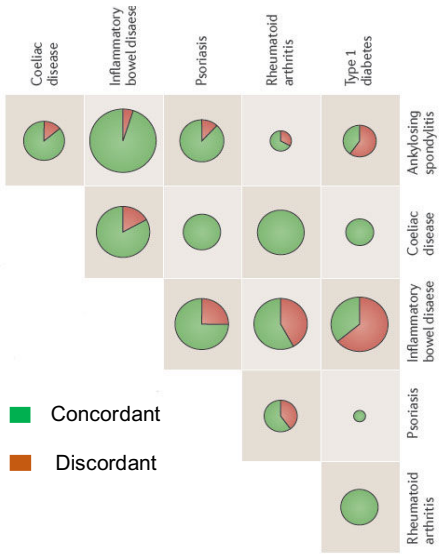

Figure 3. Shared genetic factors among different immune disorders, modified from (Parkes et al., 2013).

Based on this idea, different approaches were followed and new susceptibility regions were identified (Festen et al., 2011; Smyth et al., 2008). This issue was successfully addressed with the Immunochip project. The design of GWAS arrays was focused on the study of the common genetic polymorphisms and did not allow capturing all the genetic variation of the disease-associated loci, making it difficult to identify the true risk variants. The Immunochip was developed in order to unravel the heritability that was still missing and to refine the signals found by improving signal localization and cross-disease comparison. Around 12,000 cases and 12,000 controls were genotyped using the Immunochip and 13 additional regions associated with CD were identified (Gosia Trynka et al., 2011). Later, a reanalysis of the Immunochip identified five additional genomic regions involved in CD (Garcia-Etxebarria et al., 2016).

Overall, there is a total of 44 non-HLA regions associated with CD, containing 62 independent association signals that together contribute 5-7% to the genetic risk

(Fig4). Some of these regions pinpoint to a single candidate gene, while only 3 of the associated SNPs are linked to protein-altering variants located in exons. In other cases, potentially causative genes have been proposed due to the existence of signals near 5' or 3' regulatory regions, but as with other complex disease-associated SNPs, most variants are located in non-coding regions of the genome (promoter regions, enhancers or even in non-coding RNA genes) (Ricaño-Ponce et al., 2016).

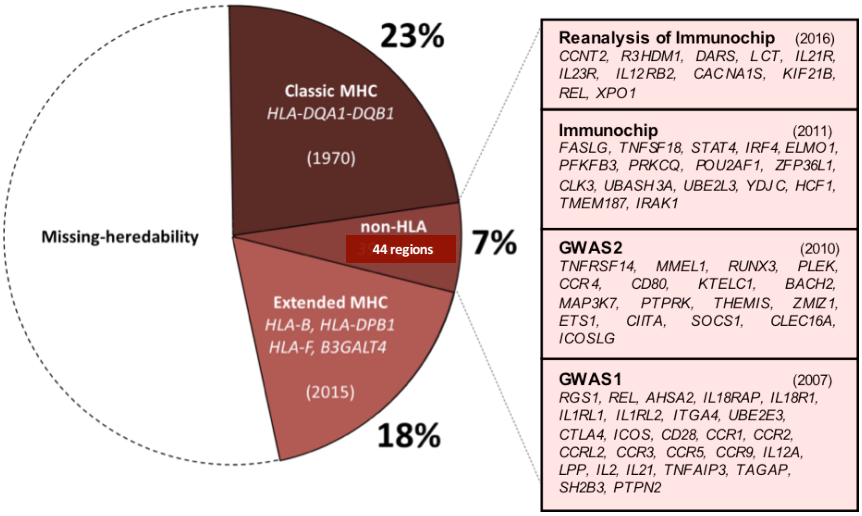

Figure 4. Heritability of CD.

Despite the success of GWAS and follow-up studies in discovering CD susceptible *loci*, the variants identified only explain a small proportion of the genetic contribution to the disease and many more remain to be found. Moreover, most of the GWAS SNPs are probably not the causal variants and it is thought that they are merely pointing to associated regions due to LD, so these regions should be more deeply scanned.

In brief, CD Genomics remains unresolved, with known genetic factors accounting approximately for half of the heritability of CD. There is a critical gap termed "missing heritability" that challenges the tremendous efforts made in Genomic Medicine. Understanding the biological consequences of associated polymorphisms is a very complicated task, which is still far from being fully completed (Farh et al., 2015). In

this line, novel approaches to elucidate the genetic component of the disease are needed. Epigenetic marks, understood as the genomic information independent of DNA sequence, as well as studies of microbiome composition are areas of growing interest in the field (Fernandez-Jimenez et al., 2019).

1.1.4. Functional studies of CD-associated SNPs

Most of the approaches made to understand the functional effects underlying the association signals have been limited to the search of possible alterations in the expression levels of nearby genes or expression quantitative trait *loci* (eQTLs), but their results have been limited, suggesting a more complex scenario in CD pathogenesis (Plaza-Izurieta et al., 2015).

More than 85% of the complex disease-associated SNPs are located on non-coding regions of the genome (promoter regions, enhancers or even in non-coding RNA genes), making it difficult to describe the molecular mechanisms in which they might be involved. Previous findings have revealed that non-coding genetic variants associated with phenotypic changes are often located in tissue-specific regulatory regions (Roadmap Epigenomics Consortium et al., 2015). These ideas have strongly motivated the study of the influence of non-coding genes in disease susceptibility.

RNA sequencing techniques, not limited to annotated transcripts, have shown that almost 70% of the non-coding human genome has transcriptional activity and contributed to the identification of novel RNAs that could be involved in the pathogenesis of disease (Ainara Castellanos-Rubio & Bilbao, 2018; Mowel et al., 2018). The families of non-coding RNAs (ncRNAs) can be divided into short ncRNAs (<30 nucleotides) and long ncRNAs (>200 nucleotides). LncRNAs are the most abundant class among these newly described elements, with up to thousands of lncRNAs that are able to regulate many different biological processes (Robinson et al., 2020).

An example of the regulatory nature of an associated SNP is a lncRNA named *lnc13* that is close to *IL18RAP* and harbors the CD-associated SNP rs917997. *Lnc13* is the only lncRNA described so far whose functional characteristics are affected by the genotype of a CD-associated, intergenic SNP and has been shown to be a key regulator of genes in the NF-κB pathway. *Lnc13* functions as a scaffold for a protein complex that binds chromatin at the transcription start site of several inflammatory genes altered in CD and inhibits their expression. The CD-risk allele binds the protein complex less efficiently causing an increase in the expression of those inflammatory genes, which will in turn predispose to disease development (Fig5) (Ainara Castellanos-Rubio et al., 2016).

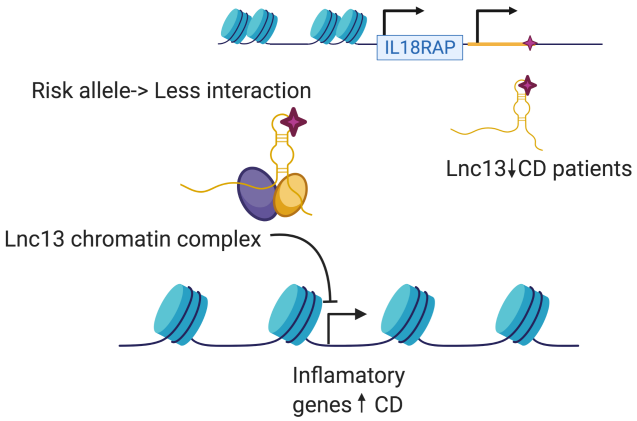

Figure 5. Functional analysis of CD-associated SNP rs917997. Modified from (Olazagoitia-Garmendia et al., 2021).

It is noteworthy that *lnc13* was differentially expressed in the tissues analyzed, pointing to a possible cell-type specific function. Moreover, as is the case for many other inflammation-related SNPs, rs917997 is also associated to other autoimmune diseases. However, while the T allele is the risk variant in CD, it is the protective allele in type 1 diabetes (T1D). A recent work published by our group that analyzed *lnc13* function in the context of T1D and pancreatic beta cell inflammation, found a totally different mechanism for *lnc13* involvement in T1D, highlighting the importance of the cell-type context for non-coding associated variants and their function (Gonzalez-Moro et al., 2020).

Until recently, protein coding genes were considered as the only functional regions of the genome, but nowadays it is widely known that non-coding regions also harbor regulatory elements that play crucial roles in gene regulation. Thus, to elucidate the functional effects of non-coding disease-associated variants is a complicated but indispensable task that would help clarify the role of immune disease-associated SNPs in genetic susceptibility.

1.2. EPITRANSCRIPTOMICS

The majority of the efforts to identify the genetic predisposition to CD have relied on SNP-association studies, but the contribution of common genetic variation identified so far, including HLA genes, account for roughly 50% of the heritability. However, other unexplored layers of genomic information that are independent from DNA sequence variation, also referred as epigenetics, could also contribute to the pathogenesis of CD.

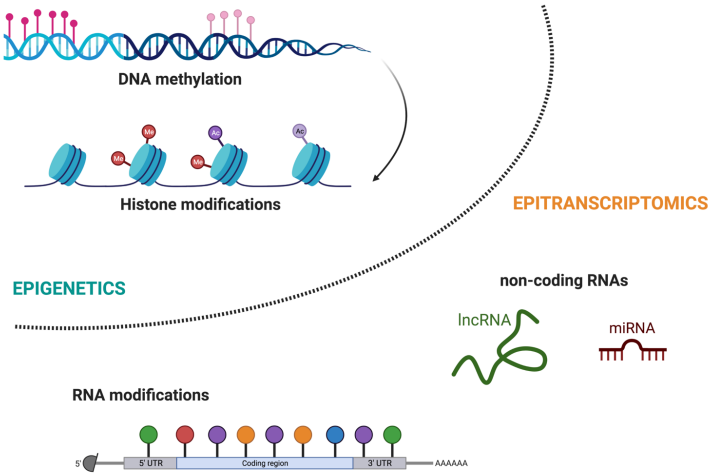

Figure 6. Epigenetic and epitranscriptomic marks that contribute to the pathogenesis of disease. Created with Biorender.

Epitranscriptomics, also named RNA epigenetics, is a branch of Epigenetics that refers to RNA editing and non-coding RNA regulation (Fig6). Epitranscriptomics plays essential roles in alternative splicing, nuclear export, transcript stability and

translation of RNAs. In addition, there is also a growing interest in SNPs that may have influence on those epigenetic marks.

To date, more than 100 types of RNA chemical modifications have been identified (Machnicka et al., 2013). Most modifications had been observed on rRNA and tRNA, whereas the modification of mRNAs was considered a rare event. Nevertheless, several modifications of mRNA molecules have been recently identified, including N^6-methyladenosine (m^6A) (Dominissini et al., 2012; Meyer et al., 2012), N^1-methyladenosine (m^1A) (Dominissini et al., 2016), inosine (I) (Slotkin & Nishikura, 2013), ^{5}-methylcytosine (m^5C) (Squires et al., 2012) and pseudouridine (ψ) (Carlile et al., 2014; Schwartz, Bernstein, et al., 2014) (Fig7). Among all those, m^6A is the most prevalent modification on mRNAs and lncRNAs.

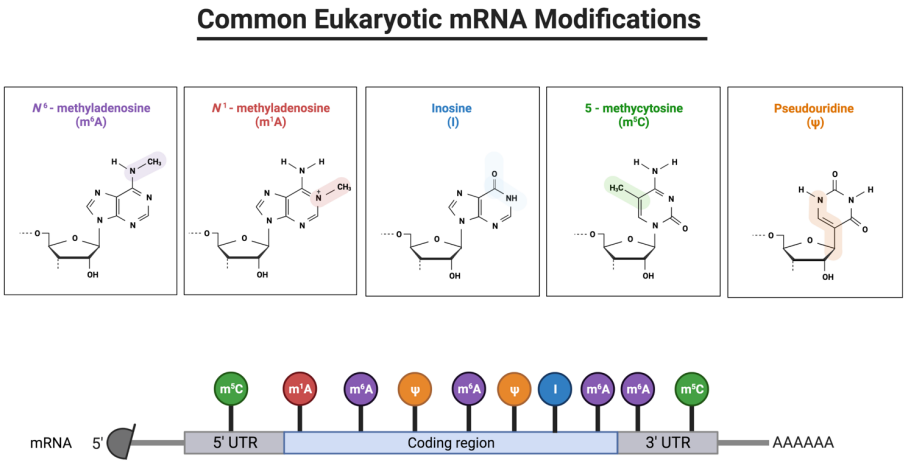

Figure 7. Common mRNA modifications. Created with Biorender.

1.2.1. N^6-methyladenosine RNA modification

N^6-methyladenosine (m^6A) was first recognized as the most abundant chemical modification of mRNAs in the 1970s (Desrosiers et al., 1974). However, little has been known about its exact location, extent of transcript identities or the cellular factors that produce and recognize m^6A until recently.

The enzyme that adds m^6A modification to RNAs was identified in the late 1990s, but the interest on this modification increased with the development of genome-wide m^6A-mapping studies, which were able to reveal the prevalence of m^6A throughout the transcriptome. Since then, m^6A modifications have been shown to be involved in multiple aspects of RNA metabolism and to play crucial roles in many cellular processes, thus they are emerging as a new layer of gene expression regulation in diverse physiological processes (Geula et al., 2015; Koranda et al., 2018; X. Wang et al., 2014, 2015).

m^6A is present in 0.1–0.4% of all adenosines in global cellular RNAs (C. M. Wei et al., 1975) and occurs mainly in the DRACH consensus sequence motif (where D = A,G, or U; R = G or A; and H = A, C or U), being mainly R=G (around 70%) (C. M. Wei et al., 1976; C. M. Wei & Moss, 1977). m^6A marks are enriched in the coding sequence (CDS) and 3' untranslated regions (3' UTR), with a particularly high enrichment around the stop codon area. However, it also occurs in 5'UTRs and NGS-based methods have shown that m^6A exists in almost every type of RNA, including lncRNAs or microRNAs (miRNAs) (Dominissini et al., 2012; Meyer et al., 2012).

The discovery of the proteins involved in m^6A regulation has been one of the most significant achievements in the field. Nowadays, m^6A writers or methylases, like the N^6-methyltransferase protein complex (METTL3/METTL14), and m^6A erasers or demethylases (FTO or ALKBH5) are known to control the levels of m^6A in RNAs by adding or removing m^6A methylation marks (Huang et al., 2020). The so-called m^6A reader proteins recognize methylated RNAs and regulate their processing (Fig8), such as nuclear RNA export, splicing, stability, translation or miRNA biogenesis (Engel et al., 2018; Roignant & Soller, 2017; Shafik et al., 2016; P. Wang et al., 2016; Y. Yang et al., 2017; Zhu et al., 2014).

m^6A modification is dynamically regulated during many physiological and pathological processes and it has been associated with numerous disorders

including inflammation, immunoregulation and carcinogenesis (Siwei Wang et al., 2017; W. Wei et al., 2017).

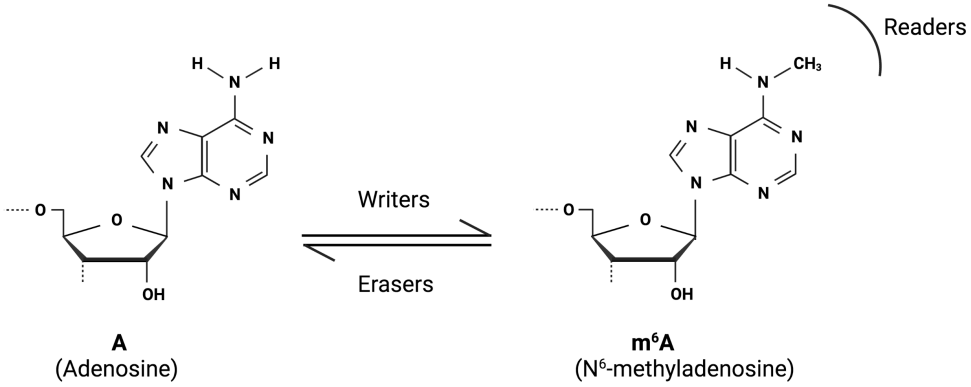

Figure 8. m^{6}A RNA modification. Created with Biorender.

1.2.1.1. m^{6}A writers, erasers and readers

1.2.1.1.1. Writers

The m^{6}A methyltransferase complex or the "writer complex" located within the nucleus deposits the m^{6}A modifications on the target RNAs. It is mainly composed of METTL3 and METTL14 heterodimers and some additional adaptor proteins.

METTL3, a 70 kDa protein, was first identified in 1997 and is the enzymatic component of the writer complex (Bokar et al., 1997). *METTL3* knockout leads to decreased m^{6}A levels and to concomitant apoptosis of human HeLa and HepG2 cells, while genomic *Mettl3* knockout in mice is embryonic lethal (Geula et al., 2015), emphasizing the biological importance of m^{6}A methylation. METTL14 is an allosteric activator that also binds to the target RNA (J. Liu et al., 2014). The complex installs the m^{6}A modification on distinct target RNAs through the methyl groups of S-adenosylmethionine (SAM) transferase (Bokar et al., 1997; J. Liu et al., 2014). WTAP, a splicing factor, acts as the third crucial component of the writer complex.

Although it does not possess any recognizable domains or motifs, WTAP binds to the METTL3-METTL14 heterodimer and regulates m^6A deposition inside the cells (Ping et al., 2014). WTAP may mediate the position of the heterodimer on nuclear speckles and recruit target RNA for m^6A modification (Ping et al., 2014) (Fig9). The writer complex also includes the ZC3H13, RBM15 or RBM15B and KIAA1429 (also known as VIRMA) subunits. ZC3H13 maintains the nuclear localization of the complex (Wen et al., 2018) and RBM15/15B (Patil et al., 2016) and KIAA1429 (Schwartz, Mumbach, et al., 2014) are thought to provide additional specificity.

These writer proteins methylate adenosine cotranscriptionally at the m^6A consensus sequence DRACH. Even if every transcript is predicted to have many potential methylation sites, the deposition of m^6A is more restricted, as only certain RNAs contain m^6A methylation marks and only a small fraction of the consensus sites within those transcripts are methylated. Moreover, the stoichiometry of m^6A (the ratio between modified and unmodified adenosines) at distinct sites can vary (Garcia-Campos et al., 2019; N. Liu et al., 2013; Zhang Zhang et al., 2019), hence many aspects of deposition specificity remain poorly understood.

In addition to the canonical writer complex, other enzymes have also been shown to act as m^6A methyltransferases. METTL16 modifies U6 small nuclear RNAs, the MAT2A transcript and possibly additional mRNAs (Pendleton et al., 2017), while ZCCHC4 and METTL5 add m^6A to18S and 28S ribosomal RNAs (Ma et al., 2019) (Van Tran et al., 2019). PCIF1 catalyzes m^6A methylation on 2-O-methylated adenines that are present at the transcription start site of m7G-capped mRNAs, thus generating N^6-2′-O-dimethyladenosine (m^6Am) (Akichika et al., 2019; Boulias et al., 2019; H. Sun et al., 2019).

1.2.1.1.2. Erasers

FTO was the first found demethylase that removes the methyl groups from m^6A (Jia et al., 2011). ALKBH5 was later identified as a demethylase and exhibits distinct physiological functions (Zheng et al., 2013). A common ALKB domain is situated in

the central regions of both FTO and ALKBH5, consisting of two active motifs that bind to Fe(II), as well as to a-ketogluterate (a-KG) and the substrate (Fig9).

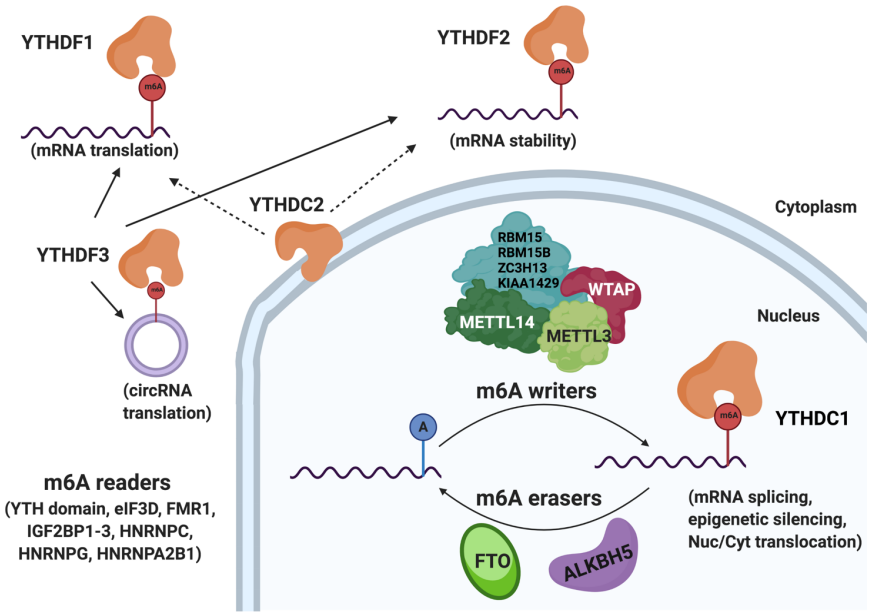

Figure 9. Regulation of m^{6}A RNA modification. Created with Biorender.

FTO and ALKBH5 have shown tissue-specificity and diverse intracellular localization. While FTO has been described to be highly abundant in adipose and cerebral tissues, ALKBH5 has been shown to be primarily expressed in the testes (Zheng et al., 2013). Thus, the demethylation performed by FTO or ALKBH5 may be tissue-specific.

FTO demethylates both m^{6}A and terminal m^{6}Am (J. Wei et al., 2018), while ALKBH5 specifically demethylates m^{6}A (Mauer et al., 2017; Zheng et al., 2013). m^{6}A erasers provide evidence that m^{6}A is a dynamically reversible RNA modification in a signal-dependent manner. Nevertheless, the potential effects of RNA demethylation in additional physiological contexts needs to be further studied.

1.2.1.1.3. Readers

The RNA-binding proteins that bind to m^{6}A are referred to as m^{6}A readers. These

proteins mediate the regulatory functions of m^{6}A-modified RNAs to confer its fate and regulate downstream functions.

The most studied m^{6}A readers are YTH domain proteins, which bind RNA in an m^{6}A-dependent manner (F. Li et al., 2014; Xu et al., 2014, 2015; Zhu et al., 2014). There are five YTH domain proteins in the mammalian genome: the family of cytosolic YTHDF proteins, comprising three highly similar paralogs (YTHDF1, YTHDF2 and YTHDF3); YTHDC1, which is broadly expressed and is predominantly localized to the nucleus (Nayler et al., 2000; Xiao et al., 2016) and YTHDC2, whose expression is tissue-restricted and can be both nuclear and cytosolic (Bailey et al., 2017; Wojtas et al., 2017) (Fig9).

YTHDF proteins share high similarity in their amino acid sequences and although there is conflicting evidence regarding whether they perform specialized effects on m^{6}A modified mRNAs or not, different functions have been described for each of the members (Patil et al., 2018). YTHDF1 was found to interact with translation initiation factors to induce translation of m^{6}A-containing mRNAs (X. Wang et al., 2015a), while YTHDF2 recruits the deadenylase complex CCR4-NOT via the YTHDF2 N-terminus and mediates RNA degradation in mammalian cells (X. Wang et al., 2014). YTHDF3 facilitates translation and decay of m^{6}A-modified RNA (Shi et al., 2017). In addition, m^{6}A modification is especially abundant in circRNA and a single m^{6}A residue seems sufficient to drive circRNA translation via recruitment of YTHDF3 and translation initiation factors eIF4G2 and eIF3A (Y. Yang et al., 2017).

YTHDC1 is a nuclear m^{6}A reader and has been linked to mRNA splicing (Kasowitz et al., 2018; Xiao et al., 2016), epigenetic silencing (Patil et al., 2016) and nuclear export of methylated RNAs (Roundtree et al., 2017).

YTHDC2 is enriched in the testes and was suggested to be involved in mRNA translation and degradation (Hsu et al., 2017). YTHDC2 knockout mice show defects mainly in spermatogenesis, supporting its suggested testis-specific function (Bailey et al., 2017; Hsu et al., 2017; Jain et al., 2018). Nonetheless, the information from

online genomic databases indicates that immune cells express moderate levels of YTHDC2, so it remains a possibility that this reader has a role in immune cells as well.

Besides the YTH domain m^{6}A readers, additional RNA-binding proteins have been reported to preferentially bind m^{6}A-containing RNAs. These include eIF3D, FMR1, IGF2BP1-3, HNRNPC, HNRNPG and HNRNPA2B1 (Alarcón et al., 2015; Arguello et al., 2017; Edupuganti et al., 2017; Huang et al., 2018; N. Liu et al., 2015, 2017; Meyer et al., 2015). However, the regulatory functions of these RNA-binding proteins, and whether they bind m^{6}A directly rather than indirectly through canonical m^{6}A binders, remain unclear. The propensity of m^{6}A to change RNA secondary structure makes it difficult to determine whether an RNA-binding protein binds directly to m^{6}A or whether it preferentially binds to m^{6}A-modified RNA due to an increase in accessibility (Spitale et al., 2015; Zaccara et al., 2019).

Table 1. List of m^{6}A writers, erasers and readers and their described functions.

Type	Protein	Function	Reference
m^{6}A writers	METTL3	Catalyzes m^{6}A modification.	(Bokar et al., 1997)
	METTL14	Assist METTL3 to recognize substrates.	(J. Liu et al., 2014)
	WTAP	Promotes METTL3-METTL14 heterodimer to the nuclear speckle.	(Ping et al., 2014)
	ZC3H13	Anchors WTAP in the nucleus to facilitate m^{6}A methylation.	(Wen et al., 2018)
	KIAA1429	Guides the methyltransferase components to specific RNA region.	(Schwartz, Mumbach, et al., 2014)

	RBM15/RBM15B	Bind the m^{6}A complex and recruit it to special RNA site.	(Patil et al., 2016)
m^{6}A erasers	FTO	Removes m^{6}A modification.	(Jia et al., 2011)
	ALKBH5	Removes m^{6}A modification.	(Zheng et al., 2013)
m^{6}A readers	YTHDF1	Promotes mRNA translation.	(X. Wang et al., 2015a)
	YTHDF2	Reduces mRNA stability.	(X. Wang et al., 2014)
	YTHDF3	Mediates translation or degradation.	(Shi et al., 2017; Y. Yang et al., 2017)
	YTHDC1	Promotes RNA splicing, epigenetic silencing and nuclear translocation.	(Kasowitz et al., 2018; Patil et al., 2016; Roundtree et al., 2017; Xiao et al., 2016)
	YTHDC2	Enhances the translation or degrades mRNA in target tissue.	(Hsu et al., 2017)

1.2.1.2. m^{6}A quantification methods

The growing interest into deciphering the mechanisms regulated by m^{6}A modifications, together with their involvement in disease development, have given rise to the need of identifying m^{6}A methylated sites. In addition, techniques that give quantitative information of the methylation status of individual sites are of special interest to compare m^{6}A levels between disease stages, among different cellular processes or in response to different stimuli. To this aim, different techniques have been developed, mostly based on high-throughput sequencing and/or use of m^{6}A antibodies or chemical modifications. These include m^{6}A-specific methylated RNA

immunoprecipitation (IP) with next-generation sequencing (m^{6}A-seq and MERIP-seq) (Fig10.A) (Dominissini et al., 2012; Meyer et al., 2012); Photo-crosslinking-assisted m^{6}A sequencing (PA-m6A-seq) (Fig10.B) (K. Chen et al., 2015); m^{6}A individual-nucleotide-resolution crosslinking and immunoprecipitation (m6A-CLIP/IP and miCLIP) (Fig10.C) (Ke et al., 2015; Linder et al., 2015); m^{6}A-level and isoform-characterization sequencing (m6A-LAIC-seq) (Fig10.D) (Molinie et al., 2016) or Site-specific cleavage and radioactive-labeling followed by ligation-assisted extraction and thin-layer chromatography (SCARLET) (Fig10.E) (N. Liu et al., 2013).

However, all these techniques require long and tedious protocols that are technically challenging. In addition, most of them require high-throughput sequencing and/or use of m^{6}A antibodies or chemical modifications, not being available and affordable to every laboratory.

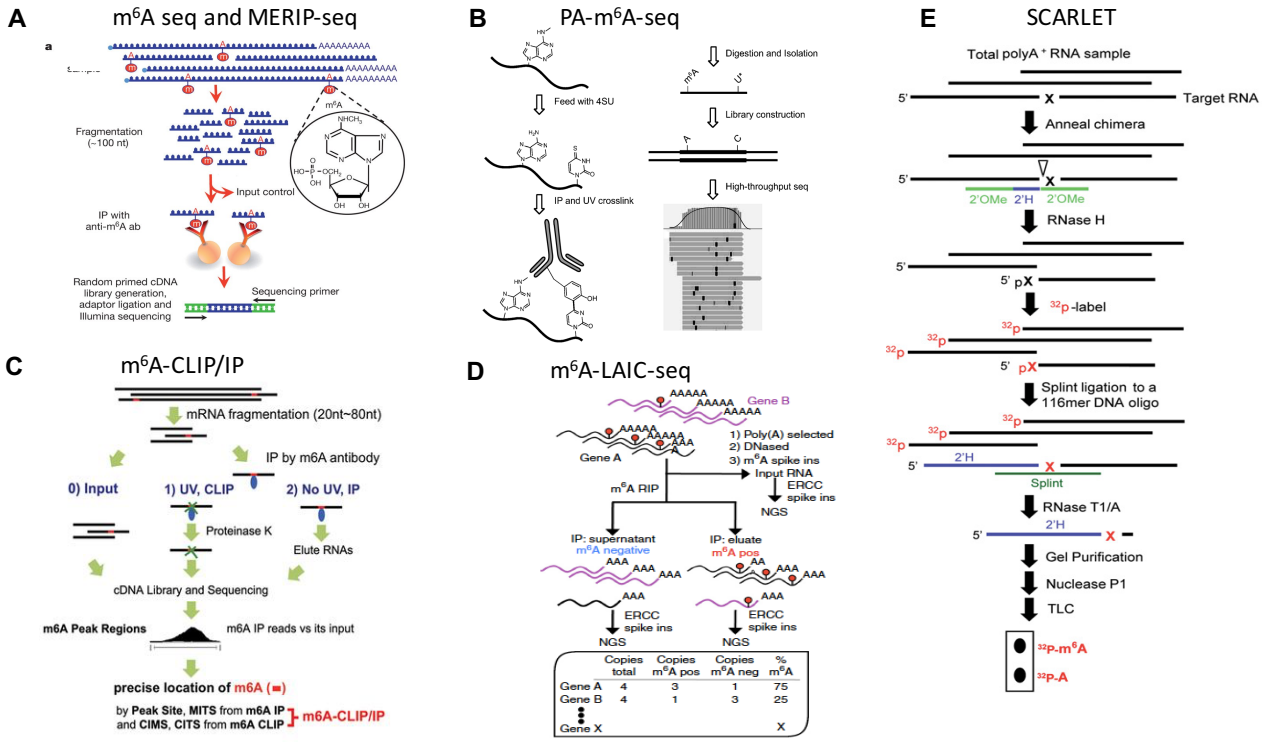

Figure 10. A) Schematic diagram of m^{6}A-seq, modified from *Dominissini et al. 2012*. **B)** Schematic diagram of PA-m^{6}A-seq, modified from *Chen et al. 2015*. **C)** Schematic diagram of

m^{6}A-CLIP/IP, modified from *Ke et al. 2015*. m^{6}A-induced truncation sites (MITSs); cross-linking-induced mutation sites (CIMSs; including single-base substitutions, deletions, and insertions) (C. Zhang & Darnell, 2011) and cross-linking-induced truncation sites (CITSs) occur (König et al., 2010). **D)** Schematic diagram of m^{6}A-LAIC-seq, modified from *Molinie et al. 2016*. **E)** Schematic diagram of SCARLET, modified from *Liu et al. 2013*.

Alternative protocols based on the reduced ability of certain polymerases (i.e. BstI) to retrotranscribe m^{6}A adenosines have been also described (Harcourt et al., 2013; Shaoru Wang et al., 2016). These enzymes have been used for single-nucleotide primer extension followed by polyacrylamide gel electrophoresis of the extension products to quantify the m^{6}A methylation levels of specific sites, but these experiments are also highly time consuming (Harcourt et al., 2013; Shaoru Wang et al., 2016; Zhou et al., 2015). Affordable and easy to apply methods are of special interest to help gain understanding of this epigenetic mark and to elucidate possible involvement in disease pathogenesis.

1.2.1.3. m^{6}A in Inflammation and Disease

The dynamicity of m^{6}A allows for a rapid response to different cellular stress signals that are implicated in several pathways related to autoimmunity and immune tolerance (Shulman & Stern-Ginossar, 2020; Winkler et al., 2019). This has increased the research on the role of m^{6}A methylation in a wide variety of pathophysiological disorders in the last years.

1.2.1.3.1. m^{6}A Methylation and Inflammatory Response

In pulpal and periapical diseases, bacterial infection is a major pathogenic factor (Feng et al., 2018) and recent findings indicate that *METTL3* expression and m^{6}A modification levels are up-regulated in LPS-treated human dental pulp cells. In addition, *METTL3* knockdown decreases the expression of LPS-induced inflammatory cytokines, including *IL6* and *IL8* among others. Moreover, the NF-κB and MAPK signaling pathways, key to inflammatory responses, are also suppressed.

1.2.1.3.2. m^{6}A Methylation and Innate Immune System

Innate immunity plays a crucial role in the early steps of the immune response, being crucial in recognizing pathogens and starting the first response against them. RNA modifications have been suggested to play a role in this recognition step, as modified nucleotides (including m^{6}A) that are added to *in vitro* transcribed RNAs suppress the activation of TLR3 and RIG-I (Durbin et al., 2016; Karikó et al., 2005). Hence, it is now thought that viruses use m^{6}A modified viral RNAs to evade innate immune recognition by the host. The presence of m^{6}A on viral RNAs was described over 40 years ago and today a wide spectrum of viruses that contain m^{6}A in their genome and transcripts are known, including positive-sense and negative-sense RNA viruses, retroviruses and DNA viruses. In addition, m^{6}A modifications in circRNAs or short interfering RNAs (siRNA) seem to reduce their immunogenicity, without any detectable effect on their activity (Imaeda et al., 2019).

While human CD4+ T cells infected by HIV-1 can trigger a massive m^{6}A increase in both T cells and HIV-1 mRNA (Lichinchi et al., 2016); a seemingly opposing mechanism of m^{6}A in type I interferon response to the herpesvirus human cytomegalovirus (HCMV) infection has been described. The decrease of m^{6}A modification results in enhanced stability of *IFNB* mRNA and sustained IFN-b production, thus triggering a stronger antiviral response to block HCMV growth (Winkler et al., 2019).

1.2.1.3.3. m^{6}A Methylation and Adaptive Immune System

m^{6}A methylation has also been associated to T cell homeostasis. The suppressor of cytokine signaling (SOCS) protein family plays a vital role in T cell proliferation and differentiation and interestingly, all three SOCS genes were found to have high m^{6}A methylation levels. m^{6}A modification was described to induce SOCS mRNA degradation and thus initiate the re-programming of naïve T cells for proliferation and differentiation (H. B. Li et al., 2017; Palmer & Restifo, 2009). Thus, this modification is likely a crucial factor in the regulation of immune homeostasis and the mitigation of various autoimmune diseases.

Another work demonstrated that m^{6}A plays a major role in the transition of dendritic cells (DCs) from immature cells into effective T cell activators that express costimulatory molecules and promote the initiation of the adaptive immune response through antigen presentation (Feng et al., 2018; H. Wang et al., 2019).

1.2.1.3.4. m^{6}A Methylation and Microbiome

The intestinal microbiota modulates host physiology and gene expression via mechanisms that are not fully understood. A recent work found that variations in gut microbiota correlate with m^{6}A modifications in the cecum, affecting pathways related to metabolism, inflammation and antimicrobial responses (Jabs et al., 2020), and stress the role of m^{6}A modifications as an additional level of communication between microbiota and the host.

1.2.1.3.5. m^{6}A Methylation and Autoimmune Diseases

Since it takes part in the regulation of a broad spectrum of biological processes, m^{6}A modification has been widely associated with multiple diseases (Jiang et al., 2021; C. Yang et al., 2020). m^{6}A has been described to regulate diverse cancer pathophysiological steps, as cancer stem cell pluripotency, regulation of cancer cell proliferation, resistance to chemo and radiotherapy or antitumor immunity (C. Yang et al., 2020). Additionally, neuronal disorders as nerve injury and malformation, several psychiatric disorders or even osteoporosis have also been described to be regulated by m^{6}A methylation. Lastly, this modification is also related to metabolic diseases such as obesity and lipid or glucose metabolism (C. Yang et al., 2020).

Perturbation of RNA methylation in T cells has been recently associated with development of colitis (Lu et al., 2020) and it has also been reported that the loss of *Ythdf1* inhibits tumor growth and host survival in a mice model (D. Han et al., 2019). Therefore, m^{6}A modification or YTHDF1 could be potential new therapeutic targets for immunotherapy in combination with other strategies.

However, the effect of SNPs associated with immune and inflammatory diseases on the variability of the epitranscriptome has not been systematically analyzed. A recent study showed that m^6A-QTLs (Quantitative Trait Loci) are enriched in complex traits as autoimmune diseases underlining the importance of performing disease-specific studies (Zijie Zhang et al., 2020). Thus, a better understanding of the way in which CD-associated SNPs can alter m^6A marks and consequently regulate the molecular mechanisms that drive the inflammatory response caused by gluten ingestion could provide a completely new layer of information regarding the pathogenesis of this disease, and open the door to the development of new therapeutic strategies.

1.3. NF-κB REGULATION, FROM GENETICS TO EPITRANSCRIPTOMICS

Nuclear factor kB transcription factors (NF-κB) are pivotal regulators of the innate and adaptive immune responses, and perturbations of NF-κB signaling contribute to the pathogenesis of immunological disorders. NF-κB is a well-known proinflammatory mediator and its deregulated activation is associated with the chronic inflammation of autoimmune diseases. NF-κB regulates inflammatory and immune response by increasing the expression of specific genes (S. C. Sun et al., 2013; Viatour et al., 2005). NF-κB pathway has been shown to be constitutively upregulated in CD mucosa and proinflammatory cytokines, adhesion molecules as well as enzymes whose gene expression is known to be regulated by NF-κB are involved in celiac disease pathogenesis (Fernandez-jimenez et al., 2014; Maiuri et al., 2003).

The NF-κB family is comprised of a group of transcription factors defined in part by their ability to bind a specific DNA sequence (Baldwin, 1996; Grilli et al., 1993). In most cell-types, NF-κB exists as a heterodimer comprising RelA (p65) and NFκB1 (p50) subunits and this heterodimer is the most potent gene transactivator in the NF-κB family (Sunil et al., 2010). NF-κB factors are normally sequestered in the cytoplasm via association with a family of inhibitory proteins, including inhibitor of

kappa B-alpha (IκB-α) and related ankyrin repeat-containing proteins (S. C. Sun et al., 2013). Stimulation of the cells triggers a series of signaling events that ultimately lead to the phosphorylation, polyubiquitination, and proteosomal degradation of IκB by the IκB-kinase (IKK) complex. Activated NF-κB is free to enter the nucleus and stimulate transcription by binding to NF-κB sites in the promoter regions of various target genes (Viatour et al., 2005) (Fig11).

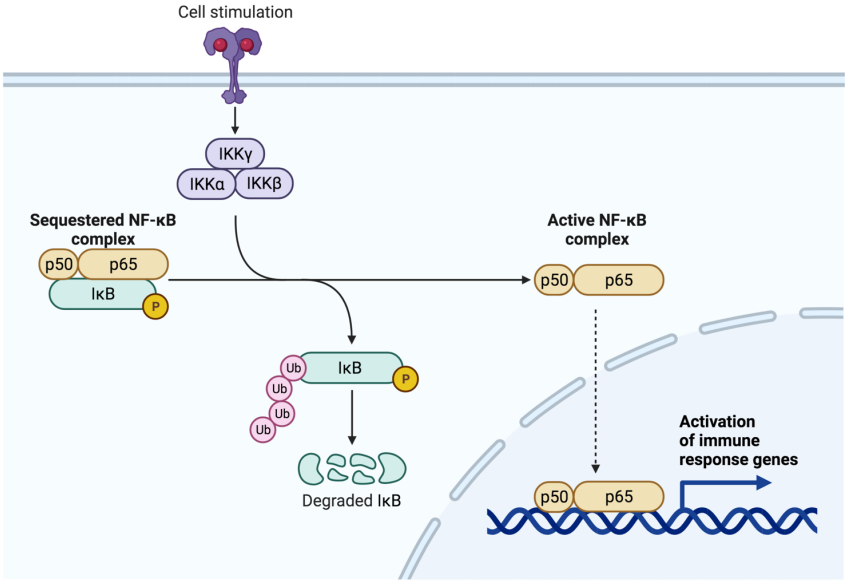

Figure 11. Schematic representation of NF-κB pathway activation. Upon stimulation, IκB is phosphorylated and further degraded by IKK complex to release the active NF-κB complex. Free active NF-κB complex is then able to enter the nucleus and bind the promoter of target genes to activate transcription of immune and inflammation related genes. Created with Biorender.

NF-κB is activated by a variety of agents, such as cytokines, growth factors, T cell mitogens, oxidative stress, bacteria, viruses and their products. Upon activation by various stimuli, NF-κB transcriptionally regulates many cellular genes involved in early inflammatory responses, including the chemokines *CXCL8* (*IL8*) (Roebuck, 1999) and *CXCL10* (Yeruva et al., 2008). IL8 is a proinflammatory CXC chemokine associated with the promotion of neutrophil chemotaxis and degranulation (Struyf et al., 2005). IL8 protein is secreted by a variety of cell types, including IECs (Fusunyan et al., 1998; H. Kim et al., 2001). Additionally, effects of gliadin on enterocytes have been shown to be mediated through oxidative stress, NF-κB activation

and *IL15* upregulation (Parmar et al., 2013), while IL8 is a gluten-responsive chemokine. So an appropriate regulation of this pathway seem to be key in the early steps of innate response. Therefore, defective or deregulated activation of NF-κB may contribute to autoimmunity and inflammation in CD, so that tight control of NF-κB signaling is of outmost importance.

The importance of this pathway in CD comes also from other key mediators that harbor CD-associated variants, such as *REL* and *TNFAIP3,* showing that heritable variation might influence this central biological pathway and predispose to CD (Fernandez-jimenez et al., 2014; G. Trynka et al., 2009).

Interestingly, epigenetic marks have been also described to control the NF-κB pathway. In fact, correlation of DNA methylation levels in CD patients was observed to be associated with the disruption of gene coexpression, suggesting a coordinated alteration of gene promoter methylation in NF-κB-related genes that could affect gene expression (Fernandez-jimenez et al., 2014).

m^6A methylation has also been reported to be involved in NF-κB pathway regulation. LPS-stimulated human dental pulp cells showed upregulated m^6A and *METTL3* expression levels, while METTL3 depletion decreased the accumulation of inflammatory cytokines and suppressed the activation of the NF-κB and MAPK signaling pathways (Feng et al., 2018). Another study described *Mettl3*-mediated m^6A effect in DC for stimulating T cell activation and further TLR4/NF-κB-induced cytokine production (H. Wang et al., 2019).

All these results show that epigenetic marks are able to regulate the NF-κB pathway, but further studies are needed on how these marks affect NF-κB and the implication of associated variants in this regulation leading to CD development.

1.3.1. NF-κB and XPO1

XPO1 is a nuclear export protein that has been described to target many proteins and RNAs involved in diverse cellular processes (Sendino et al., 2018). IκB-α is a cargo of XPO1 and inhibits the NF-κB transcription factor by sequestering the latter in an inactive state in the cytoplasm, and preventing NF-κB from entering the nucleus and binding to its DNA targets (Johnson C. 1999; Krappmann D. 1997; Scott ML. 1993).

Upregulation and mutations in *XPO1* have been implicated in different malignancies, evolving as an interesting therapeutic target for diverse types of cancer (Gravina et al., 2014; Tan et al., 2014). One consequence of XPO1 overexpression in cancer cells is excessive nuclear export of IκB-α to the cytoplasm where it is inactivated by proteasome-mediated degradation (Viatour et al., 2005). The resulting upregulation of NF-κB transcriptional activity promotes inflammation and tumorigenesis (Kashyap et al., 2016). It has been suggested that differential patterns of degradation of the IκB isoforms represent an important mechanism in the regulation of NF-κB activation (Maiuri et al., 2003), pointing XPO1 as an interesting regulator.

Indeed, a reanalysis of the Immunochip described that *XPO1* harbors a CD-associated SNP in the 5'UTR of the coding gene (Garcia-Etxebarria et al., 2016). Taking into account that NF-κB pathway is upregulated in CD mucosa and that IL8 is upregulated in CD patients upon gluten simulation (Tye-Din et al., 2020), elucidating *XPO1* function in the regulation of NF-κB and downstream IL8 could bring new insights towards understanding CD pathogenesis.

2.AIMS OF THE STUDY

The present work has four main objectives that aim to contribute to our understanding of the implication of non-coding genetic variants and epitranscriptomic modifications as m^6A methylation in CD pathogenesis:

1. To develop a new technique to quantify m^6A methylation.

    a. To quantify site-specific m^6A methylation in different cell lines and human samples.

    b. To quantitatively measure m^6A level alterations upon stimuli or between different disease stages.

2. To confirm the involvement of m^6A methylation in CD.

    a. To quantify m^6A levels in CD patients.

    b. To determine m^6A machinery expression in CD patients.

3. To study the implication of CD-associated rs3087898 non-coding SNP and m^6A modification in *XPO1* gene.

    a. To study SNP genotype effect in m^6A methylation modification.

    b. To show how non-coding SNP can affect key inflammatory genes as *XPO1*.

4. To analyze gluten involvement in m^6A modification and inflammatory response.

    a. To check if gluten alters m^6A methylation levels.

    b. To study the involvement of gluten-induced m^6A methylation changes in CD-characteristic inflammatory environment.

3.MATERIALS AND METHODS

3.1. MATERIALS

3.1.1. PT-Gliadin

PT-Gliadin was prepared by enzymatic digestion as described previously (Jauregi-Miguel et al., 2019) with minor modifications. Briefly, 2.5 g of gliadin (Sigma-Aldrich, #G3375) was dissolved in 25 ml of 0.2 N HCl and incubated stirring o/n at 37°C with 25 mg of pepsin (Sigma-Aldrich, #6887). pH was adjusted to 7.4 using 1 N NaOH and the resultant dilution was further digested adding 25 mg of trypsin (Sigma-Aldrich, #T9201). The solution was stirred vigorously at 37°C for 5 h, boiled (100°C) for 1 h, centrifuged 10 min at 2000 g, supernatant filtered and aliquots of the resulting solution were kept at -80ºC until used.

3.1.2. Human patients and samples

In pediatric patients, celiac disease was diagnosed according to the ESPGHAN (European Society of Pediatric Gastroenterology Hematology and Nutrition) criteria in force at the time of recruitment, including anti-gliadin (AGA), anti-endomysium (EMA) and anti-transglutaminase antibody (TGA) determinations. A confirmatory small bowel biopsy and analyses were performed after informed consent was obtained from all subjects or their parents.

All newly diagnosed adult CD patients had elevated TGA titers and displayed characteristic small intestinal histopathologic abnormalities, including villous atrophy, crypt hyperplasia and intraepithelial lymphocytosis. The samples were obtained after informed consent and using a protocol approved by the institutional review board of Columbia University.

The study was approved by the Basque Country Clinical Research Ethics Board (CEIC-E ref. PI2019133). All experiments were performed in accordance with relevant guidelines and regulations. Biopsy specimens from the distal duodenum of each patient were obtained during routine diagnosis endoscopy. None of the patients suffered from any other concomitant immunological disease. None of the controls

showed small intestinal inflammation or any other immunological disease at the time of the biopsy. None was taking any kind of medication. Details on human samples used is included in Table 2.

Table 2. List of human biopsy samples.

	Dx	ORIGIN	AGE (years)	SEX	HLA	Celiac Serology	Marsh (0-3)
ADULTS	CD n=6	100% USA	34.2 ± 19.5	83.3% FEMALE 16.7% MALE		100% +	100% 3
	CTR n=22	31.8% USA 68.2% SPAIN	45.2 ± 11.3	77.3% FEMALE 22.7% MALE	13.6% DQ2 4.5% DQ8	100% -	100% 0
	GFD n=6	100% USA	37.3 ± 11.4	33.3% FEMALE 66.7% MALE		100% -	83.3% 0 16.7% 1
	Dx	**ORIGIN**	**AGE (years)**	**SEX**	**HLA**	**Celiac Serology**	**Marsh (0-3)**
PEDIATRICS	CD n=28	100% SPAIN	4.6 ± 3.7	48.5 FEMALE 51.5 % MALE	69.7% DQ2 9.1% DQ2/ DQ8	81.8% + 12.1% -	20% 0 80% 3
	CTR n=16	100% SPAIN	8.1± 3.6	68.75% FEMALE 31.25% MALE	-	100% -	100% 0
	GFD n=12	100% SPAIN	2 ± 0.7	69.2% FEMALE 30.8% MALE	69.2% DQ2 23.1% DQ2/ DQ8	7.7% + 92.3% -	84.6% 0 7.7% 1 7.7% 3

3.1.2.1. Treatments

For biopsy stimulation experiments, two biopsy portions, taken from active celiac patients were incubated without any compound or in the presence of 250 µg/ml PTG in 150 µl RPMI-1640 10X medium (Thermofisher, #11875093) at 37°C and 5% CO_2 during 4 h (Fig12).

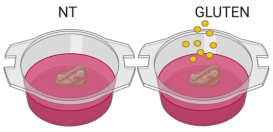

Figure 12. Representative figure of PTG stimulation approach in active CD patients' biopsies.

3.1.3. Cell lines

Human intestinal cell lines HCT116 (cat. no. CCL-247) and HCT15 (cat. no. CCL-225) and embryonic kidney cell line HEK293FT (cat. no. CRL-1573) were obtained from the American Type Culture Collection (ATTC, Manassas, VA, USA). Murine intestinal cell line C26 was kindly provided by Dr Beatriz Arteta.

All cell lines were cultured following manufacturer's protocol in RPMI (Lonza, #12-115F) supplemented with 10 % FBS (Millipore, Burlington, MA, USA #S0115), 100 units/ml penicillin and 100 µg/ml streptomycin (Lonza, #17-602E) or in DMEM (Lonza, Basel, Switzerland, #12-604F) supplemented with 10 % FBS, 100 units/ml penicillin and 100 µg/ml streptomycin.

3.1.3.1. Treatments

For cycloleucine treatment, HCT15 cells were incubated with 100 mM cycloleucine (Sigma Aldrich, #A48105) for 3 hours prior to RNA extraction.

For actionomycin experiments, HCT116 cells were treated with actinomycin D (Sigma-Aldrich, #A9415) at a final concentration of 5 µg/ml for 3 h and 6 h for mRNA stability assay.

For XPO1 and NF-κB inhibition, XPO1 inhibitor leptomycin B (LMB; Apollo Scientific, Cheshire, UK, #BIL2101) and NF-κB inhibitor BAY-11-7082 (Sigma Aldrich #B5556-10MG) were used at a final concentration of 6 ng/ml and 10 uM for 24 h and 48 h respectively.

For PTG stimulations, 100.000 HCT116 cells were plated and incubated o/n at 37ºC. Next day cells were incubated with a low-dose of 30 µg/mL PT-Gliadin (PTG) and incubated for 48 h. Then treatment with PTG at a final concentration of 350 µg/mL was performed and after 24 h supernatants and cells were harvested for further RNA and protein analysis (Fig13).

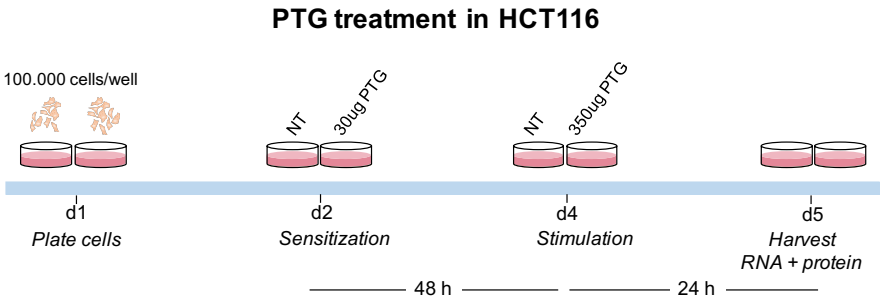

Figure 13. Schematic representation of the gliadin treatment set up *in vitro*. HCT116 cells were cultured for 48 h with a low-dose PTG concentration (30 µg/mL) and subsequently challenged with a higher dose of PTG (350 µg/ml) for 24 h.

3.1.4. Mouse models

For *in vivo* PTG exposure experiments, C57BL/6 mice, purchased from Janvier Labs, France, were used as wild type controls. Briefly, breeders were maintained on GFD (Altromin #C1074) for at least 4 weeks, and experiments were performed using their progeny.

For *in vivo* PTG exposure experiments in CD-risk model, specific pathogen free mice transgenic for HLA-DQ2 (human haplotype DR3-DQ2) with mouse $CD4^+$ cells exclusively, originally generated at the University of Melbourne (de Kauwe et al., 2009), were bred at McMaster University's Central Animal Facility on a gluten-free

diet (Teklad, Harlan Laboratories, Indianapolis, IN) for at least 2 generations. Local animal ethics approval was obtained.

For the study of YTHDF1 reader in our pathway, *Ythdf1* KO mice were received from Dr. He's lab (D. Han et al., 2019) and sacrificed at 4 weeks of age. Tissue sections of the duodenum from *Ythdf1* KO mice were processed for RNA and protein extraction.

3.1.4.1. Treatments

In *in vivo* PTG experiments, C57BL/6 mice were orally sensitized at 4 weeks of age using CT and PTG (500 µg PTG + 25µg CT) once a week for 3 weeks (Enzo Life Sciences, #BML-G117-000). Control mice received CT alone. Control and PTG-treated mice were housed in different cages to avoid PTG exposure through feces in control mice. After the last gavage the mice were sacrificed, and sections of the duodenum processed for RNA and protein extraction (Fig14). The Animal Experimentation Ethics Committee of the University of Barcelona (CEEA-UB) approved all the procedures with mice. Permits for procedure were obtained from the Government of Catalonia, according to European Directive 2010/63/EU.

For the CD-risk model, one group of HLA-DQ2 mice was gavaged orally using 25µg cholera toxin (CT) (Sigma Aldrich) and 500 µg PTG once a week, for 3 weeks. Controls received CT alone. At sacrifice, duodenal sections were processed for RNA extraction.

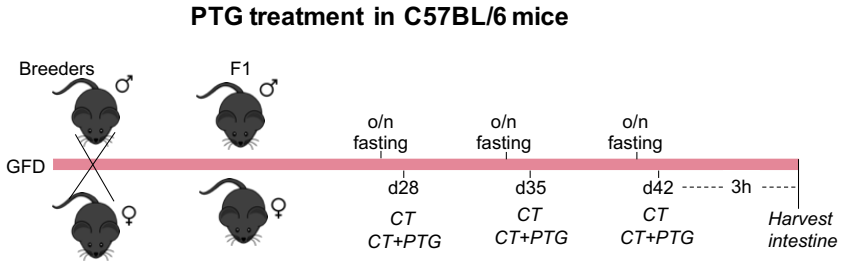

Figure 14. Schematic representation of the gliadin treatment set up *in vivo.* Mice were gavaged with PTG and CT (PTG) during 3 weeks, once a week. Control mice received only CT (NT).

For *ex vivo* stimulation experiments, epithelial cells isolated from duodenal fractions from WT and *Ythdf1* KO mice were divided into two wells and cultured in DMEM + FBS and P/S. PTG stimulation was further performed in freshly isolated cells using 250 µg/mL PTG for 4 h and non-stimulated cells were used as control.

3.2. METHODS

3.2.1. DNA, RNA and protein extraction

For human biopsies NucleoSpin TriPrep kit (Macherey-Nagel, Düren, Germany, #740966.50) was used following manufacturer instructions. Protein pellets were resuspended in RIPA buffer (150 mM NaCl, 1.0 % NP-40, 0.5 % NaDeoxycholate, 0.1 % SDS, 50 mM TrisHCl, 1 mM EDTA) with 1x protease inhibitor cocktail (PI) (Roche, Basel, Switzerland, #11836153001).

For mice samples Direct-zol RNA miniprep kit (Zymo research, Irvine, USA, #R2053) was used for RNA extraction. Proteins were lysed in RIPA buffer with 2x PI.

For HCT116, HCT15, HEK293FT and C26 cell lines RNA extraction was performed using NucleoSpin RNA Kit (Macherey Nagel, #740984.50) and cells were lysed in RIPA buffer.

Epithelial and immune subcellular fractions from human intestinal biopsies were obtained following the previously described protocol (Romero-Garmendia et al., 2018). Briefly, cells were mechanically separated from fresh biopsies by rotation-agitation in 10 ml of RPMI medium supplemented with 2% FBS, 1% DTT and 5 nM EDTA for 1 hour. The lamina propria and debris were removed by filtration through 30 µm pre-separation filters (cat. no. 130-041-407) and dead cell removal kit (cat. no. 130-090-101) was used to prepare a viable single-cell homogenous suspension. Live cells were labelled with CD45 magnetic microbeads (cat. no. 130-045-801) in the presence of FcR blocking reagent (cat. no. 130-059-901) to increase the

specificity of antibody labelling. The antibody-labelled cell-suspension was applied to a magnetic separation column (cat. no. 130-042-201) and unlabelled CD45- cells (mainly the epithelial CD326+ fraction) were collected with the flow-through, while CD45+ cells were recovered after removing the column from the magnet.

3.2.2. Gene expression analyses

500-1000 ng of RNA were used for the retrotranscription reaction using iScript cDNA Synthesis Kit (BioRad, CA, USA, #1708890). Expression values were determined by qPCR using Taqman Gene Expression Assays (Thermofisher, Waltham, MA) or by qPCR using Sybr Green (iTaq SYBR Green Supermix, Bio-Rad, #1725124) and specific primers. *HPRT* gene was used as endogenous control both in human and murine samples. Reactions were run in a BioRad CFX384 and melting curves were analyzed to ensure the amplification of a single product. All qPCR measurements were performed in duplicates and expression levels were analyzed using the $2^{-\Delta\Delta Ct}$ method. All Taqman Gene expression Assays and primers are listed in Table 3 and Table 4.

IL8 expression in complete human intestinal biopsies, as well as in epithelial and immune fractions from non-celiac controls and active disease patients was analyzed using a previously performed RNAseq from our group (Fernandez-Jimenez et al., 2019).

Table 3. List of used qPCR primers.

Gene	Primer Sequence
XPO1 (5'UTR)	Fw: TGTTCCAGTCTTTGCTGCTG Rv: AAGGCTCGCCTAAACTTTCC
METTL3	Fw: TCGAGAGCGAAATTTTTCAAC Rv: GGAGATAGAGAGCCTTCTGAACC
YTHDF1	Fw: ACCTGTCCAGCTATTACCCG Rv: TGGTGAGGTATGGAATCGGAG
HPRT	Fw: ACCAGTCAACAGGGGACATAA Rv: CTTCGTGGGGTCCTTTTCACC
TUG1	Fw: ATTCCACGACCATGGTTGTC Rv: ATTCACCACCAACCACACAG
SOCS1	Fw: AGACCCCTTCTCACCTCTTG Rv: AGTTAAGCTGCTACAACAACCAG
IL8	Fw: ACTGAGAGTGATTGAGAGTGGAC Rv: AACCCTCTGCACCCAGTTTTC
5'UTR Xpo1	Fw: GGTGGGAAAACTGTGAAACCC Rv: ACTGCTTCTTCCTTCCTTGTCC
Ythdf1-/-	Fw: CCTGCATTCTCAGCATGG Rv: GCTCCAGACTGTTCATCC
Hprt	Fw: CTGGTGAAAAGGACCTCTCGAAG Rv: CCAGTTTCACTAATGACACAAACG
Mip2a	Fw: CCAACCACCAGGCTACAGG Rv: GCGTCACACTCAAGCTCTG
Cxcl1	Fw: CTGGGATTCACCTCAAGAACATC Rv: CAGGGTCAAGGCAAGCCTC

Table 4. List of used qPCR assays.

Gene	Assay ID
XPO1	C__16006954_10
MALAT1	Hs00273907_s1
RPLPO	Hs99999902_m1
Mettl3	Mm01316319_m1
Ythdf1	Mm00620538_m1
Rplpo	Mm00725448_s1

3.2.3. SNP genotyping

Genotyping of the SNP rs3087898 was performed in DNA samples extracted from human biopsies using a custom rhAmp SNP Assay (IDT, Newark, NJ, USA) following the manufacturer's instructions.

3.2.4. Bioinformatic packages

3.2.4.1. RNAfold

RNAfold web server available at Vienna RNA web services (Hofacker, 2003) was used to predict the secondary structure of the allele specific *XPO1* 5'UTRs. The RNAfold web server predicts secondary structures of single stranded RNA sequences up to 7,500 nt.

3.2.4.2. MeT-DB V2.0

MeT-DB V2.0 m^6A database (H. Liu et al., 2018) was used to assess the existence of m^6A peaks in the 5'UTR of *XPO1*. MeT-DB V2.0 records predicted transcriptome-wide m^6A peaks and single-base m^6A sites from a significantly expanded collection of Methylated RNA Immunoprecipitation Sequencing (MeRIP-Seq) samples. It provides a genome browser to help visualize the m^6A sites from different studies. The user can search by genes or genomic location to visualize the relationship of m^6A sites from different studies.

3.2.4.3. miCLIP data from GEO

m^6A individual-nucleotide-resolution cross-linking and immunoprecipitation (miCLIP) data of HCT116 cells was downloaded from GEO repository (GSE128699). Sequence runs SRR8767363 and SRR8767364, corresponding to the m^6A mapping (mCLIP) results of wild-type HCT116 cells deposited in GEO (https://www.ncbi.nlm.nih.gov/geo) experiments GSM3682895 and GSM3682896, respectively, were obtained from the Sequence Read Archive (https://www.ncbi.nlm.nih.gov/sra) and reads were aligned against the *XPO1* 5'UTR sequence using NCBI Nucleotide Blast (https://blast.ncbi.nlm.nih.gov). Alignments were downloaded as plain text files, and the number of total matches and mismatches in each position were counted using MS Excel.

3.2.5. m^6A detection methods

3.2.5.1. Dot Blot

300 ng of RNA were crosslinked into a nitrocellulose membrane using UV. Membrane was blocked using 5 % milk in 0.1 % PBST (0.1 % Tween in PBS). Membrane was incubated overnight with a m^6A antibody (1:200) (Abcam, Cambridge, UK, #ab151230) at 4ºC. After washing in 0.1 % PBST, membranes were incubated with a secondary HRP-conjugated anti-rabbit antibody (1:10000) (Santa Cruz Biotechnology, #sc-2357) and the membrane was developed using Clarity Max ECL Substrate (BioRad, #1705062).

3.2.5.2. m^6A RNA immunoprecipitation

For cell lines, 4 µg of precleared RNA per sample were fragmented with RNA fragmentation buffer (100 mM Tris, 2 mM $MgCl_2$) for 3 min at 95ºC and placed on ice immediately after heating. For epithelial and immune fractions isolated from human intestinal biopsies a pool of 18 human biopsy fractions was used for a total of 2 µg RNA per fraction. 10 % of RNA was kept as input. 1 µg of m^6A antibody (Abcam, #ab151230) and control antibody (IgG, Santa Cruz Biotechnologies, Dallas, USA, #sc-2025) were coupled to agarose A beads (GE Healthcare, Chicago, USA) in a rotation wheel for 1 h at 4ºC. After incubation, beads were washed twice in reaction buffer (150 mM NaCl, 10 mM Tris-HCl, 0.1 % NP-40). RNA was added to the antibody-coupled beads and incubated for 3 hours at 4ºC in a rotating wheel. Subsequently, beads were washed 2X in reaction buffer, 2X in low salt buffer (50 mM NaCl, 10 mM TrisHCl and 0.1 % NP-40) and 2X in high salt buffer (500 mM NaCl, 10 mM TrisHCl and 0.1 % NP-40). After the last wash, beads were resuspended in Lysis buffer and RNA was extracted using the PureLink RNA extraction kit (Invitrogen, Carlsbad, USA, #12183016). In human intestinal HCT116 cell line *SOCS1* and *HPRT* were used as positive and negative controls respectively. In murine intestinal cell line C26 *Hprt* and *Rplp0* were used as positive and negative controls respectively.

3.2.5.3. m^{6}A RT-qPCR

m^{6}A methylation quantification was assessed by a new simple and cost-effective RT-qPCR method (A. Castellanos-Rubio et al., 2019; Olazagoitia-Garmendia & Castellanos-Rubio, 2021).

Primers used for retrotranscription (RT) were design considering specific conditions (Fig15.A). A reverse positive (+) primer to measure the relative methylation of the candidate methylated Adenosine (m^{6}A) within a m^{6}A motif (DR-**A**-CH) was first designed. Last nucleotide of the 3' end of primer had to be adjacent to the candidate m^{6}A. Then a reverse negative (-) primer located in a closeby A (not within a motif), and that did not overlap with the (+) primer covered region, was designed. Last nucleotide of the 3' end of primer need to be adjacent to the non-methylated A.

For the qPCR primer design, we took advantage of the lower retrotranscription ability of BstI enzyme, as this will result in shorter cDNA products. For this reason, the closer the qPCR primers were located from the RT primers the better.

For the m^{6}A-retrotranscription reaction, 75–150 ng of RNA, 100 nM of each primer, 50 µM dNTPs and 0.1U of BstI (NEB) or 0.8U of MRT (ThermoScientific) were used. The cycling conditions were as follows: 50 °C -15 min, 85 °C-3 min, 4°-∞.

For the PCR, 1 µl of the RT reaction was amplified using Dream Taq polymerase (ThermoScientific) and 100 nM of each primer. Cycling conditions were as follows: 95 °C-3min, 40 cycles x (95 °C-30sg, 60 °C- 30sg, 72 °C-30sg), 4 °C-∞.

For the qPCR, 1.5 µl of the retrotranscription reaction was used together with 100 nM of each primer and 2X iTaq SYBR green (BioRad). Reactions were run in an Illumina Eco Real Time System and melting curves were analyzed to ensure the amplification of a single product (Fig15.B).

For data analysis the difference of Cts between the two enzymes using primer (+) was calculated:

Delta (+) = Ct BstI (+) - Ct MRT (+).

Then the difference of Cts between the two enzymes using primer (-) was calculated:

Delta (-) = Ct BstI (-) - Ct MRT (-).

If Delta (+) > Delta (-) the candidate m^{6}A was considered as methylated, while if Delta (+) ≤ Delta (-) the candidate m^{6}A was considered as non-methylated.

To calculate relative m^{6}A levels $2^{-((Ct\ Bst\ (-)\ -\ Ct\ MRT\ (-))/(Ct\ Bst\ (+)\ -\ Ct\ MRT\ (+))}$ formula was used; where values above 0.5 were considered as positive for methylation and below 0.5 as negative for methylation.

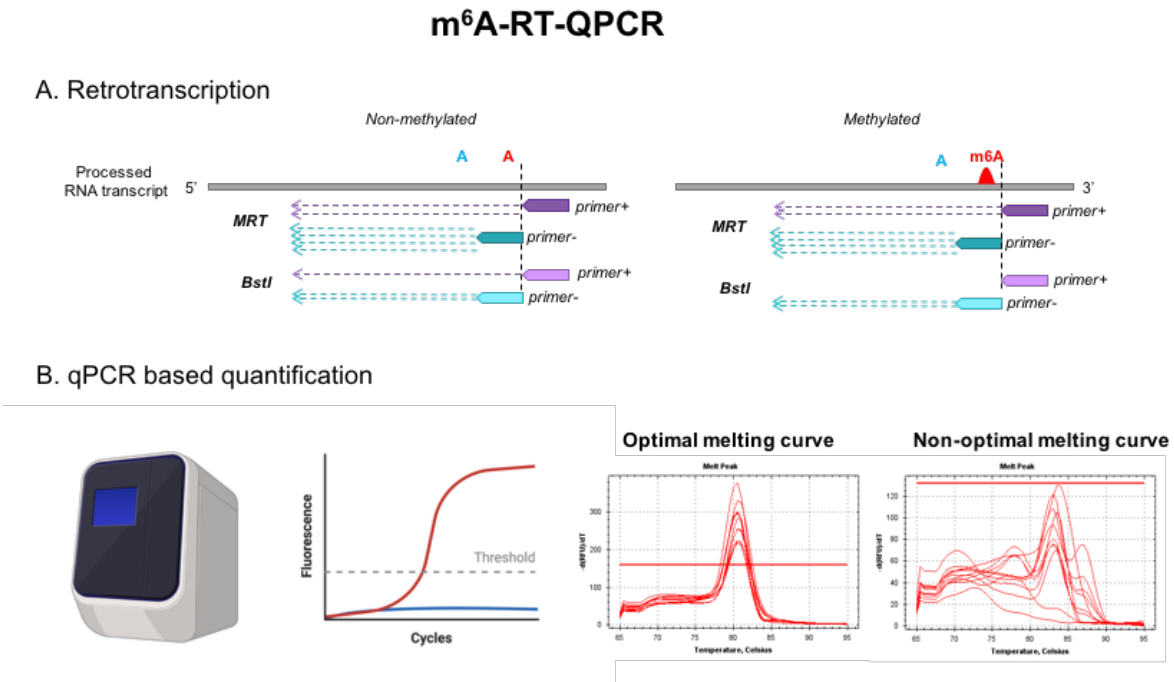

Figure 15. Relative quantification of residue specific m^{6}A RNA methylation using m^{6}A-RT-QPCR, modified from (Olazagoitia-Garmendia & Castellanos-Rubio, 2021).

RT-qPCR based method was also used for the confirmation of residue specific methylation of *XPO1* 5'UTR in HCT116 cell line. (+) primers for the 3 m^{6}A motifs together with a (-) primer, all located in the *XPO1* 5'UTR, were designed. *TUG1* and *HPRT* were used as positive and negative controls respectively. The sequence of

the primers used is in table 5.

Table 5. Primer sequences for the *TUG1* positive and *HPRT* negative controls and *XPO1* target gene.

Primer name	Primer sequence
HPRT+	CCTCCTACAACAAACTTGTCTGGAATT
HPRT-	CTTCGTGGGGTCCTTTTCACC
HPRTF	ACCAGTCAACAGGGGACATAA
TUG1+	TTCCAGTGAGCCCGCTTGCTAAAAG
TUG1-	ATTCACCACCAACCACACAGCC
TUG1F	ATTCCACGACCATGGTTGTC
XPO1.1+	ACAGGCAGCAGCAGAAGCGGCAGGAGTAGG
XPO1.2+	AGGGAAGGGGGAGGGAACGGGGTCAAG
XPO1.3+	GGGGAGACGCTCTGCTGCCAGTTGCAG
XPO1-	AAGGCTCGCCTAAACTTTCC
XPO1F	AAGGCTCGCCTAAACTTTCC

3.2.5.4. m^{6}A ELISA

RNA from HCT116 cells or from intestinal samples of non-celiac controls, active celiac disease patients and celiac disease patients in a gluten free diet were collected for determination of m^{6}A levels using a commercially available m^{6}A ELISA kit (Epigentek, NY, USA, # P-9005-96).

3.2.6. Protein quantification methods

3.2.6.1. Western Blot

The cells were lysed in RIPA buffer (150 mM NaCl, 1.0 % NP-40, 0.5 % NaDeoxycholate, 0.1 % SDS, 50 mM TrisHCl, 1 mM EDTA) for protein extraction. Laemmli buffer (62 mM Tris-HCl, 100 mM dithiothreitol (DTT), 10 % glycerol, 2 % SDS, 0.2 mg/ml bromophenol blue, 5 % 2-mercaptoethanol) was added followed by heat denaturation. Proteins were migrated on 10 % SDS-PAGE gels. Following electrophoresis, proteins were transferred into nitrocellulose membranes using a Transblot-Turbo Transfer System (Biorad) and blocked in 5 % non-fatty milk diluted in TBST (20 mM Tris, 150 mM NaCl and 0.1 % Tween 20) at room temperature for

1 h. The membranes were incubated overnight at 4ºC with primary antibodies diluted 1:1000 -1:5000 in TBST. Immunoreactive bands were revealed using the Clarity Max ECL Substrate (BioRad, #1705062) after incubation with a horseradish peroxidase-conjugated anti-mouse (1:10000 dilution in 2.5 % non-fatty milk) or anti-rabbit (1:10000 dilution in 2.5 % non-fatty milk) secondary antibody for 1 h at room temperature. The immunoreactive bands were detected using a Bio-Rad Molecular Imager ChemiDoc XRS (BioRad) and quantified using the ImageJ software.

The following antibodies were used for Western Blotting: XPO1 (Cell Signalling, Leiden, The Netherlands, #46249S), METTL3 (Abcam, #195352), YTHDF1 (Abcam, #220162), YTHDF1 (Proteintech, Rosemont, USA, #17479-1-AP) ß-ACTIN (Santa Cruz Biotechnologies, #sc47778), a-TUBULIN (Sigma-Aldrich, #T9026 and Cell Signalling, #2144S), HSP90 (Cell Signaling; #4874), H3 (Abcam; #ab1791), p50 (Abcam, #ab7971),GAPDH (Novus, St Louis, MI, USA, #ND300-221), GAPDH HRP (Santa Cruz Biotechnologies, #sc-166574 HRP).

3.2.6.2. ELISA

Protein extracts from human biopsies or cell culture supernatants were collected for determination of human XPO1 protein levels (Cloud-Clone Corp, Houston, USA, #SEC258Hu) and secreted IL8 chemokine levels. Quantifications were done using commercially available ELISA kit (R&D Systems, Abingdon, UK; #D8000C) following the manufacturer's instructions.

3.2.7. *In vitro* transcription

TUG1 amplicon was amplified using a forward primer with a T7 sequence. After purification, 100 ng of DNA were used for *in vitro* transcription using T7 polymerase and rNTPs from Takara (Clonthech) following manufacturer's instructions. The IVT product was purified using the Direct-zol miniprep kit (Zymo Research).

3.2.8. Plasmid construction

XPO1 5'UTR was amplified from human cDNAs containing T or C allele for rs3087898 SNP and cloned into a modified pIS0 vector (Addgene, #12178) using NcoI restriction sites.

pLKO.1-TRC Cloning vector (Addgene, #10878) was used for the construction of plKO.1-shMETTL3 and plKO.1-shYTHDF1 plasmids. Following Addgene's protocol shRNAs were designed to knock down human *METTL3* (AAGGAACAATCCATTGTTCTCGAGAACAATGGATTGTTCCTT) and *YTHDF1* (AACGGCAGAGTCGAAACAAACTCGAGTTTGTTTCGACTCTGCCGTTC).

For allele-specific overexpression experiments, mammalian expression plasmids containing XPO1 5´UTR sequence followed by the cDNA encoding human full-length XPO1 protein (1071 amino acids) were generated. Two different constructs, named *5´UTR-XPO1*T* and *5´UTR-XPO1*C*, were generated, carrying the rs3087898 T or C allele, respectively. To generate these plasmids, a partial *XPO1* cDNA fragment, from nucleotide 187 to the stop codon, was first amplified by PCR using a previously described pEYFP-CRM1 plasmid (Rodríguez & Henderson, 2000) as template. This PCR product was cloned into the pEYFP-C1 vector (Clontech) as a SalI/BamHI fragment. Next, the EYFP-coding sequence from the resulting plasmid was excised as a NheI/SalI fragment, and replaced by a DNA sequence containing *XPO1* 5´UTR fused to the first 187 nt of *XPO1* cDNA, which was generated using a two-step overlapping PCR approach.

3.2.9. Luciferase Assay

150000 cells/well were seeded and transfection was performed with X-TremeGENE HP DNA transfection reagent (Sigma-Aldrich, #6366546001) using 250 ng per plasmid during 48 h. Empty vector pIS0 was used as control. Dual-Luciferase Reporter Assay System (Promega, Madison, USA, #E1910) was used following manufacturer's protocol.

3.2.10. Overexpression

For METTL3 overexpression experiments 250 ng plasmid from Addgene (#53739) were used. 150000 cells/well were seeded and transfected using X-TremeGENE HP DNA transfection reagent (Sigma-Aldrich, #6366546001), cells were harvested 48 h post-transfection.

For XPO1 overexpression, 1 µg of *5´UTR-XPO1*T* or *5´UTR-XPO1*C* plasmids were used. 100000 cells/well were seeded and transfection was performed with X-TremeGENE HP DNA transfection reagent (Sigma-Aldrich, #6366546001) for 48 h.

3.2.11. Silencing experiments

Viral particles were produced in HEK293FT cells transfected with 1 µg pLKO.1 shRNA plasmid, 750 ng psPAX2 packaging plasmid (Addgene, #12260) and 250 ng pMD2.G envelope plasmid (Addgene, #12259) using X-TremeGENE HP DNA transfection reagent (Sigma-Aldrich, #6366244001) in DMEM without antibiotics and cells were incubated o/n at 37ºC. Transfection media was replaced with fresh complete DMEM and viral particle containing media was harvested twice; after 24 h and after 48 h. Collected media was centrifuged and viral particles were stored as working aliquots at -80ºC. HCT116 cells were infected with sh-METTL3, sh-YTHDF1 or plKO.1 as negative control and selection was performed by puromycin resistance (2 µg/mL).

For YTHDF1 silencing in PTG stimulated cells, 30 nM of 2 different siRNAs against YTHDF1 (IDT, # hs.Ri.YTHDF1.13.1 and hs.Ri.YTHDF1.13.2) or negative control siRNA (IDT # 51-01-14-01) were transfected into cells sensitized with PTG and 16 h prior to 350 µg/mL PTG treatment using Lipofectamine RNAimax reagent (Thermo Fisher Scientific).

3.2.12. Cellular fractionation

For the quantification of RNA amounts in nuclear and cytoplasmic compartments, nuclei were isolated using C1 lysis buffer (1.28 M sucrose, 40 mM Tris-HCl pH 7.5, 20 mM $MgCl_2$, 4 % Triton X-100). The amounts of *XPO1-T/C*, *MALAT1* (nuclear

control) and *RPLPO* (cytoplasmic control) mRNAs were measured by q-PCR and compared to the total amount of those RNAs in the whole cell lysate.

For the quantification of protein amounts in nuclear and cytoplasmic compartments, cells were resuspended in NARA buffer (10 mM HEPES pH 7,9, 10 mM KCl, 0.1 mM EDTA) with proteinase inhibitors (PI) and incubated on ice for 10 minutes. After adding NP-40 to final concentration 0.05 %, lysates were incubated on ice for 5 minutes and centrifuged at 400 g for 2 minutes. The supernatant was the cytosolic fraction. Pellet was washed 3 times with NARA buffer and resuspended in NARC buffer (20 mM HEPES, 400 mM NaCl, 1 mM EDTA) + PI, shaken at 4ºC for 30 minutes and centrifuged at 16000 g for 10 minutes. The supernatant was the nuclear extract.

3.2.13. RNA immunoprecipitation assay (RIP)

For RIP experiments, cells were lysed in RIP buffer (150 mM KCl, 25 mM Tris, 0.5 mM DTT, 0.5 % NP-40, PI), kept on ice for 15 minutes and homogenized using a syringe. Lysates were pre-cleared with protein A-Agarose beads (GE Healthcare, Chicago, USA) for 1 h in a wheel shaker at 4ºC. A-Agarose beads were blocked with 20 % BSA and mixed with pre-cleared lysates and 1 µl of anti-IgG antibody (negative control; Santa Cruz Biotechnologies, #sc-2025) or antibody of interest (METTL3, Abcam or YTHDF1, Abcam). After overnight incubation in a wheel shaker at 4ºC, beads were washed three times with RIP buffer, three times with low salt buffer (50 mM NaCl, 10 mM Tris-HCl, 0.1 % NP-40) and three times with high salt buffer (500 mM NaCl, 10 mM Tris-HCl, 0.1 % NP-40). After the washes, 70 % of beads were resuspended in RNA extraction buffer and 30 % was used for WB. *SOCS1* and *HPRT* were used as positive and negative controls respectively.

3.2.14. Gel shift assay

Nuclear lysates were prepared from HCT116 cells transfected with an empty vector or overexpressing *XPO1*T* form by incubating them on ice with C1 lysis buffer for 15 min and collecting nuclei by centrifugation for 15 min at 700 g. Nuclei were extracted

with EMSA lysis buffer (50 mM KCl, 25 nM HEPES, 125 uM DTT and 0.5 % NP-40). Electrophoretic mobility shift assays were performed by incubating 40 µg of nuclear extracts in 50 µl reaction volume in EMSA binding buffer (50 µg BSA, 20 mM Tris, 50 mM KCl, 0.05 % NP-40, 5 % glycerol, 10 mM b-mercaptoethanol,1 mM EDTA and 0.1 M DTT) with 60 nM of the fluorescently labeled oligos containing the NF-κB consensus sequence in the *IL8* promoter as described in LASAGNA TFBS web server (Lee & Huang, 2013) for 30 min at room temperature. For competition assay 10x of the unlabeled oligos were added to the reaction. Samples were then loaded on a 1 % non-denaturing agarose gel and run at 60 V for 2 h.

3.2.15. Statistical analysis

The data are represented as the mean and standard error of the mean of at least three biological replicates. Mean comparisons were performed by Student's t-test, Mann Whitney test or ANOVA test. Correlation analyses were done using Pearson correlation. The statistically significance level was set at $p< 0.1$.

4.RESULTS

4.1. RESIDUE SPECIFIC m^{6}A METHYLATION QUANTIFICATION BY A NOVEL RT-qPCR METHOD

As it has been mentioned before, the available methods to quantify m^{6}A methylation are tedious and/or require high-throughput sequencing not affordable for all laboratories. In this line, our group described a new protocol where site-specific m^{6}A quantification is achieved by taking advantage of the diminished capacity of BstI enzyme to retrotranscribe methylated RNAs. Retrotranscription is followed by an accurate, quantitative PCR (qPCR) (A. Castellanos-Rubio et al., 2019; Olazagoitia-Garmendia & Castellanos-Rubio, 2021).

We have shown that this method is useful to relatively quantify m^{6}A methylation levels in RNA from cell line RNA extracts (Fig16) as well as from human derived samples (Fig18.B). Using our m^{6}A-RT-qPCR method, we confirmed *TUG1* positive values (above 0.5) together with *HPRT* negative values (below 0.5) in various cell lines. Additionally, we were able to confirm the methylation of several genes that had been previously described to be methylated by other techniques (Fig16.A-C), showing the cell-type specificity of this modification in some of the genes. Indeed, using RNA from HEK293FT cells, because it was the material used in the immunoprecipitation experiments, we compared our results with previously published m^{6}A immunoprecipitation data of the same regions available at the Met-DB v2.0 database (H. Liu et al., 2018). Eight out of the ten gene regions analyzed by relative m^{6}A RT-qPCR method presented concordant results in terms of methylation status (methylated or non-methylated) when compared with those available in the database (Fig16.D), confirming the high efficiency of this method.

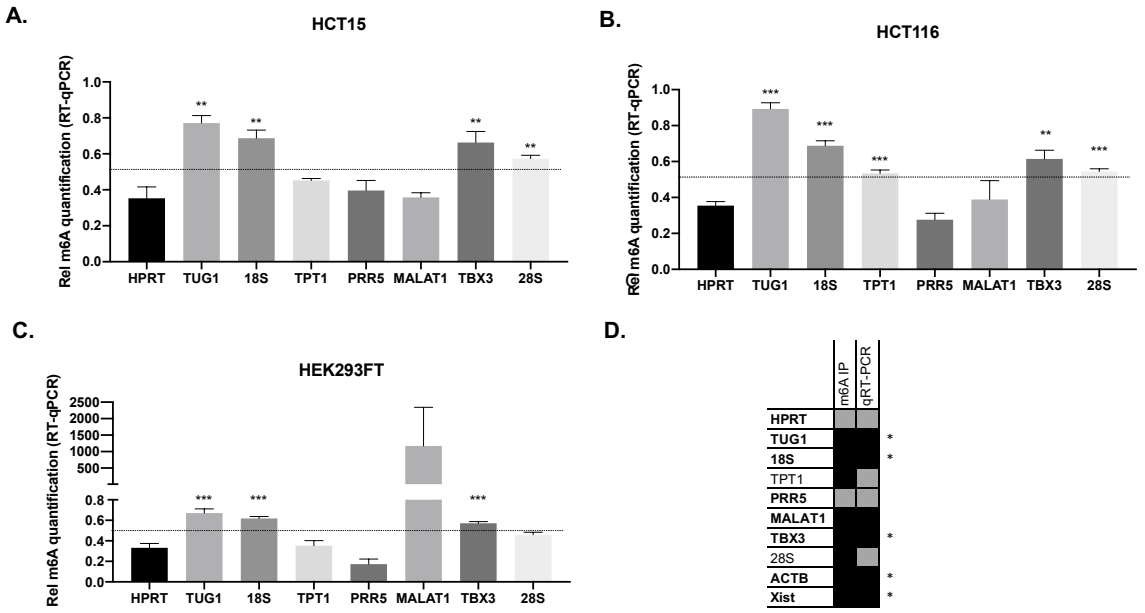

Figure 16. Relative quantification of residue specific m^{6}A RNA methylation using m^{6}A-RT-qPCR in **A)** HCT15, **B)** HCT116 and **C)** HEK293FT cell lines. n=3-4, values are mean ± SEM (**p<0.01, ***p<0.001 according to Student's t-test relative to negative control HPRT). **D)** Comparison of m^{6}A IP data from the Met-DBv2.0 database and relative m^{6}A-RT-qPCR results in different genes using the HEK293FT cell line. Genes in bold showed concordant results using both methods. Grey boxes represent negative (non-methylated) and black boxes represent positive (methylated) results. n=4, values are mean ± SEM (*p<0.05 according to Student's t-test relative to negative control HPRT).

We also confirmed that our method is useful to quantitatively measure m^{6}A methylation levels. When IVT *TUG1* RNA was mixed with HCT15 cell line lysate we observed that increasing the amount of unmethylated IVT *TUG1* in the sample led to an overall decrease in m^{6}A methylation (Fig17.A) as measured by m^{6}A dot blot. We further quantified the difference among these conditions using our m^{6}A-RT-qPCR method and showed that it is able to provide site-specific quantitative information on m^{6}A methylation level changes (Fig17.B).

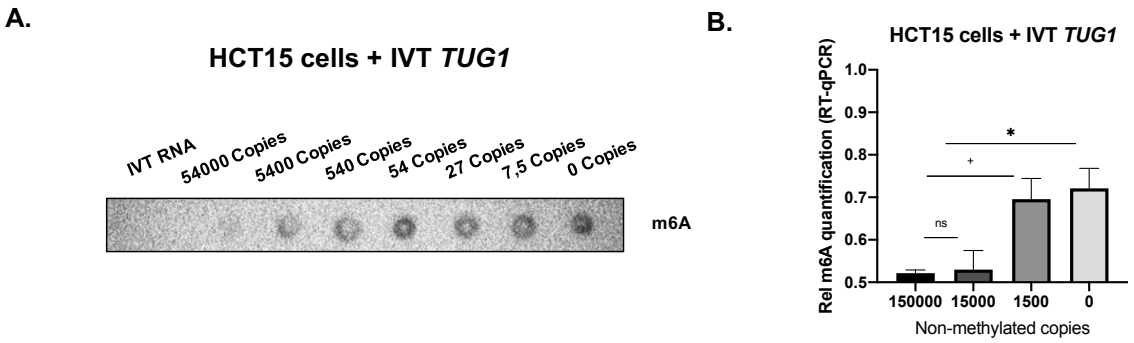

Figure 17. A) Total m^{6}A quantification by m^{6}A dot blot in basal RNA (0) and in RNA mixed with increasing amount of copies of *in vitro* transcribed non-methylated RNA. **B)** Relative m^{6}A quantification of *TUG1* motif in basal RNA (0) and in RNA mixed with increasing amount of copies (1500, 150000 and 1500000) of *in vitro* transcribed non-methylated RNA. n=3, values are mean ± SEM (*p<0.05 according to Student's t-test relative to 1500000 copies condition).

This method has been also shown to be useful to quantify relative m^{6}A changes in response to stimuli or at different disease stages (Fig18. A, B). HCT15 cells treated with cycloleucine (a chemical compound that removes m^{6}A methylation) showed reduced total m^{6}A methylation levels in an m^{6}A dot blot (Fig18. A left). In addition, using our m^{6}A-RT-qPCR method, the quantitative reduction of m^{6}A in *TUG1* could also be assessed (Fig18. A right).

Noteworthy, m^{6}A methylation changes in human intestinal biopsies from healthy controls and active celiac disease (CD) patients could also be quantified using the m^{6}A-RT-qPCR method described (Fig18.B). We were able to detect differences in RNA methylation levels between CD patients and non-celiac controls (18.B).

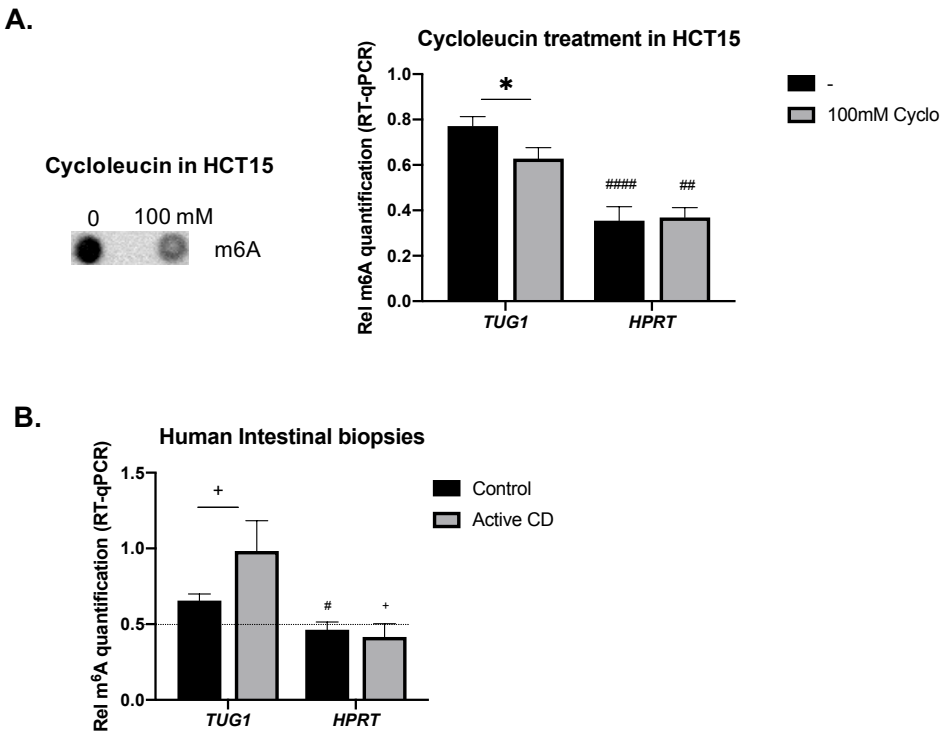

Figure 18. A) Representative m^{6}A RNA dot blot of basal and 100 mM cycloleucine treatment of 4 independent experiments (left). Relative quantification of the m^{6}A levels in the selected motifs of *TUG1* in RNA extracted from non-treated (−) and 100 mM cycloleucine treated cells. n=4, values are mean ± SEM (*p<0.05 according to Student's t-test. ##p<0.01, ####p<0.0001 according to Student's t-test relative to negative control HPRT) (right). **B)** Relative m^{6}A quantification of *TUG1* and *HPRT* motifs in intestinal biopsies of celiac patients (n = 8) and controls (n = 6), values are mean ± SEM (+p<0.1 according to Student's t-test. +p<0.1, #p<0.05 according to Student's t-test relative to negative control HPRT).

Thus, our results demonstrate that the newly developed m^{6}A-RT-qPCR method is an affordable and easy method useful to relatively quantify m^{6}A methylation sites in RNA samples from human tissues or cell cultures as well as changes in m^{6}A levels. Hence, we have provided a new technique that could help elucidate the implication of this RNA modification in diverse disorders.

4.2. m^{6}A RNA METHYLATION IN CD

Considering that m^{6}A methylation is involved in the development of various disorders, we aimed to quantify overall m^{6}A levels in small intestinal biopsies from control and CD individuals.

RNA was extracted from intestinal biopsies from controls (CTR), active celiac patients (CD) and celiac patients on GFD (GFD) and overall m^{6}A RNA methylation was measured. Biopsies in the active (newly diagnosed) CD group showed higher degree of methylation compared to control individuals (Fig19. A).

Higher expression of m^{6}A writer *METTL3* and *YTHDF1* m^{6}A reader was also observed in the active CD group compared to controls (Fig19. B,C). More interestingly, when gluten had been removed from the CD patients' diet (GFD), total m^{6}A levels as well as the expression of m^{6}A machinery genes reverted to normal values (Fig19. A-C).

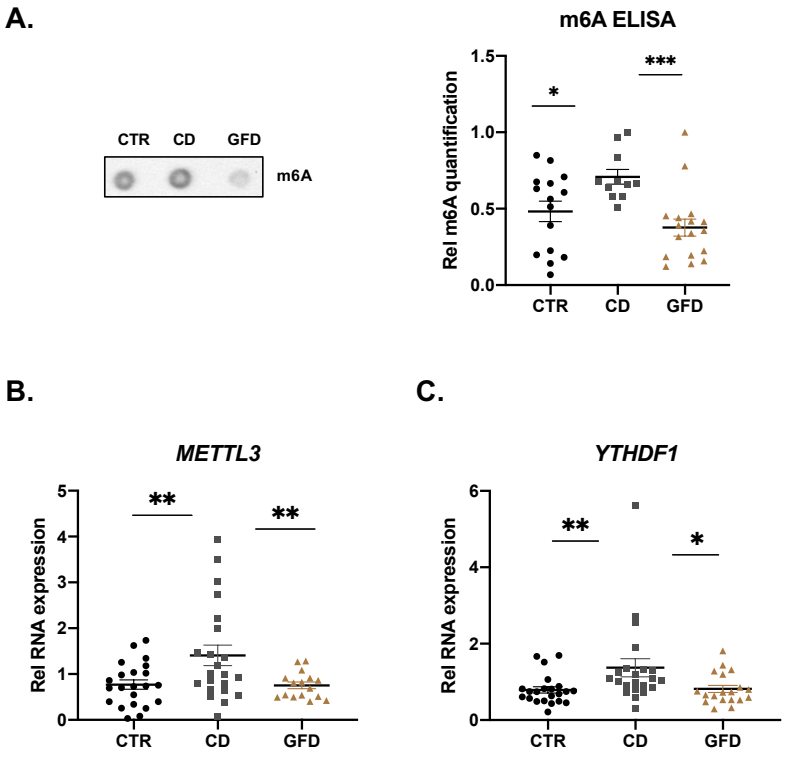

Figure 19. A) Total m^{6}A quantification by m^{6}A dot blot (left) and a commercial m^{6}A Elisa kit (right), n=15-17. (*p<0.05, ***p<0.001 according to an ANOVA test). The expression of **B)**

METTL3 and **C)** *YTHDF1* measured by RT-qPCR in RNA extracted from adult and pediatric individuals, n=6-16. (*p<0.05, **p<0.01, according to ANOVA test).

These results confirm that m^{6}A methylation is altered in CD patients and suggest that gluten exposure could enhance m^{6}A machinery expression, pointing to the involvement of this pathway in the acute response observed upon gluten ingestion in CD patients. Thus, we have discovered a previously undescribed pathway that could play a key role in CD development.

4.3. XPO1 AS A CANDIDATE: FUNCTIONAL CHARACTERIZATION IN THE CD INFLAMMATORY ENVIRONMENT

Considering that m^{6}A methylation is altered in CD patients, we wondered if non-coding, CD-associated SNPs could influence m^{6}A modification and hence contribute to the predisposition to develop CD. Here we present the functional study of the CD-associated Immunochip SNP rs3087898, which is located in the 5'UTR of protein-coding gene *XPO1* (Fig20.A). Vienna Package online tool (Hofacker, 2003) predicts a change in the secondary structure of the 5'UTR based on the SNP genotype (Fig20.B), with 3 m^{6}A motifs (GGACT) located near the SNP. This indicates that the SNP genotype and m^{6}A methylation may affect function of the *XPO1* gene and thus contribute to the risk to develop CD.

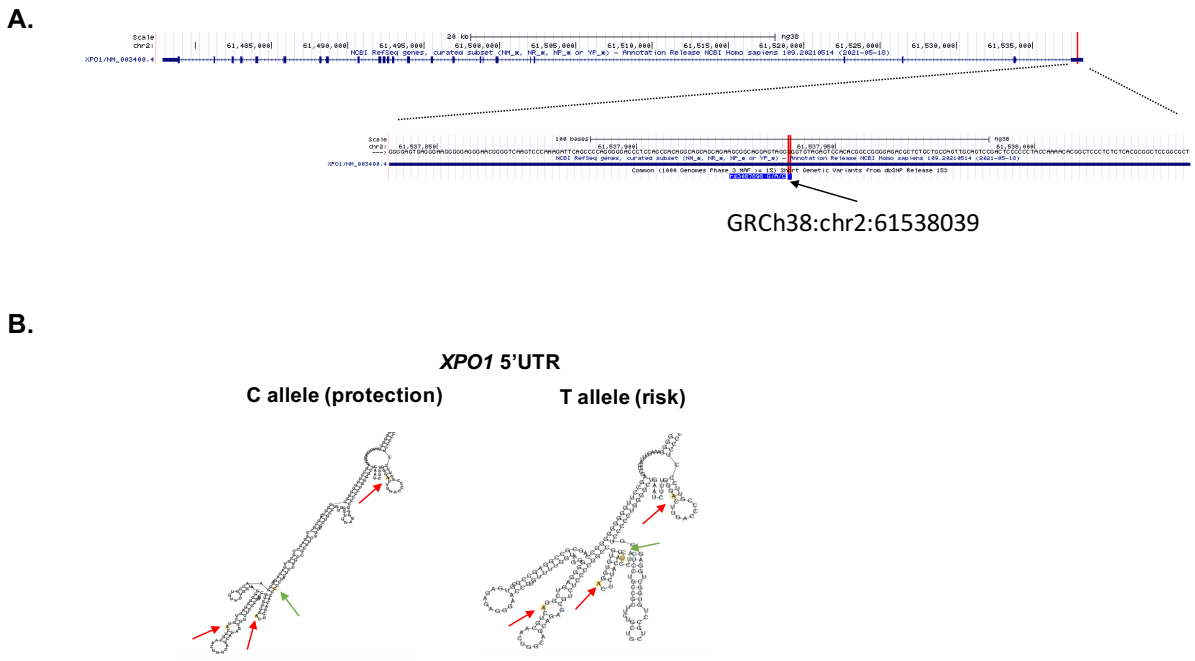

Figure 20. A) Chromosomal location of rs3087898 SNP in the 5'UTR of *XPO1* according to GRCH38. **B)** Zoomed secondary structure of each of the human 5'UTR *XPO1* forms as predicted by Vienna package. rs307898 SNP (green arrows) and putative m^6A methylated adenines (red arrows) are highlighted.

4.3.1. rs3087898 genotype effect in CD patients

To validate the involvement of SNP rs3087898 in CD patients in our cohort, small intestinal biopsies from celiac patients and non-celiac controls were used.

Genotyping of the human samples showed that although the expression levels of *XPO1* did not change significantly depending on the SNP genotype (Fig21.A), biopsies from individuals carrying the risk allele (rs3087898 genotypes CT and TT) presented higher amounts of XPO1 protein (Fig21.B). This result shows that the genotype of the CD-associated SNP affects XPO1 protein levels (protein Quantitative Trait Loci, pQTL), which in turn could increase predisposition to develop the disease (Minor Allele $Frequency_{controls}$0.41/Minor Allele $Frequency_{CD}$0.44) (Dubois et al., 2010).

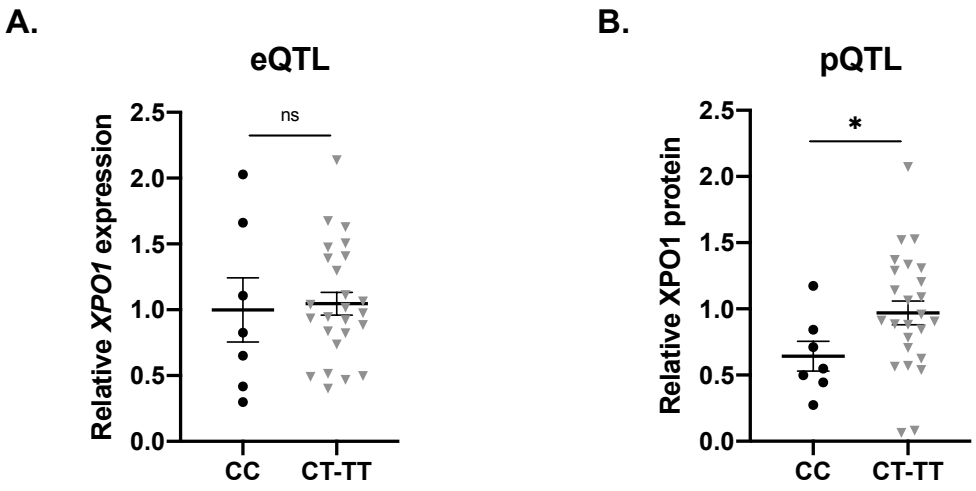

Figure 21. A) Expression quantitative trait loci (eQTL) of *XPO1* levels compared between individuals with the protection genotype (CC) and individuals harboring the risk allele (CT+TT) n=7-25. Values are means ± S.E.M. (ns: non-significant, according to a Mann Whitney test). **B)** Protein quantitative trait loci (pQTL) of XPO1 protein levels compared between individuals with the protection genotype (CC) and individuals harboring the risk allele (CT+TT), n=7-25. Values are mean ± SEM (*p<0.05 according to a Mann Whitney test).

4.3.2. RNA methylation and *XPO1* levels in CD patients

Having observed that total m^{6}A levels and m^{6}A machinery expression are altered in CD patients and that there are 3 m^{6}A motifs near the disease associated SNP, we next wanted to analyze the RNA methylation levels in XPO1.

The MeT-DB V2.0 m^{6}A database (H. Liu et al., 2018) revealed m^{6}A peaks in the human 5'UTR of *XPO1* (Fig22.A), suggesting that the motifs near the SNP can be methylated. m^{6}A methylation in the 5'UTR of *XPO1* was analyzed by m^{6}A RNA immunoprecipitation (meRIP) followed by RT-qPCR in immune (CD45+) and epithelial (CD326+) fractions from human intestinal biopsies. Only the RNA from the epithelial fractions of human duodenal biopsies appeared to be methylated, revealing that m^{6}A methylation could be influencing *XPO1* function specifically in epithelial cells (Fig22.B).

XPO1 mRNA and protein amounts were quantified in pediatric and adult patient biopsies from controls (CTR), active celiac disease patients (CD) and patients on gluten free diet (GFD) (Fig22. C, D). Higher expression of *XPO1* in the active CD group compared to controls was observed, and these levels reverted to normal values when patients were following a gluten free diet.

The results indicate that, as previously observed in m^{6}A, *METTL3* and *YTHDF1*, the induction of *XPO1* may be, at least in part, gluten-dependent. Moreover, the methylation of the 5'UTR of *XPO1* occurs mainly in epithelial cells, suggesting that this mechanism could be influencing *XPO1* levels in CD patients in a cell type-specific manner.

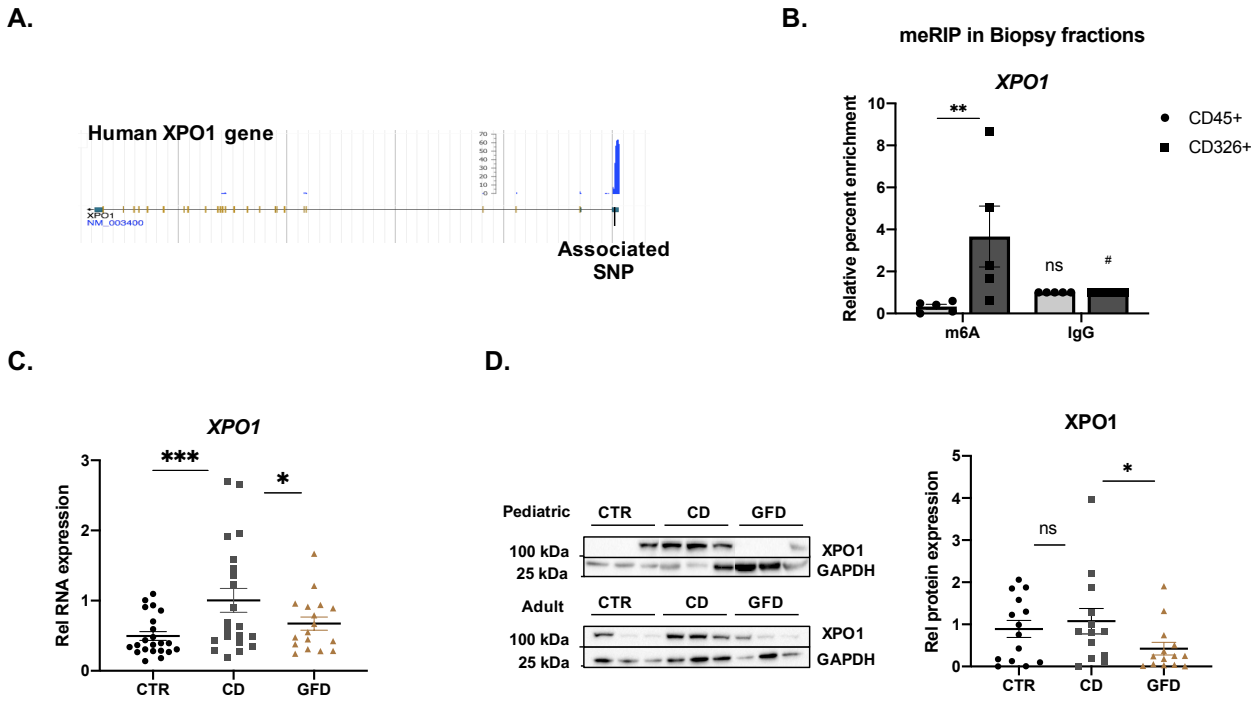

Figure 22. A) m^{6}A signals in the human *XPO1* gene retrieved from the Metdb v2 database. Blue peaks correspond to meRIP-seq reads, yellow and green boxes are exons and UTR's respectively. Location of the CD-associated SNP rs3087898 is marked. **B)** m^{6}A RNA immunoprecipitation (meRIP) followed by RT-qPCR in immune (CD45+) and epithelial (CD326+) fractions from human intestinal biopsies. n=pool of 18 individuals. (**p<0.01 according to ANOVA test. Enrichment relative to control IgG #p<0.05, ns: non-significant according to ANOVA test). **C)** The expression of *XPO1* measured by RT-qPCR in RNA extracted from adult and pediatric

individuals, n=6-16. (*p<0.05, ***p<0.001 according to ANOVA test). **D)** Representative immunoblot of 5-10 samples per group (left) and quantitative summary of immunoblot (right) for XPO1 in both pediatric and adult biopsies from CTR, CD and GFD, n=14-16. (*p<0.05, ns: non-significant according to ANOVA test).

Our results showed that the SNP genotype affects XPO1 protein levels and that XPO1 is increased in CD patients. We verified that the 5'UTR of *XPO1* is actually methylated in human intestinal RNA samples, more specifically in the epithelial cell fractions. Considering these results, further *in vitro* and *in vivo* studies were performed to functionally characterize the involvement of rs3087898 and m^6A methylation in *XPO1* levels and their effects on downstream inflammation.

4.3.3. Functional characterization of SNP rs3087898 and m^6A RNA methylation in *XPO1*

4.3.3.1. Effect of rs3087898 SNP and m^6A levels in XPO1 in vitro

4.3.3.1.1. HCT116 intestinal cell line

As we observed that the 5'UTR of *XPO1* is only methylated in human epithelial fractions, we decided that the most adequate *in vitro* model for this study was the HCT116 intestinal cell line, which is heterozygous for rs3087898 SNP.

Using online available m^6A individual-nucleotide-resolution cross-linking and immunoprecipitation (miCLIP) data from HCT116 cells (Van Tran et al., 2019) we confirmed that the three m^6A consensus motifs in the 5'UTR (Fig20.B) are actually methylated in these cells (Fig23.A). We further confirmed m^6A methylation in HCT116 using m^6A RNA immunoprecipitation (meRIP) followed by RT-qPCR of the 5'UTR of *XPO1* in this intestinal cell line (Fig23.B). Moreover, the previously described m^6A-RT-qPCR method was also used to verify that the three motifs are methylated (Fig23.C). In addition, taking advantage of the heterozygosity of the

HCT116 cell line for the CD-associated SNP, we found that the mRNA transcript carrying the CD-risk allele (*XPO1*T*) is more methylated than its alternative, protective form (*XPO1*C*) (Fig23.D).

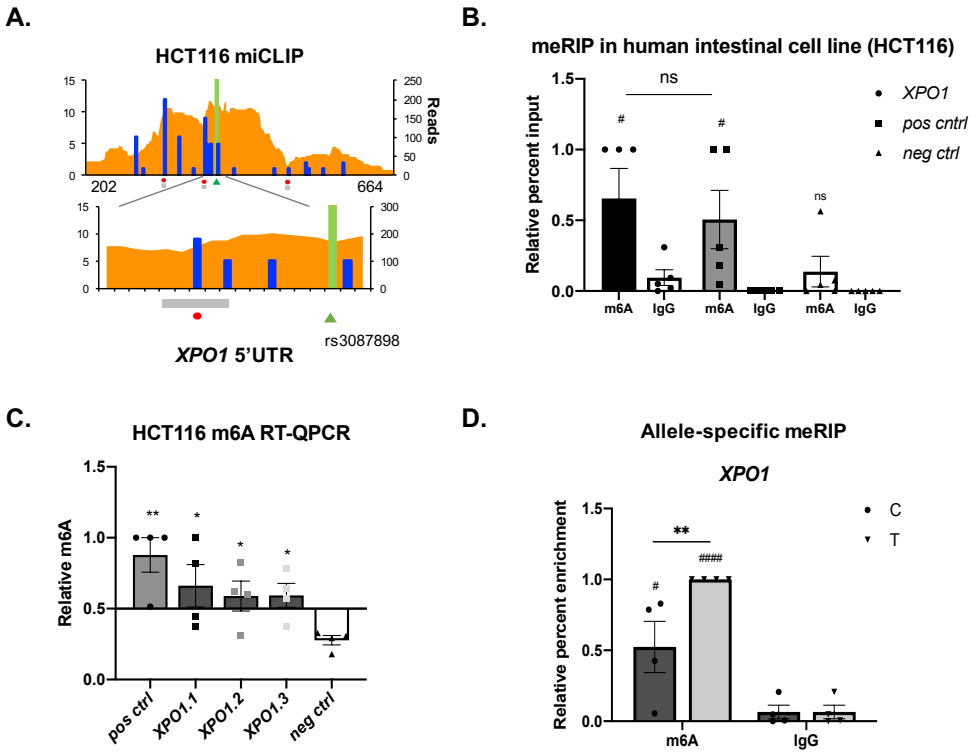

Figure 23. A) Quantitative representation of miCLIP reads (orange) and mutations (blue) in the 5'UTR of *XPO1* from HCT116 cells (heterozygous for rs3087898). Grey squares represent GGACT motifs, red dots represent methylated As and the green triangle and bars corresponds to the associated SNP. **B)** m^6A RNA immunoprecipitation (meRIP) followed by RT-qPCR of the 5'UTR of *XPO1* and positive and negative controls in HCT116 intestinal cell line, n=5. (****p<0.0001; ns: non-significant according to ANOVA test. Enrichment relative to control IgG #p<0.05, ###p<0.001, ####p<0.0001 according to ANOVA test). **C)** m^6A-RT-qPCR of the 3 m^6A motifs in the 5'UTR of *XPO1* and positive and negative controls in intestinal cells, n=4. Significance was calculated relative to the negative control. (*p<0.05,**p<0.01 according to a ANOVA test). **D)** Allele-specific m^6A levels in the 5'UTR of *XPO1* in HCT116 cells as assessed by meRIP-qPCR, n=4. (**p<0.01 according to ANOVA test. Enrichment relative to control IgG #p<0.05, ####p<0.0001 according to ANOVA test).

4.3.3.1.2. 5'UTR methylation of XPO1 and RNA metabolism

It is known m^{6}A methylation is involved in diverse RNA metabolic processes, so we wanted to elucidate the effects of this differential methylation on *XPO1* mRNA.

We did not observe any differences in mRNA cellular localization (Fig24.A) or stability (Fig24.B) when comparing the protective (*XPO1*C*) and risk (*XPO1*T*) mRNA forms. However, the analysis of translation efficiency using a luciferase reporter preceded by the 5'UTR of *XPO1,* showed higher luciferase activity in the presence of the T allele (Fig24.C), suggesting an implication of this SNP in the translation process. These results were confirmed in constructs with each of the 5'UTR forms upstream of the *XPO1* coding sequence, where we observed higher XPO1 protein production from the risk allele form (Fig24.D, E).

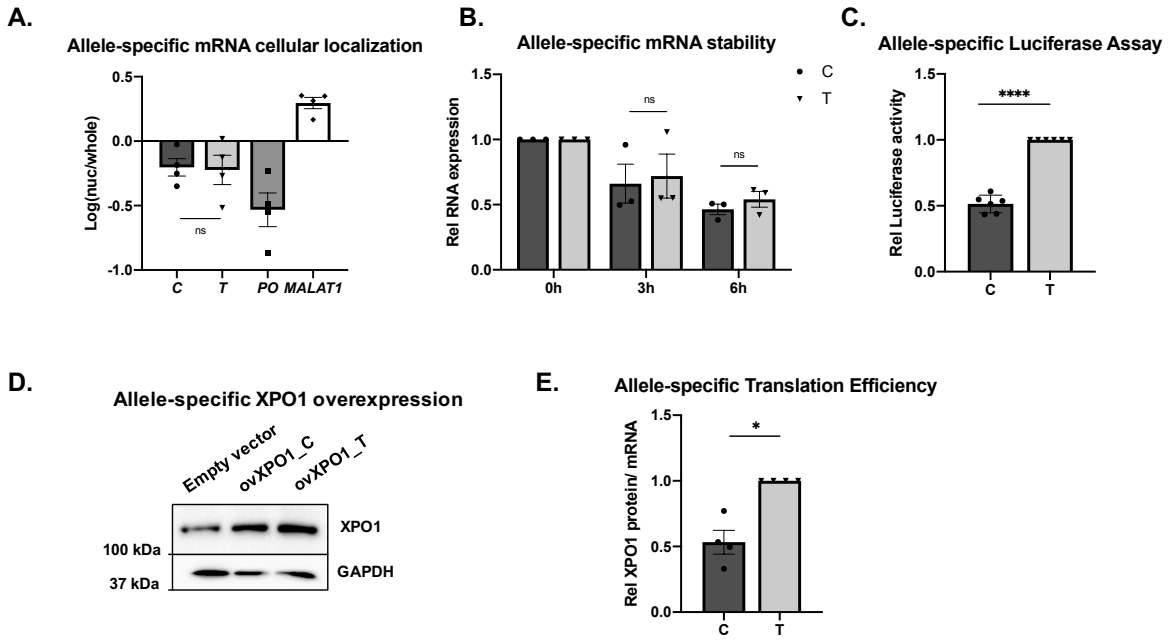

Figure 24. A) Cellular localization of both *XPO1* mRNA forms *XPO1*C* (C) and *XPO1*T* (T) and *PO* (cytoplasmic) and *MALAT1* (nuclear) controls, n=4. (ns: non-significant according to ANOVA test). **B)** mRNA stability of both *XPO1* mRNA forms *XPO1*C* (C) and *XPO1*T* (T) in cells treated with actinomycin D for 3 h and 6 h, n=3. (ns: non-significant according to ANOVA test). **C)** Translation efficiency of each allele of the 5'UTR of *XPO1* assessed by dual-reporter luciferase assay, n=6. (****p<0.0001 according to Student's t-test). Translation efficiency assessed by transfection of both forms of the 5'UTR cloned upstream the *XPO1* cDNA, **D)** representative

immunoblot and **E)** quantitative summary data of XPO1 levels, n=4. (*p<0.05 according to Student's t-test). All values are mean ± SEM.

4.3.3.1.3. Regulation of XPO1 by METTL3 and YTHDF1

Taking into account a recent m^{6}A-QTL study confirming upregulation of translation by YTHDF1 in human cells (Zijie Zhang et al., 2020), and considering that we have observed that *XPO1* translation is allele-specific and that the risk allele shows higher methylation, we hypothesized that the m^{6}A reader protein YTHDF1 could differentially bind each of the alleles and influence their translation (X. Wang et al., 2015).

To clarify whether METTL3 and YTHDF1 proteins interact with the *XPO1* 5'UTR in an allele-specific manner, we performed RNA immunoprecipitation (RIP) assays and quantified the amount of immunoprecipitated allele-specific *XPO1* mRNA (Fig25). While METTL3 showed no preferential binding for any of the alleles (F25.A), YTHDF1 was preferentially bound to the risk allele (*XPO1*T*) (F25.B), in accordance with the higher translation efficiency observed for this allele.

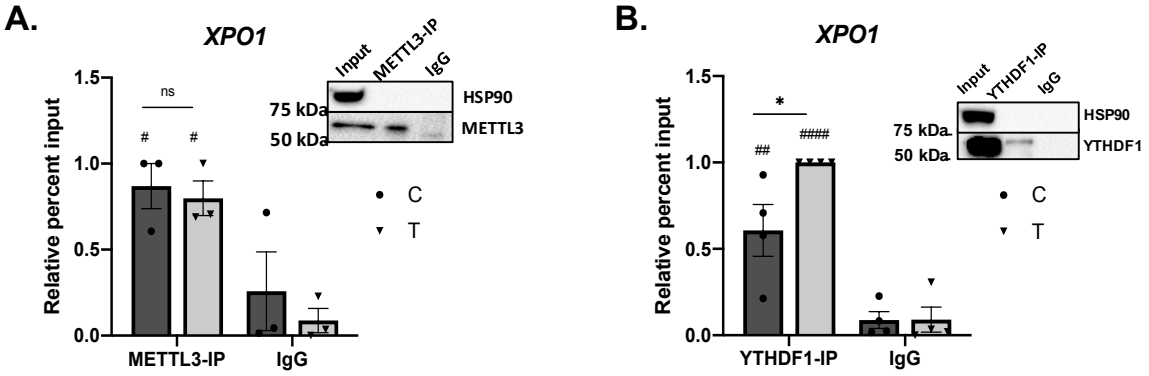

Figure 25. A) Allele-specific binding of *XPO1* in METTL3 immunoprecipitation (IP) followed by RT-qPCR, n=3. (ns: non-significant according to ANOVA test. Enrichment relative to control IgG #p<0.05 according to ANOVA test). Representative immunoblot of the IP experiment with HSP90 as negative control for the IP (right). **B)** Allele-specific binding of *XPO1* in YTHDF1 immunoprecipitation (IP) followed by RT-qPCR, n=4. (*p<0.05 according to ANOVA test. Enrichment relative to control IgG ##p<0.01, ####p<0.0001 according to ANOVA test).

Representative immunoblot of the IP experiment with HSP90 as a negative control for the IP (right).

To study more deeply the implication of m^{6}A machinery in XPO1 protein levels, we created stable *METTL3* and *YTHDF1* KD HCT116 cell lines (Fig26). Upon *METTL3* knock down we obtained an overall decrease of m^{6}A levels (F26.A) and more than a 70% reduction in mRNA (F26.B) and protein (F26.C) levels of METTL3 and YTHDF1.

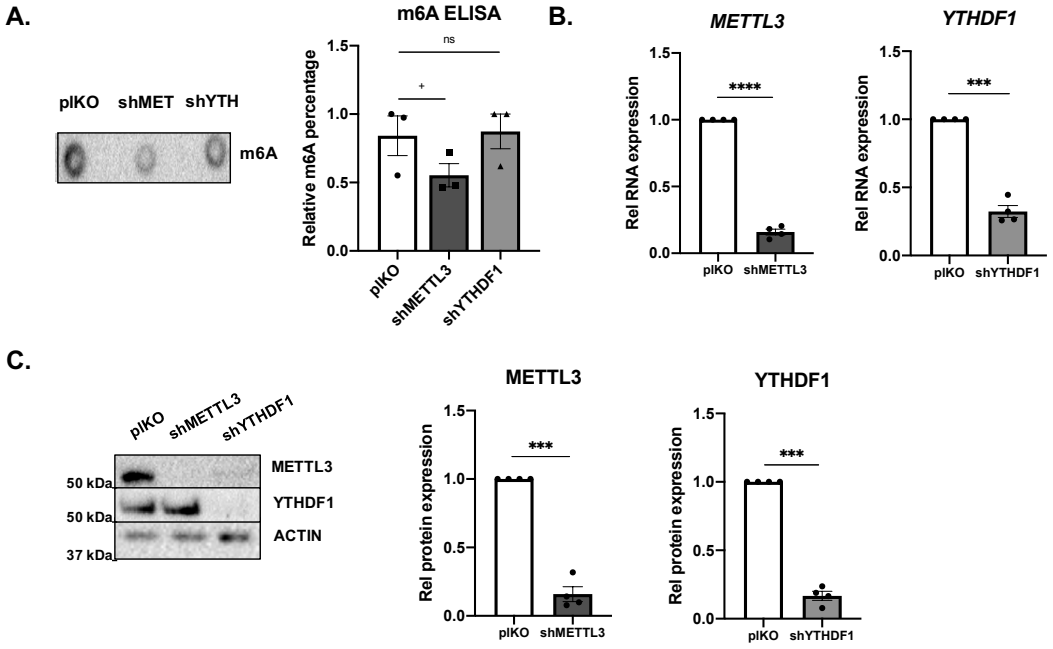

Figure 26. A) Overall RNA methylation measured by m^{6}A dot blot (left) and quantified using a commercial m^{6}A Elisa kit (right) of METTL3 and YTHDF1 knock down cells, n=3. (+p<0.1; ns: non-significant according to Student's t-test). **B)** Relative RNA expression measured by RT-qPCR of METTL3 and YTHDF1 knock down cells, n=4. (***p<0.001, ****p<0.0001 according to Student's t-test). **C)** Representative immunoblot (left) and quantitative summary (right) of METTL3 and YTHDF1 immunoblot of METTL3 and YTHDF1 knock down cells, n=4. (***p<0.001 according to Student's t-test).

Taking advantage of these KD cells, we analyzed the changes of *XPO1* expression as a result of m^{6}A deregulation. The reduction of total m^{6}A levels in the *METTL3* KD

resulted in less methylation of the 5'UTR of *XPO1* (Fig27.A). Consequently, lower *XPO1* mRNA and protein amounts were observed in this condition (Fig27.B, C). *XPO1* mRNA and protein levels were also decreased when *YTHDF1* was knocked down (Fig27.B, C), although the overall m^{6}A levels did not vary in these cells (Fig26.A and Fig27.A).

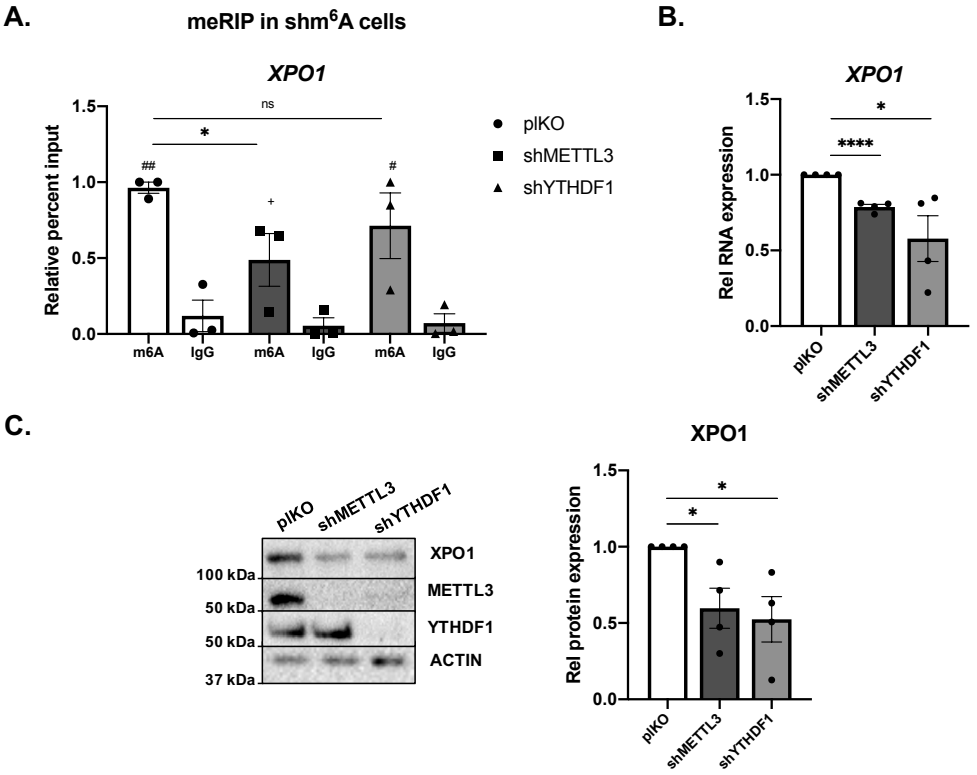

Figure 27. A) m^{6}A RNA immunoprecipitation (meRIP) followed by RT-qPCR of the 5'UTR of *XPO1* (*p<0.05; ns: non-significant according to ANOVA test. Enrichment relative to control IgG +p<0.1, #p<0.05, ##p<0.01 according to ANOVA test). **B)** Relative RNA expression measured by RT-qPCR of *XPO1* of METTL3 and YTHDF1 knock down cells (*p<0.05, ****p<0.0001 according to Student's t-test). **C)** Representative immunoblot (left) and quantitative summary (right) of the XPO1 immunoblot, n=4. (*p<0.05 according to Student's t-test).

These results show that methylation of the 5'UTR is necessary to maintain *XPO1* transcript levels and an adequate translation, suggesting that XPO1 translation is mediated by the recognition of the methylated 5'UTR mRNA by reader protein YTHDF1.

4.3.3.2. Effect of m^{6}A levels in XPO1 in vivo

4.3.3.2.1. Yhdf1 influence in Xpo1 *in vivo*

Using the murine intestinal cell line C26, we first confirmed that the 5'UTR of *Xpo1* is methylated in mice too (Fig28.A).

To further confirm the involvement of m^{6}A and YTHDF1 in *XPO1* translation, we studied a *Ythdf1* knockout mouse model. Intestinal epithelial cells isolated from the duodenum of WT and *Ythdf1* KO mice (Fig28. B, C) were used to confirm *in vivo* our previous results.

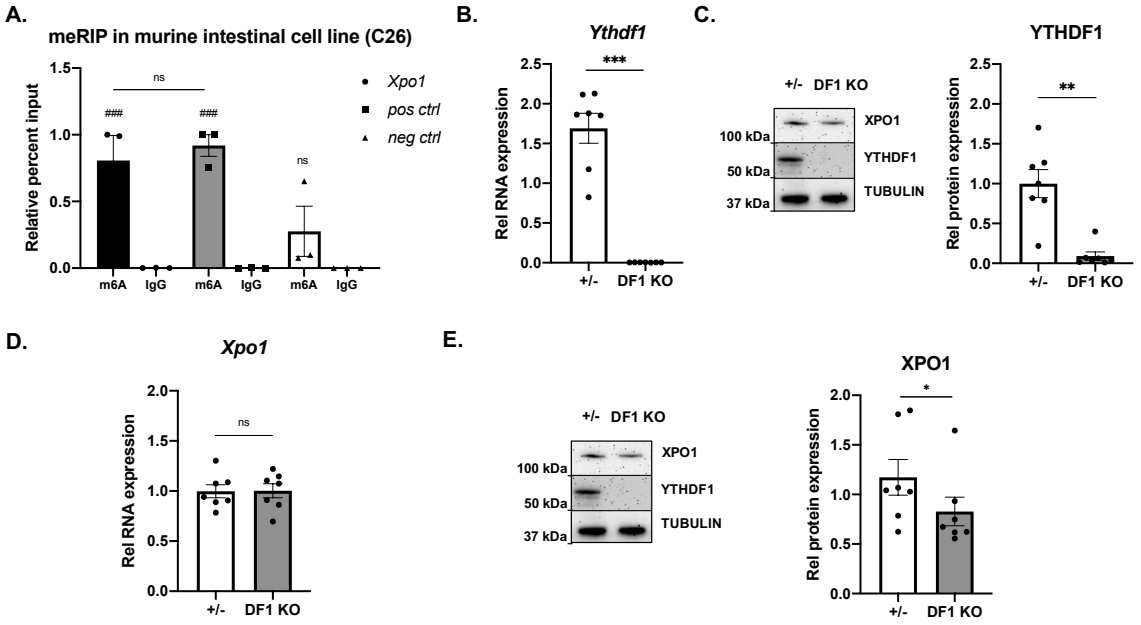

Figure 28. A) m^{6}A immunoprecipitation (meRIP) RT-qPCR values for *Xpo1* 5'UTR and m^{6}A positive and negative controls in C26 mouse intestinal cells, n=3. (ns: non-significant according to ANOVA test. Enrichment relative to control IgG ###p<0.001 according to ANOVA test). **B)** Relative expression of *Ythdf1* measured by RT-qPCR in WT (+/-) and *Ythdf1* KO mice (DF1 KO), n=7. (***p<0.001 according to Mann Whitney test). **C)** Representative immunoblot (left) and quantitative summary data (right) of YTHDF1 immunoblot, n=7. (**p<0.01, according to Mann Whitney test). **D)** Relative expression of *Xpo1* measured by RT-qPCR in WT (+/-) and *Ythdf1* KO mice (DF1 KO), n=7. (**p<0.01, ***p<0.001, ns: non-significant according to Mann Whitney test). **E)** Representative immunoblot (left) and quantitative summary data (right) of XPO1 immunoblot, n=7. (*p<0.05, according to Mann Whitney test). All values are mean ± SEM.

In addition, quantification of *Xpo1* levels in intestinal epithelial cells from the duodenum of WT and *Ythdf1* KO mice confirmed the involvement of YTHDF1 in the regulation of XPO1 protein amounts *in vivo*. Indeed, even if no significant differences were observed at the mRNA level (Fig28.D), *Ythdf1* KO mice showed significantly lower amounts of XPO1 protein in the epithelial cells isolated from the duodenum than their WT littermates (Fig28.E).

Results *in vivo* confirmed that reader YTHDF1 binds the methylated 5'UTR of *XPO1* to facilitate its translation.

4.3.3.3. XPO1 role in CD-related inflammation

We have so far demonstrated that the CD-associated SNP affects XPO1 protein levels by differential methylation of the risk allele. But we also wanted to study further how this association increases risk to develop CD. *XPO1* inhibitors have been widely tested as anti-cancer drugs due to their ability to downregulate NF-κB activity (M, 2016) and NF-κB is known to be upregulated in CD patients (Fernandez-jimenez et al., 2014; Maiuri et al., 2003). Thus we wanted to determine whether the increased m^6A levels and subsequent induction of XPO1 protein in *XPO1*T* form affect NF-κB and downstream inflammatory pathway in human intestinal cells.

As described above, the higher m^6A levels present in the risk allele form (*XPO1*T*) lead to greater XPO1 protein amounts (Fig24.E). In accordance with our hypothesis, we observed that cells overexpressing the *XPO1*T* form showed significantly higher induction and activation of the NF-κB subunit p50 (F29.A-C).

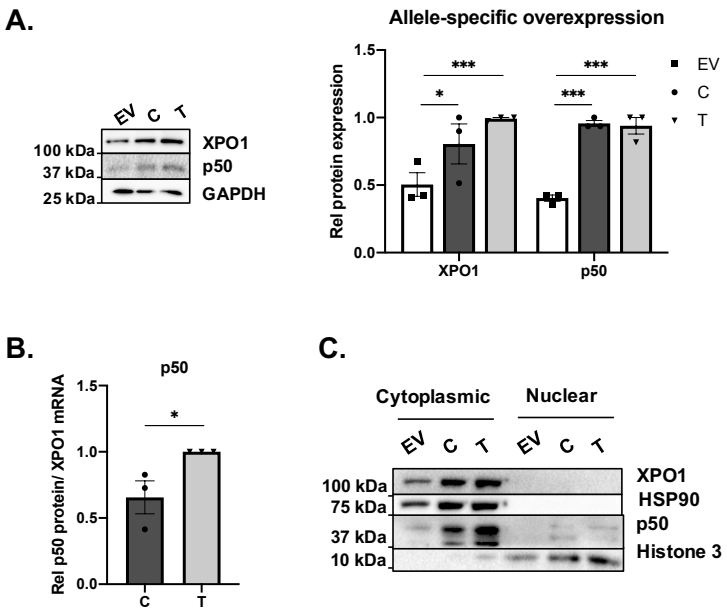

Figure 29. A) Representative immunoblot (left) and quantitative summary (right) of immunoblot for XPO1 and p50 in *XPO1* overexpressed cells, n=3. (*p<0.05, ***p<0.001 according to ANOVA test). **B)** Quantitative summary data of p50 relative to XPO1. (*p<0.05. according to Student's t-test). **C)** Activation of p50 assessed by nuclear localization in *XPO1* overexpressed cells, HSP90 was used as a cytoplasmic loading control and H3 as a nuclear loading control.

The activation of NF-κB implies an increased binding to target gene promoters in order to induce their transcription. Chemokine *IL8* appeared to be a good candidate as it had been previously identified as a cytokine that is induced by gluten (Tye-Din et al., 2017) and it is a NF-κB target (Roebuck, 1999), which is also regulated by *XPO1*.

In fact, *IL8* expression was induced in active CD patients and was reduced after removal of gluten from diet (Fig30.A). *IL8* expression was then quantified in the immune (CD45+) and epithelial (CD326+) fractions from complete biopsies of controls and active celiac patients, to confirm the implication of the epithelial cells in this pathway. We observed that even though immune cells seem to be the main producers of *IL8*, the differences observed between control and active CD individuals come from the epithelial fraction (Fig30.B).

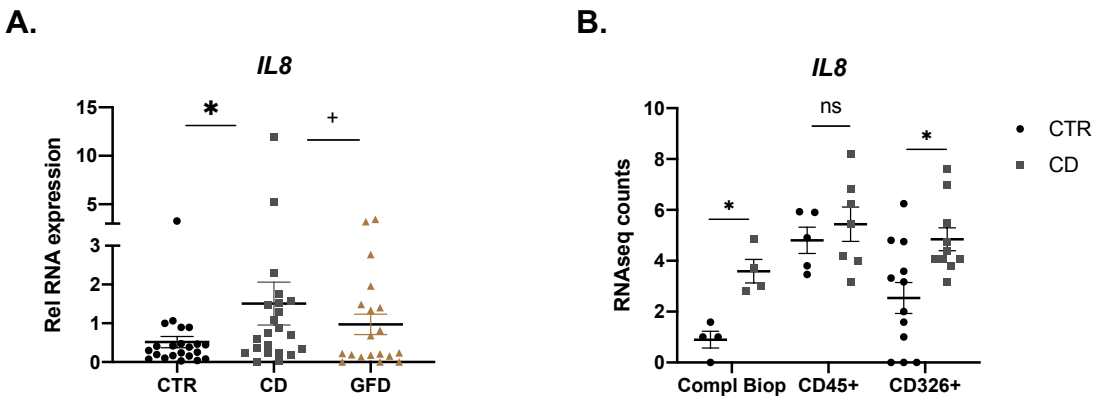

Figure 30. A) The expression of *IL8* measured by RT-qPCR in RNA extracted from adult and pediatric individuals, n=6-16. (+p<0.1; *p<0.05 according to ANOVA test). **B)** *IL8* expression by RNAseq counts from a previous RNAseq study (Fernandez-Jimenez et al., 2019) in complete biopsies, CD45+ immune cell fractions and CD326+ epithelial cell fractions from CTR and CD, n=4-12. (*p<0.05, ns: non-significant according to ANOVA test).

To further analyze the involvement of XPO1 in IL8 induction, Electrophoretic Mobility Shift Assay (EMSA) experiments were performed in HCT116 cells. We showed that nuclear extracts of cells overexpressing *XPO1* exhibit higher protein binding to the NF-κB consensus sequence of the *IL8* promoter (Fig31.A). Moreover, as it was the case for p50 protein activation, we observed that *IL8* expression is higher in cells overexpressing *XPO1* (Fig31.B), and again, that this induction is further increased in the presence of the *XPO1*T* form (Fig31.C). We also confirmed that this XPO1-mediated *IL8* increase is NF-κB-dependent, as treatment with BAY 11-7082 (an NF-κB inhibitor) counteracted the *IL8* increase in XPO1-overexpressing cells (Fig31. B, D).

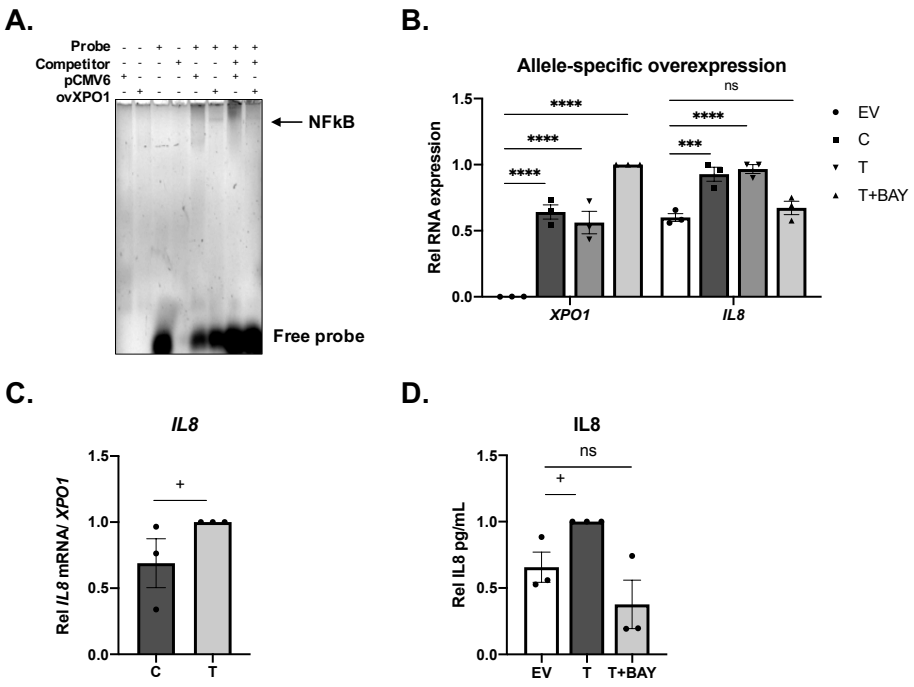

Figure 31. A) Nuclear extracts from HCT116 cells transfected with an empty vector (EV) or XPO1 expression plasmid (*ovXPO1*) were analyzed, with 10X unlabeled probe as competitor. A representative gel of 2 independent experiments is shown. **B)** Relative expression measured by RT-qPCR of *XPO1* and *IL8* in cells transfected with an empty vector (EV), overexpressing both forms of *XPO1* (C and T) and cells overexpressing *XPO1* and treated with the NF-κB inhibitor Bay (T+BAY), n=3. (***p<0.001, ****p<0.0001, ns: non-significant according to ANOVA test)**. C)** *IL8* expression quantified by RT-qPCR in cells overexpressing both forms of *XPO1*; n=3. (+p<0.1, according to Student´s t-test). **D)** Secreted IL8 measured by ELISA in the medium of cells transfected with an empty vector (EV) or overexpressing *XPO1*T* in the absence (T) or presence of the NF-κB inhibitor BAY 11-7082 (T+BAY), n=3. (+p<0.1, ns: non-significant according to ANOVA test).

These results show that increased *XPO1* levels from the risk allele form (*XPO1*T*) lead to a higher induction of NF-κB-mediated inflammatory response, thus increasing susceptibility to develop CD.

4.4. CONTRIBUTION OF GLUTEN TO m^{6}A METHYLATION AND *XPO1* PATHWAY

4.4.1. Gluten stimulation in human biopsy

Removal of gluten from CD patients' diet seemed to affect the m^{6}A machinery, *XPO1* and downstream *IL8* expression levels, so we wanted to confirm the role of gluten in this pathway. To this aim, biopsies from active CD patients were cut into two pieces and incubated with or without PTG for 4 h (Fig12).

We detected a trend towards increased *METTL3*, *YTHDF1* and *XPO1* mRNA levels (Fig32.A) together with enhanced XPO1 protein levels (Fig32.B) in PTG-challenged biopsies. We could also confirm the overexpression of *IL8* in the PTG-treated biopsy portions (Fig32.C), further indicating a role of gluten in this process.

Interestingly, the PTG-induced increase of *YTHDF1* in intestinal biopsies significantly correlated with the increase of *XPO1* (Fig32.D), confirming the importance of this m^{6}A reader in the gluten-dependent *XPO1* induction observed in our tissue stimulation model.

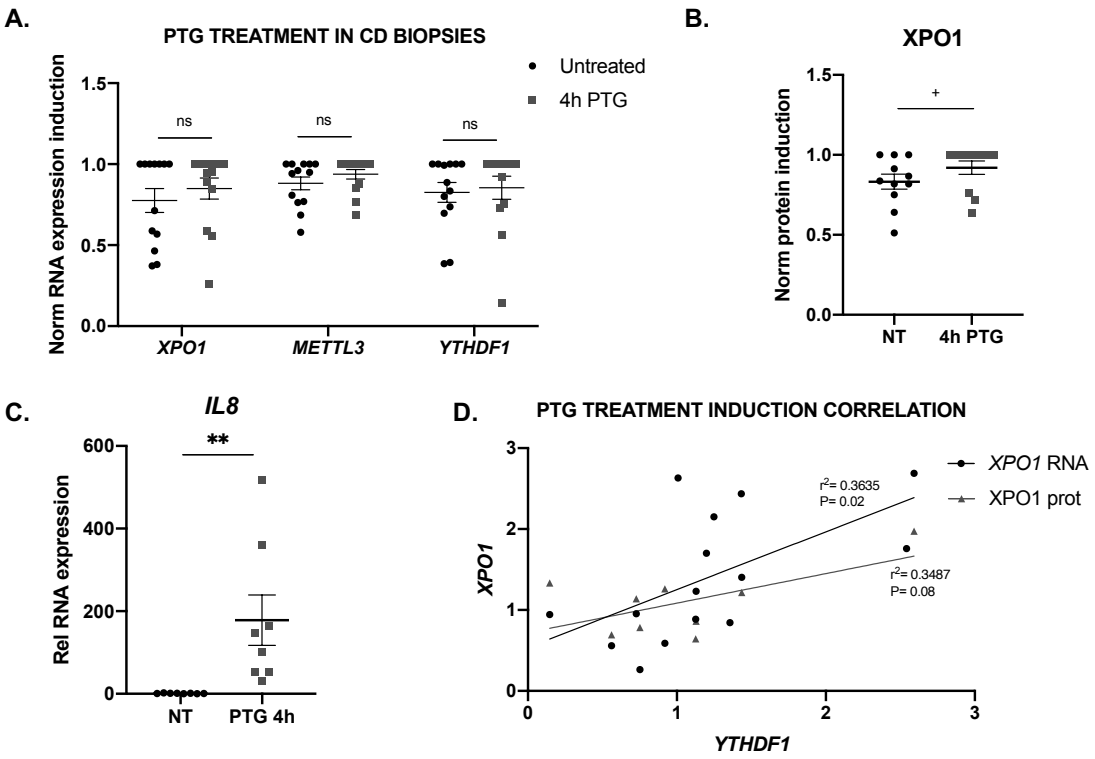

Figure 32. A) RNA expression of *XPO1*, *METTL3* and *YTHDF1* measured by RT-qPCR in untreated and PTG incubated biopsies, n=15. Values are means of induction ± S.E.M. (+p<0.1, ns: non-significant according to Mann Whitney test). **B)** XPO1 protein levels measured by ELISA in biopsies untreated (NT) and incubated with gliadin for 4 h (PTG), n=13. (+p< 0.1 according to a Mann Whitney test). **C)** *IL8* expression measured by RT-qPCR in untreated (NT) and PTG-incubated biopsies. (**p<0.01 according to Mann Whitney test). All values are mean ± SEM. **D)** Correlation of the induction between *YTHDF1* and *XPO1* in PTG treated biopsies. Triangles correspond to *XPO1* mRNA and dots to XPO1 protein induction. n=9-15, (R and p were calculated by Pearson correlation).

As we observed a possible implication of gluten in the m^{6}A machinery and in *XPO1* regulation, together with the downstream induction of inflammation, our next objective was to elucidate how gluten regulates this pathway.

4.4.2. Gluten stimulation *in vitro* model

4.4.2.1. Gluten and m^{6}A methylation

We wanted to understand how gluten could be influencing *XPO1* levels and if this regulation was somehow regulated by m^{6}A methylation. m^{6}A marks in 5'UTRs of mRNAs have been described to be key factors in the activation of translation upon stress stimuli (Coots et al., 2017). In order to determine whether provocation with gliadin (the environmental trigger of CD) intensifies m^{6}A marks and leads to an increase in *XPO1* levels, we stimulated intestinal cells with PTG (Fig13).

Concordant with the results obtained with human samples, we observed an increase in overall m^{6}A levels (Fig33. A), together with higher *METTL3*, *YTHDF1* and *XPO1* expression (Fig33. B), as well as higher protein levels (F33.C) when HCT116 cells were stimulated with PTG.

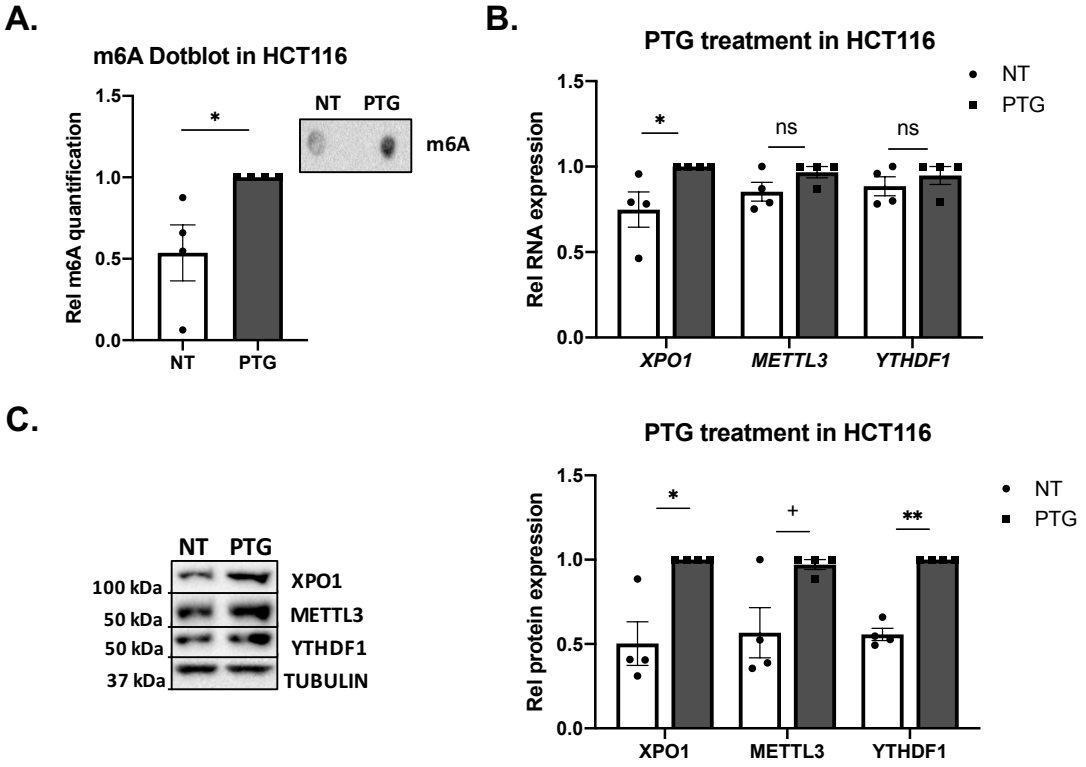

Figure 33. A) Overall RNA methylation quantification by m^{6}A dot blot and a representative m^{6}A dot blot (top right) in untreated (NT) and PTG-treated cells, n=4. (*p<0.05 according to Student's t-test). **B)** Relative expression measured by RT-qPCR for *XPO1*, *YTHDF1* and *METTL3* in

untreated (NT) and PTG-treated cells, n=4. (*p<0.05, **p<0.01, ****p<0.0001, ns: non-significant according to Student's t-test). **C)** Representative immunoblot (left) and quantitative summary data (right) of XPO1, METTL3 and YTHDF1 immunoblot in untreated (NT) and PTG-treated cells. n=4. (+p<0.1, *p<0.05, **p<0.01, according to Student's t-test).

As expected, we also observed that the levels of m^{6}A in the 5'UTR of *XPO1* were higher after PTG stimulation (Fig34. A), suggesting that the gliadin-induced increase in XPO1 protein levels is mediated by an m^{6}A increase of the 5'UTR. Further supporting this idea, when PTG stimulations were performed in *YTHDF1*-silenced cells, XPO1 levels did not vary (Fig34.B).

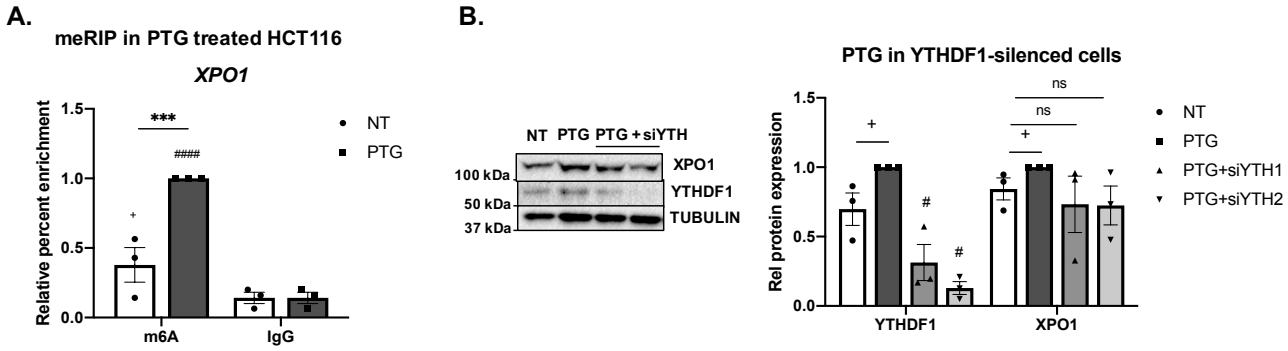

Figure 34. A) m^{6}A levels in the 5'UTR of *XPO1* assessed by meRIP-qPCR in untreated (NT) and PTG-treated cells, n=3. (***p<0.001 according to ANOVA test. Enrichment relative to the control IgG +p<0.1; ####p<0.0001 according to ANOVA test). **B)** Representative immunoblot (left) and quantitative summary (right) of XPO1 and YTHDF1 immunoblot in untreated (NT), PTG-treated (PTG) and PTG-treated and YTHDF1-silenced (PTG+siYTH) cells, n=3. (+p<0.1, ns:non-significant, according to Student's t-test). Silencing efficiency compared to NT cells (#p<0.05, according to Student's t-test).

Taken together, our results show that gliadin activates the m^{6}A machinery, increasing methylation levels in the 5'UTR of *XPO1* and leading to a YTHDF1-dependent increase of XPO1 protein amounts.

4.4.2.2. Gluten and m^{6}A-dependant inflammation

It is known that gliadin induces NF-κB activation and further cytokine release in human immune (Jelínková et al., 2004) and intestinal epithelial cells (Capozzi et al., 2013). However, the cell-type specificity and the mechanisms underlying gliadin-induced inflammation are not totally understood. We have demonstrated that increased m^{6}A levels in *XPO1*T* induce NF-κB and increase *IL8*. Thus, we wanted to determine whether the activation of the m^{6}A machinery and subsequent *XPO1* increase in response to PTG is able to activate the NF-κB and downstream inflammatory pathways in human intestinal cells.

Indeed, cells treated with PTG, which showed activated m^{6}A machinery and increased *XPO1* levels (Fig33), also showed increased amounts of p50 (Fig35).

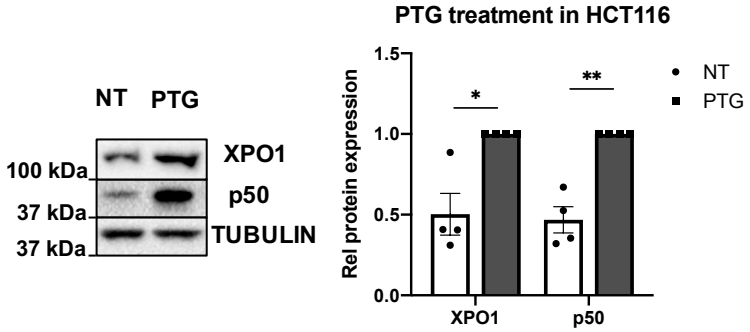

Figure 35. Representative immunoblot (left) and quantitative summary (right) of the immunoblot for XPO1 and p50 in untreated cells (NT) and cells treated with PTG, n=4. (*p<0.05, **p<0.01 according to Student's t-test).

We confirmed that the PTG induction of p50 is m^{6}A-dependent, as PTG-stimulation did not increase NF-κB in YTHDF1-silenced cells (F36.A). Moreover, when PTG-stimulated cells were treated with the XPO1 inhibitor leptomycin B (LMB), we observed a decline in the induction of p50, confirming that the inflammatory environment induced by PTG is, at least in part, dependent on XPO1 (F36.B).

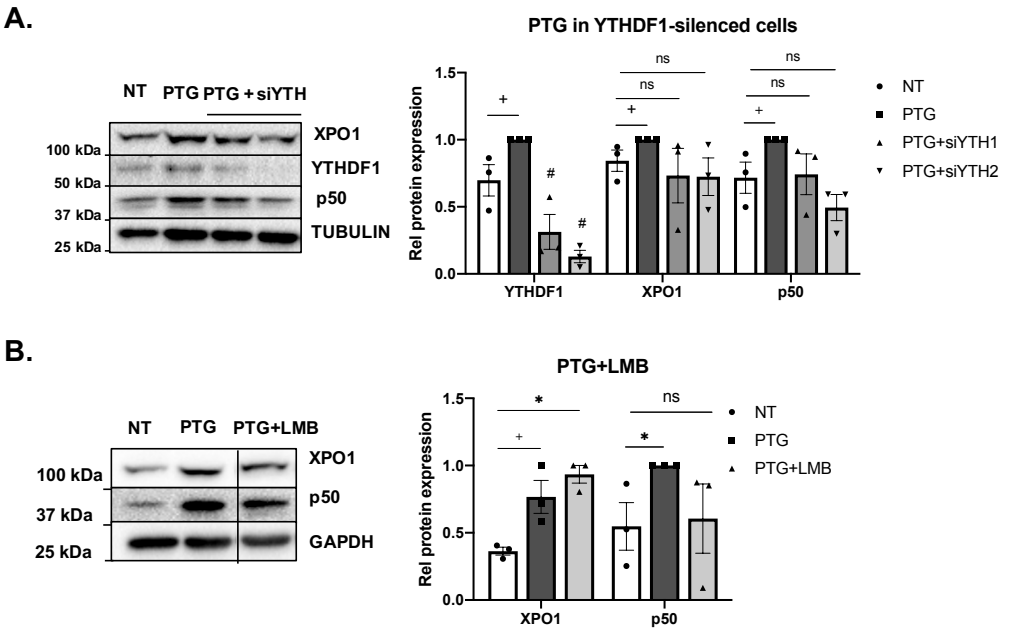

Figure 36. A) Representative immunoblot (left) and quantitative summary (right) of immunoblot for YTHDF1, XPO1 and p50 in untreated (NT), PTG-treated (PTG) and PTG-treated +YTHDF1-silenced (PTG+siYTH) cells, n=3. (+p<0.1, ns: non-significant according to Student's t-test). Silencing efficiency compared to NT cells (#p<0.05, according to Student's t-test). **B)** Representative immunoblot (left) and quantitative summary (right) of immunoblot for XPO1 and p50 in untreated (NT), PTG-treated (PTG) and cells treated with PTG + the XPO1 inhibitor leptomycin B (PTG+LMB), n=3. (+p<0.1, *p<0.05, ns: non-significant according to ANOVA test).

Additionally, we confirmed that *IL8* was also induced by PTG (Fig37. A) in an XPO1-dependent manner (Fig37. B), as the inhibition of XPO1 significantly reduced the levels of *IL8* in response to PTG.

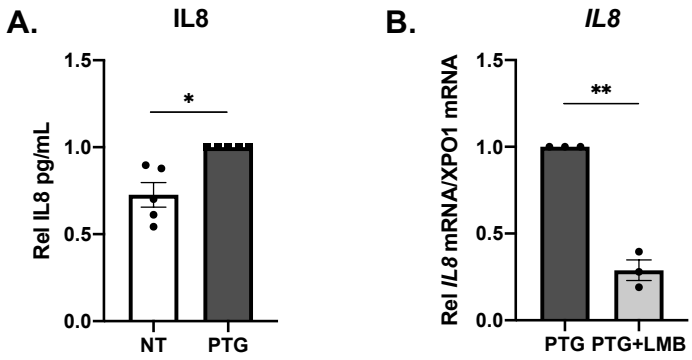

Figure 37. A) Secreted IL8 levels and **B)** *IL8* expression quantified by ELISA and RT-qPCR in untreated (NT), PTG-treated and PTG+LMB-treated cells, n=3-5 (*p<0.01; **p<0.01 according to Student´s t-test).

Altogether, these results suggest that the gliadin-induced increase of both m^{6}A and *XPO1* activates the NF-κB pathway and provokes a downstream inflammation in intestinal epithelial cells *in vitro*.

4.4.3. Gluten stimulation *in vivo* model

4.4.3.1. Gluten and m^{6}A methylation

To analyze whether gliadin is also able to enhance the m^{6}A machinery and boost *XPO1* translation *in vivo*, we treated C57BL/6 mice, previously naïve to gluten exposure, with PTG and cholera toxin (CT) as an adjuvant (Fig14).

In accordance with the *in vitro* model, we observed that tissues from mice treated with PTG had increased m^{6}A methylation (Fig38. A) together with *Ythdf1* and *Xpo1* induction at the mRNA and protein levels (Fig38. B, C) compared with those treated only with CT, confirming *in vivo* the gliadin induction of m^{6}A and *XPO1* previously observed.

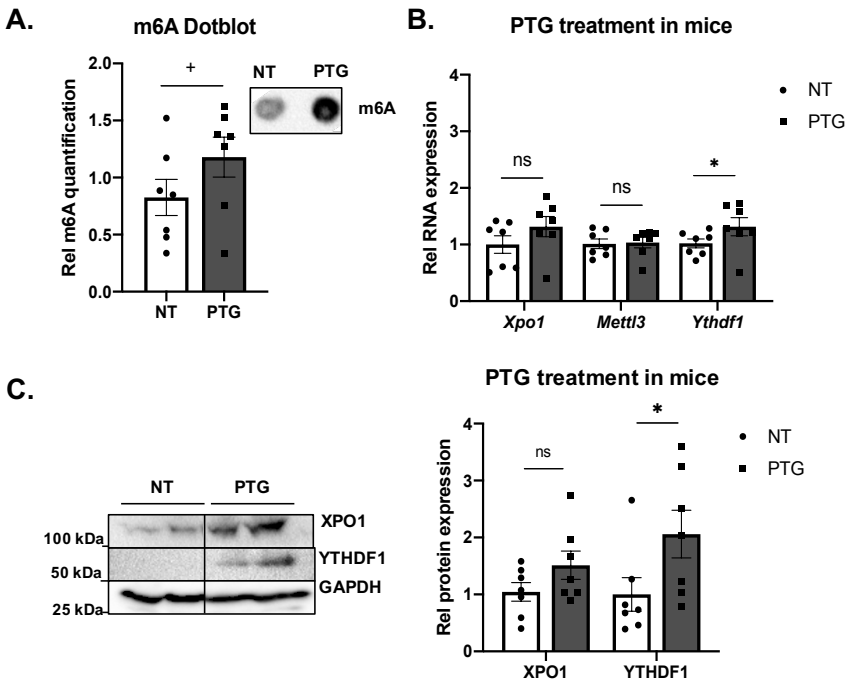

Figure 38. A) Overall m^{6}A RNA levels measured by m^{6}A Dot blot and a representative dot blot (top right) in WT control (NT) or PTG-treated mice (PTG), n=7. (+p<0.1 according to Mann Whitney test). **B)** Relative expression measured by RT-qPCR for *Xpo1*, *Ythdf1* and *Mettl3*, n=7. (*p<0.05, ns: non-significant according to Mann Whitney test). **C)** Representative immunoblot (left) and quantitative summary (right) of immunoblot for XPO1 and YTHDF1 in untreated (NT) and PTG-treated mice (PTG). n=7 (+p<0.1, *p<0.05, ns: non-significant according to Mann Whitney test).

In addition, YTHDF1 involvement in gliadin-mediated *XPO1* induction was further confirmed as epithelial cells from *Ythdf1* KO mice barely showed PTG-mediated *XPO1* increase when compared to WT (Fig39).

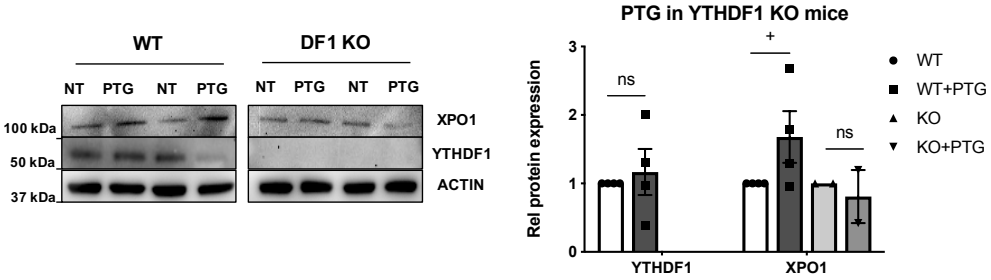

Figure 39. Representative immunoblot (left) and quantitative summary (right) of immunoblot for YTHDF1 and XPO1 in untreated (-) and PTG-treated cells (+PTG) derived from wild type (WT)

or Ythdf1 KO (KO) mice, n=2-4 (+p<0.1, ns:non-significant according to ANOVA test). All values are means ± S.E.M.

Human biopsy samples and *in vitro* results showed that the CD-associated genotype influences m^{6}A machinery and *XPO1* levels. Therefore, we wanted to see how mice harboring the major risk factor for CD (HLA DQ2 alleles) respond to our PTG stimulation model. Interestingly, when small intestinal samples from HLA-DQ2 mice were studied, a stronger response to gliadin could be observed at the RNA levels in mice treated with PTG versus controls (Fig40.A-C).

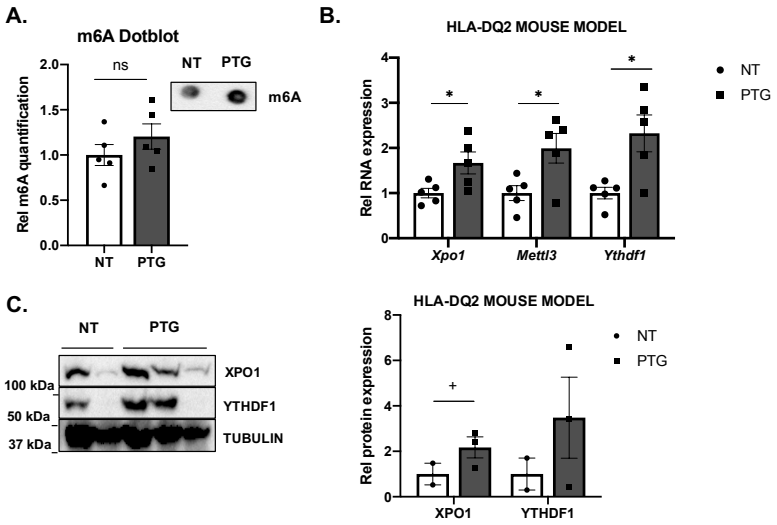

Figure 40. A) Overall m^{6}A RNA levels measured by m^{6}A Dot blot and a representative dot blot (top right) in WT control (NT) or PTG-treated mice (PTG), n=7. (ns: non-significant according to Mann Whitney test). **B)** Relative expression measured by RT-qPCR for *Xpo1*, *Ythdf1* and *Mettl3* in untreated (NT) and PTG-treated mice (PTG), n=5. (*p<0.05 according to Mann Whitney test). **C)** Representative immunoblot (left) and quantitative summary (right) for XPO1 and YTHDF1 protein levels in untreated (NT) and PTG-treated mice (PTG), n=2-5 (+p<0.1, ns: non-significant according to Mann Whitney test).

These results confirm that gluten activates the m^{6}A machinery and leads to higher XPO1 protein amounts *in vivo.* In addition, we observed that mice with HLA risk

genotype showed an increased response in this pathway, pointing that additional CD predisposing genotype can cause a more severe response.

4.4.3.2. Gluten and m^{6}A-dependant inflammation

To further confirm that the m^{6}A-mediated XPO1 increase leads to an induction of intestinal inflammation, the p50 NF-κB subunit was quantified in PTG-treated mice. Both mice models, WT (C57BL/6) and HLA-DQ2 mice, showed an induction of NF-κB upon gliadin stimulation (Fig41. A, B).

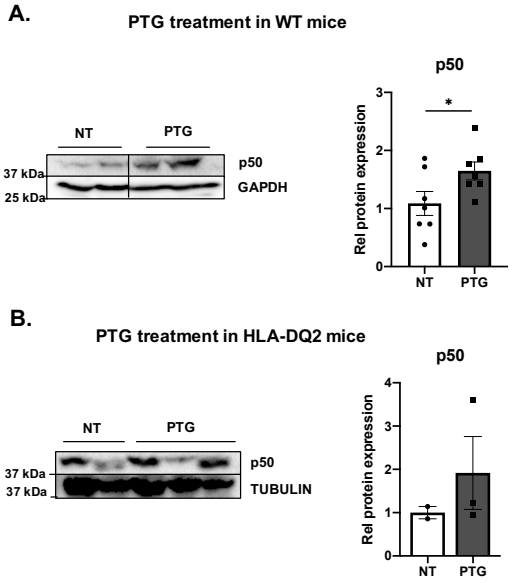

Figure 41. A) Representative immunoblot (left) and quantitative summary (right) of immunoblot for p50 protein levels in untreated (NT) and PTG-treated WT mice. n=7 (*p<0.05 according to Mann Whitney test). **B)** Representative immunoblot (left) and quantitative summary (right) of immunoblot for p50 protein in humanized HLA-DR3-DQ2 control mice (NT) or PTG-treated mice (PTG). n=2-3 (*p<0.05 according to Mann Whitney test).

As in the *in vitro* model, we expected an increase of inflammatory cytokines upon NF-κB activation. *Cxcl1* is the mouse functional homolog for *IL8* (Hol et al., 2010), which showed higher expression levels in PTG-treated mice (Fig42. A, B), confirming the physiological effect of gliadin stimulation *in vivo*. Interestingly, HLA-DQ2 mice which showed a more pronounced response to gliadin, also presented higher *Cxcl1* levels.

Moreover, PTG treatment in *Ythdf1* KO mice-derived epithelial cells did not show an increase in *Cxcl1 ex vivo* (Fig42. C), further demonstrating that gliadin-induced inflammation is m^{6}A and *YTHDF1*-dependent.

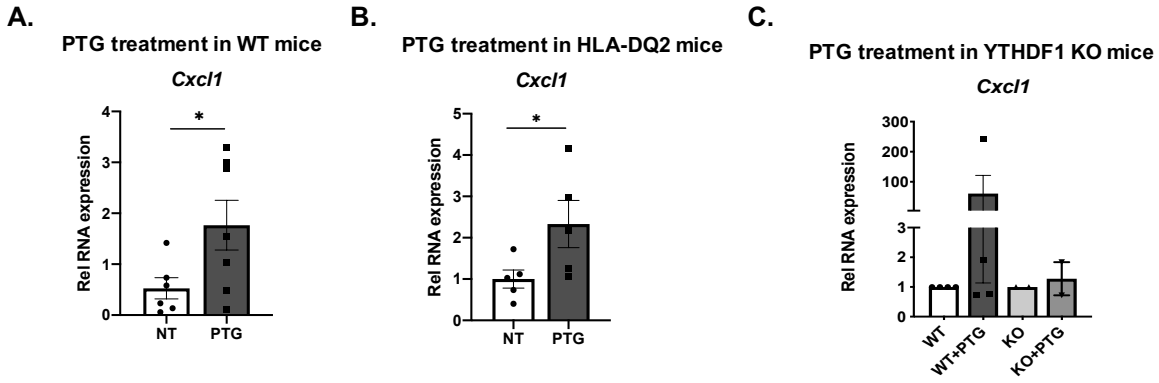

Figure 42. Expression of mouse *IL8* functional homolog chemokine *Cxcl1* quantified by RT-qPCR in **A)** untreated (NT) and PTG-treated WT mice, n=7. (*p<0.05, according to Mann Whitney test); **B)** untreated (NT) and PTG-treated humanized HLA-DQ2 mice, n=5. (*p<0.05 according to Mann Whitney test) and **C)** untreated (-) and PTG-treated cells (+PTG) derived from wild type (WT) or *Ythdf1* KO (KO) mice, n=2-4. All values are means ± S.E.M.

All these results from human samples and *in vitro* and *in vivo* models present a new m^{6}A-mediated and gluten responsive pathway, provide novel functional implications of CD-associated SNPs and open new possible therapy targets for the disease.

5.DISCUSSION

During the last two decades, large-scale genotyping approaches like GWAS or the Immunochip project have helped to identify new genomic regions related to autoimmune-disease susceptibility and also to pinpoint potentially disrupted pathways in those disorders. However, these approaches have not been sufficient and the Genetics of CD is still far from being fully understood. Indeed, half of the heritability of CD is still to be discovered, as the so-called "missing heritability". More recent approaches, including the study of Epigenetics and ultimately, epitranscriptomics might harbor the clues to further decipher this missing heritability. In CD, a few works relating DNA methylation to CD pathogenesis (Fernandez-jimenez et al., 2014; Fernandez-Jimenez et al., 2019) or describing the involvement of different lncRNAs in the context of CD (Ainara Castellanos-Rubio et al., 2016; Olazagoitia-Garmendia et al., 2021) have been published so far.

In this line, RNA modifications are emerging as a new layer of gene regulation and there is an increasing number of studies describing the involvement of RNA modifications in different diseases (Jonkhout et al., 2017). However, there are still many unknown aspects regarding RNA modifications and their biological function. Although several new methodologies to identify, detect and/or quantify RNA modifications are being published (X. Li et al., 2016), many of those techniques are not fully reliable and have several drawbacks (use of modified nucleotides, need to manipulate cells with crosslinking methods, limitations to develop high-throughput techniques, etc.). In addition, some of those methods are not robust enough and there are often discrepancies between studies when measuring the same modification using different or even the same technique (Y. S. Chen et al., 2021; X. Li et al., 2016; McIntyre et al., 2020). So one of the main objectives regarding RNA modification studies is to find more accurate and reliable techniques so that it is possible to draw the real RNA modification map and study these marks in terms of their implication in disease.

N^6-Methyladenosine (m^6A) is the most abundant internal modification of mammalian RNAs constituting a new layer of gene regulation that is involved in different

biological processes, as T-cell responses or tumorigenesis (Cui et al., 2017; H. B. Li et al., 2017). Moreover, it has been shown that this modification plays important roles in the development of several disorders, including neuronal disorders, immune-mediated diseases, obesity and cancer (Maity & Das, 2016). Nevertheless, so far there is no study relating m^6A modification of RNA and CD.

Several techniques have been developed to map and quantify m^6A residues (K. Chen et al., 2015; Dominissini et al., 2012; Ke et al., 2015; Linder et al., 2015; N. Liu et al., 2013; Meyer et al., 2012; Molinie et al., 2016), but as it is the case of Epitranscriptomics in general, the methods available today are laborious or involve next-generation sequencing. In addition, as mentioned above, there are some discrepancies among studies from different groups regarding m^6A site-specific quantification (X. Li et al., 2016; McIntyre et al., 2020), so new approaches are needed to measure the m^6A levels in selected transcripts that could be involved in the development of disease.

Taking all these into consideration, our group has developed a new technique that takes advantage of the previously described reduced efficiency of *BstI* enzyme to retrotranscribe m^6A nucleotides that are located adjacent to the priming oligo (Harcourt et al., 2013; Shaoru Wang et al., 2016). This method has been shown to be able to confirm the methylation motifs described by other techniques in a cost-affordable and time-efficient way, in lncRNA *TUG1,* among other transcripts. Additionally, when we compared the results of specific residues using our method to those obtained with m^6A immunoprecipitation experiments that evaluate a whole region, we found that the methylation status is concordant in eight out of ten of the RNAs assessed, further supporting the validity of the method.

This method is also useful for the rapid, relative quantification of changes in the percentage of molecules that are methylated at a specific residue within a transcript. In fact, results obtained using m^6A-RT-qPCR decreased when non-methylated RNA is spiked into an RNA sample (decreasing the relative amount of m^6A) or when

cycloleucine is used to reduce the overall levels of RNA methylation in the cell. These results confirm the validity of this technique to evaluate whether a certain residue presents alterations in its methylation rates in response to different stimuli or is affected by disease status.

Indeed, we have demonstrated that this technique can be used with the limited amounts of RNA extracted from human tissues that are normally insufficient to perform RNA immunoprecipitation experiments and also that the relative amount of m^6A marks in candidate regions could be easily quantified. However, the limitation of this technique is that it cannot be used for high-throughput studies as only information of a single site of interest will be obtained. Nevertheless, identification of the variability of the m^6A methylation in interesting candidates using this technique could help understand their contribution in disease pathogenesis.

A recently published m^6A-QTL (quantitative trait loci) study (Zijie Zhang et al., 2020) has shown the need to study RNA modifications that are altered by disease-associated SNPs. Analyzing the involvement of SNPs in m^6A methylation changes may help to elucidate the missing heritability of many autoimmune disorders as CD. In this line, we first wanted to assess the overall involvement of m^6A in CD. We showed that human biopsy samples from pediatric and adult active celiac patients (on a gluten containing diet) presented elevated total m^6A methylation levels, together with the overexpression of m^6A writer *METTL3* and reader *YTHDF1* compared to non-celiac individuals. This pointed to an alteration of m^6A methylation in CD, so that studying the implication of CD-associated SNPs in m^6A methylation could help to better understand CD pathogenesis.

We have specifically studied the involvement of m^6A and non-coding SNP rs3087898 in the *XPO1* transcript and have shown that genotype-dependently altered RNA methylation levels activate the NF-κB inflammatory pathway. However, we believe that there could be more pathways affected by m^6A alterations in CD, so

more studies are needed to elucidate the role of RNA modifications in CD pathogenesis, as well as in other autoimmune disorders.

In particular, this study reveals how the genotype of the CD-associated noncoding SNP rs3087898, located in the 5'UTR of protein-coding gene *XPO1*, affects mRNA methylation and its subsequent translation. We also found that the SNP genotype affects the RNA binding affinity of RBP YTHDF1, so that it preferentially binds to the CD-risk allele resulting in increased translational activity of the mRNAs that carry risk allele *XPO1*T.* Interestingly, the predicted secondary structure of the 5'UTR of *XPO1* was also genotype-dependent, suggesting that rs308789 could alter not only the binding of proteins but also the RNA structure, leading to alterations in m^6A levels and YTHDF1-dependent translational features, in accordance with results from a recent m^6A QTL study (Zijie Zhang et al., 2020). Further studies would be needed in order to elucidate how m^6A levels change upon those genotype-specific structures.

We have shown, both *in vitro* and *in vivo,* that in intestinal epithelial cells, increased methylation confers higher translation efficiency of the mRNA molecules that carry the risk allele (*XPO1*T*), an effect that is mediated by the m^6A reader YTHDF1. It is important to emphasize that in contrast to what is observed in enterocytes, immune cells appear to have fewer (or no) methylation marks on the 5'UTR of *XPO1*, suggesting that this m^6A-mediated mechanism is specific of intestinal epithelial cells. Our work demonstrates that non-coding SNPs associated with susceptibility to immune and inflammatory diseases can alter m^6A levels and functionally contribute to disease pathogenesis via cell type-specific activation of an inflammatory response, confirming what has been recently shown by a transcriptome-wide m^6A QTL analysis (Zijie Zhang et al., 2020). These results also emphasize the importance of performing functional studies in the appropriate biological models as the effects of non-coding SNPs have been shown to be predominantly cell-type specific (Roadmap Epigenomics Consortium et al., 2015).

We also observed that individuals harboring the risk allele produce higher amounts

of XPO1 protein, and this would explain the association of this SNP with disease susceptibility, as individuals homozygous for the risk allele (TT) are predicted to have higher levels of basal inflammation, because of the increase in XPO1 protein amounts. Our results highlight the importance of performing functional studies of disease-associated SNPs, because as in this case, the mechanisms by which SNPs regulate the candidate gene can be more complex than simply affecting transcription of the candidate gene.

We have also described the biological implication of the m^6A-dependent increase of *XPO1* levels in CD. *XPO1* is a nuclear export receptor involved in critical signaling pathways and cellular functions that has been associated with several malignancies. Appropriate shuttling of IκB-α via XPO1 nuclear export has been linked to the activation of the NF-κB pathway and downstream secretion of cytokines. Moreover, it has been shown that cells treated with *XPO1* inhibitors display lower NF-κB activity and a subsequent decrease in cytokine release (Sendino et al., 2018). We have shown that increased XPO1 protein levels, a consequence of the more abundant m^6A marks in the *XPO1*T* mRNA, promote the induction of NF-κB, a hallmark of CD, providing a functional explanation for the association of this SNP with CD.

Although an increased inflammatory response, as evidenced by activated NF-κB, has been reported in CD, there are still many gaps in our understanding of CD pathogenesis. It is known that CD is characterized by the destruction of the small intestinal epithelial barrier caused by intraepithelial lymphocyte (IEL) infiltration and an exacerbated activation of macrophages and other immune cells. A recent study using transgenic mice has underlined the complexity of CD pathogenesis; in the CD-like mouse model, activation and regulation of intestinal epithelial cells (IEC) as well as immune cells are needed to develop the characteristic immune response and villous atrophy that are seen in human CD patients (Abadie et al., 2020). The role of various immune cells in cytokine secretion has been well studied, but less is known about the contribution of IECs. It has been described that different cytokines secreted by IECs play key roles in the activation and early steps of the immune

response in CD (Abadie et al., 2020). In this line, we have studied the role of *IL8*, a neutrophil attractant chemokine, in our pathway. IL8 is known to play a key role in tissue-damage and activation of the innate immune response and it has been proposed that in CD patients, IL8 is specifically secreted after gluten ingestion (Diosdado et al., 2007; Tye-Din et al., 2020). So far, most studies have been performed in CD-derived immune cells and PBMCs (Goel et al., 2019; Lammers et al., 2011; Manavalan et al., 2010), however, this is the first study where it is shown that CD intestinal epithelial cells can also secrete IL8.

In accordance with an allele-specific NF-κB activation, we observed higher transcription of *IL8* and secretion in the presence of the *XPO1* risk allele. We have also seen that even if they are not the main producers, active CD patients show increased *IL8* expression in epithelial cells when compared to controls, confirming that m^{6}A-XPO1- NF-κB activation in CD patients come mainly from a dysregulation in gut epithelial cells.

In terms of how m^{6}A could influence CD pathogenesis, it is known that the rapid kinetics of m^{6}A methylation provides cells with the ability to quickly respond to external stimuli, activating distinct pathways in different cell types (Engel et al., 2018; Winkler et al., 2019). Viral infections or microbiome composition are thought to contribute to CD development, and the microbiome has recently been involved with the levels of m^{6}A methylation present in the gut (Jabs et al., 2020). However, the main antigens triggering CD are gliadin peptides derived from gluten (Abadie et al., 2020; Capozzi et al., 2013; Garrote et al., 2008). Although gliadin has been proposed as an activator of the innate immune response, little is known about the early steps that lead to gluten intolerance, so we wanted to study the effect of gluten stimulus on the m^{6}A mechanism.

Interestingly, we observed that upon GFD treatment in CD patients, the levels of total m^{6}A, *METTL3*, *YTHDF1*, *XPO1* and *IL8* expression reverted to normal, indicating that this pathway could be affected by gluten exposure. Our *in vitro* and *in vivo*

experiments, together with results from human biopsies, relate for the first time gliadin stimulation with an overall increase of m^{6}A and YTHDF1, which in turn results in augmented XPO1 protein levels. We have shown that the gluten-induced m^{6}A-mediated increase of XPO1 activates the NF-κB pathway, a characteristic of CD. Moreover, we also show that the XPO1-mediated induction of NF-κB is dependent of YTHDF1, thus supporting the implication of m^{6}A methylation in the gluten-induced inflammatory response in intestinal epithelial cells that is observed in CD. In addition, *Cxcl1*, considered a functional murine homolog of *IL8* (Hol et al., 2010), was also upregulated in the intestine of mice challenged with gliadin, confirming the XPO1-mediated activation of intestinal inflammation in response to the stress stimulus. Hence, as described for *IL15* (Abadie et al., 2020), it is possible that our mechanism could be involved in the initiation of a response against gluten and promote the activation of immune cells.

This novel link between m^{6}A modifications and gliadin exposure adds a completely new and unexplored layer to the already complex scenario of CD pathogenesis, and also opens the door to novel therapeutic approaches for individuals with CD. In addition, considering that viral infections and microbiome have been linked both to CD and to changes in m^{6}A methylation, further studies with different CD triggering agents could help us understand the factors involved in the development of innate immunity in CD.

In summary, our data stress the importance of the m^{6}A machinery in the gluten-mediated XPO1 increase that enhances NF-κB expression and subsequently leads to the induction of *IL8* in the enterocytes of CD patients (Fig44). The only reliable treatment for CD so far is a strict, lifelong removal of gluten from the diet, which reverses most of the disease symptoms, but negatively affects patients' quality of life and psychological well-being. This impacts long-term adherence to GFD and increases the risk of complications, including gastrointestinal cancers (Y. Han et al., 2015). Indeed, both *XPO1* and *IL8* levels are increased in tumor tissues from colon and colorectal adenocarcinomas (as observed in TGCA data) while YTHDF1 has

been described to regulate tumorigenicity in human colorectal adenocarcinomas (Bai et al., 2019). Interestingly, studies show that the risk to develop colon cancer in CD patients is lower in patients on GFD (Holmes et al., 1989).

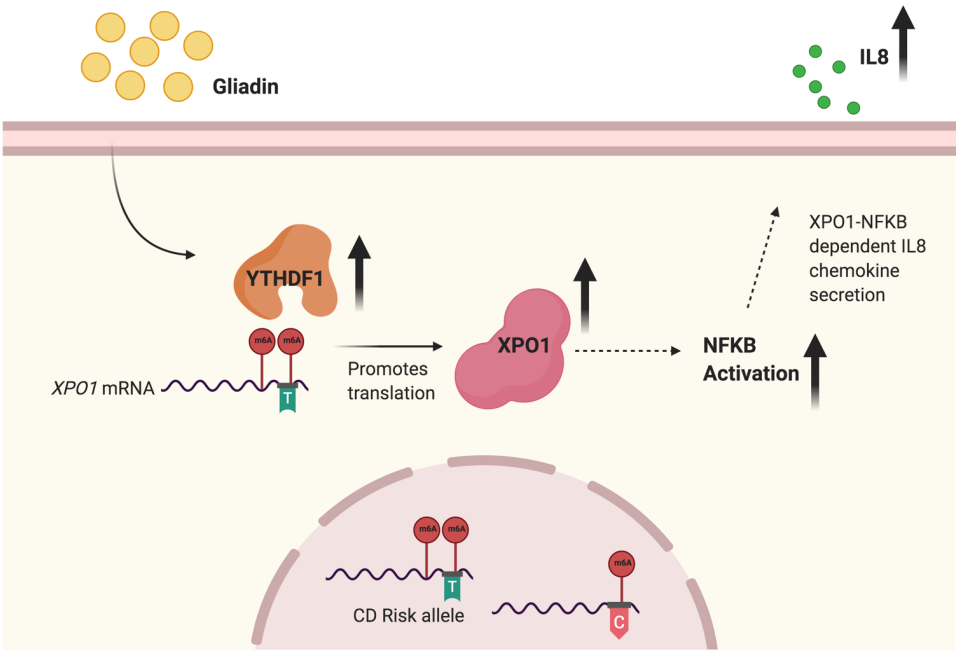

Figure 44. A gluten-responsive m^{6}A-*XPO1*-NF-κB pathway in epithelial cells. Gluten induces m^{6}A machinery and increase m^{6}A methylation levels in *XPO1* mRNA. Interaction between YTHDF1 reader and *XPO1* methylated mRNA promotes translation. Higher XPO1 levels activate NF-κB inflammatory pathway, leading to IL8 proinflammatory chemokine secretion.

Small molecules targeting m^{6}A readers and erasers have already been suggested as potential therapies for different types of cancer (Huang et al., 2020) and emerge as an option for protection against inflammation in CD patients. Furthermore, XPO1 inhibitors are already in use or in advanced clinical trials as anticancer therapeutic agents and have shown to have the ability to decrease NF-κB activity via nuclear retention of IκB-α (Sendino et al., 2018; Syed, 2019).

Thus, this study provides the first experimental evidence of the involvement of a gluten-responsive m^{6}A-*XPO1*-NF-κB pathway in the pathogenesis of CD, presenting novel potential therapeutic targets for this disease. The involvement of m^{6}A, *XPO1* and NF-κB in diverse intestinal malignancies supports that the m^{6}A-*XPO1*-NF-κB

axis may possibly function in response to small intestinal epithelial injury by other agents, which may have direct implications in the treatment of a variety of gastrointestinal disorders.

6.CONCLUSIONS

1. We developed a m^{6}A-RT-qPCR technique that is useful for m^{6}A methylation quantification. It uses the reduced ability of BstI enzyme as retrotranscriptase and it is followed by a quantitative PCR.

    a. This technique is capable of identifying site-specific m^{6}A methylation sites in different cell lines as well as in human samples.

    b. m^{6}A methylation changes upon cell stimulation or different disease stages can be quantified by our method.

2. We showed that overall m^{6}A methylation levels and m^{6}A writer *METTL3* and *YTHDF1* reader are increased in CD patients. Thus we have described for the first time that RNA m^{6}A modification is altered in CD.

    a. CD patients present increased total m^{6}A, *METTL3* and *YTHDF1* m^{6}A machinery genes.

    b. Gluten removal from CD patients' diet results in decreased m^{6}A, *METTL3* and *YTHDF1* levels.

3. The risk allele of the non-coding rs3087898 SNP in the 5'UTR of *XPO1* gene influences m^{6}A methylation levels resulting in higher XPO1 protein amounts.

    a. Risk allele (*XPO1*T*) is more methylated and induces higher XPO1 translation by preferential binding of YTHDF1 reader to the risk allele.

    b. m^{6}A-dependent increased XPO1 levels in the risk allele form activate NF-κB and downstream IL8 chemokine secretion, inducing a more severe inflammatory response and thus predisposing to develop CD.

4. Gluten, the main triggering agent in CD, activates m^6A machinery increasing methylation levels in the 5'UTR of *XPO1* and further inducing NF-κB-mediated inflammation.

    a. Gliadin stimulations show an induction of the m^6A machinery, what leads to an increase of m^6A methylation in *XPO1* 5'UTR and higher XPO1 levels.

    b. We showed that the increased NF-κB and downstream *IL8* levels characteristic in CD are, at least in part, m^6A and XPO1-dependent.

5. We present a novel m^6A-XPO1-NF-κB pathway that seems key in the early inflammatory response in intestinal cells upon gluten ingestion, offering new putative therapeutic targets for CD.

7.BIBLIOGRAPHY

Abadie, V., Kim, S. M., Lejeune, T., Palanski, B. A., Ernest, J. D., Tastet, O., Voisine, J., Discepolo, V., Marietta, E. V., Hawash, M. B. F., Ciszewski, C., Bouziat, R., Panigrahi, K., Horwath, I., Zurenski, M. A., Lawrence, I., Dumaine, A., Yotova, V., Grenier, J. C., … Jabri, B. (2020). IL-15, gluten and HLA-DQ8 drive tissue destruction in coeliac disease. *Nature*, *578*(7796), 600–604. https://doi.org/10.1038/s41586-020-2003-8

Abadie, V., Sollid, L. M., Barreiro, L. B., & Jabri, B. (2011). Integration of Genetic and Immunological Insights into a Model of Celiac Disease Pathogenesis. *Annual Review of Immunology*, *29*(1), 493–525. https://doi.org/10.1146/annurev-immunol-040210-092915

Akichika, S., Hirano, S., Shichino, Y., Suzuki, T., Nishimasu, H., Ishitani, R., Sugita, A., Hirose, Y., Iwasaki, S., Nureki, O., & Suzuki, T. (2019). Cap-specific terminal N 6 -methylation of RNA by an RNA polymerase II–associated methyltransferase. *Science*, *363*(6423). https://doi.org/10.1126/science.aav0080

Alarcón, C. R., Goodarzi, H., Lee, H., Liu, X., Tavazoie, S., & Tavazoie, S. F. (2015). HNRNPA2B1 Is a Mediator of m6A-Dependent Nuclear RNA Processing Events. *Cell*, *162*(6). https://doi.org/10.1016/j.cell.2015.08.011

Arguello, A. E., Deliberto, A. N., & Kleiner, R. E. (2017). RNA Chemical Proteomics Reveals the N6-Methyladenosine (m6A)-Regulated Protein-RNA Interactome. *Journal of the American Chemical Society*, *139*(48). https://doi.org/10.1021/jacs.7b09213

Bai, Y., Yang, C., Wu, R., Huang, L., Song, S., Li, W., Yan, P., Lin, C., Li, D., & Zhang, Y. (2019). YTHDF1 regulates tumorigenicity and cancer stem cell-like activity in human colorectal carcinoma. *Frontiers in Oncology*, *9*(MAY), 1–12. https://doi.org/10.3389/fonc.2019.00332

Bailey, A. S., Batista, P. J., Gold, R. S., Grace Chen, Y., de Rooij, D. G., Chang, H. Y., & Fuller, M. T. (2017). The conserved RNA helicase YTHDC2 regulates the transition from proliferation to differentiation in the germline. *ELife*, *6*. https://doi.org/10.7554/eLife.26116

Baldwin, A. S. (1996). The NF-κB and IκB proteins: New discoveries and insights.

Annual Review of Immunology, *14*. https://doi.org/10.1146/annurev.immunol.14.1.649

Barone, M. V., Troncone, R., & Auricchio, S. (2014). Gliadin peptides as triggers of the proliferative and stress/innate immune response of the celiac small intestinal mucosa. In *International Journal of Molecular Sciences* (Vol. 15, Issue 11). https://doi.org/10.3390/ijms151120518

Bokar, J. A., Shambaugh, M. E., Polayes, D., Matera, A. G., & Rottman, F. M. (1997). Purification and cDNA cloning of the AdoMet-binding subunit of the human mRNA (N6-adenosine)-methyltransferase. *RNA*, *3*(11).

Boulias, K., Toczydłowska-Socha, D., Hawley, B. R., Liberman, N., Takashima, K., Zaccara, S., Guez, T., Vasseur, J. J., Debart, F., Aravind, L., Jaffrey, S. R., & Greer, E. L. (2019). Identification of the m6Am Methyltransferase PCIF1 Reveals the Location and Functions of m6Am in the Transcriptome. *Molecular Cell*, *75*(3). https://doi.org/10.1016/j.molcel.2019.06.006

Caio, G., Volta, U., Sapone, A., Leffler, D. A., De Giorgio, R., Catassi, C., & Fasano, A. (2019). Celiac disease: A comprehensive current review. *BMC Medicine*, *17*(1), 1–20. https://doi.org/10.1186/s12916-019-1380-z

Capozzi, A., Vincentini, O., Gizzi, P., Porzia, A., Longo, A., Felli, C., Mattei, V., Mainiero, F., Silano, M., Sorice, M., & Misasi, R. (2013). Modulatory Effect of Gliadin Peptide 10-mer on Epithelial Intestinal CACO-2 Cell Inflammatory Response. *PLoS ONE*, *8*(6). https://doi.org/10.1371/journal.pone.0066561

Carlile, T. M., Rojas-Duran, M. F., Zinshteyn, B., Shin, H., Bartoli, K. M., & Gilbert, W. V. (2014). Pseudouridine profiling reveals regulated mRNA pseudouridylation in yeast and human cells. *Nature*, *515*(7525). https://doi.org/10.1038/nature13802

Castellanos-Rubio, A., Santin, I., Olazagoitia-Garmendia, A., Romero-Garmendia, I., Jauregi-Miguel, A., Legarda, M., & Bilbao, J. R. (2019). A novel RT-QPCR-based assay for the relative quantification of residue specific m6A RNA methylation. *Scientific Reports*, *9*(1). https://doi.org/10.1038/s41598-019-40018-6

Castellanos-Rubio, Ainara, & Bilbao, J. R. (2018). Profiling Celiac Disease-Related

Transcriptional Changes. In *International Review of Cell and Molecular Biology* (Vol. 336, pp. 149–174). Elsevier Inc. https://doi.org/10.1016/bs.ircmb.2017.07.003

Castellanos-Rubio, Ainara, Fernandez-Jimenez, N., Kratchmarov, R., Luo, X., Bhagat, G., Green, P. H. R., Schneider, R., Kiledjian, M., Bilbao, J. R., & Ghosh, S. (2016). A long noncoding RNA associated with susceptibility to celiac disease. *Science*, *352*(6281), 91–95. https://doi.org/10.1126/science.aad0467

Castellanos-Rubio, Ainara, Santin, I., Irastorza, I., Castaño, L., Carlos Vitoria, J., & Bilbao, J. R. (2009). TH17 (and TH1) signatures of intestinal biopsies of CD patients in response to gliadin. *Autoimmunity*, *42*(1). https://doi.org/10.1080/08916930802350789

Chander, A. M., Yadav, H., Jain, S., Bhadada, S. K., & Dhawan, D. K. (2018). Cross-talk between gluten, intestinal microbiota and intestinal mucosa in celiac disease: Recent advances and basis of autoimmunity. In *Frontiers in Microbiology* (Vol. 9, Issue NOV). https://doi.org/10.3389/fmicb.2018.02597

Chen, K., Lu, Z., Wang, X., Fu, Y., Luo, G. Z., Liu, N., Han, D., Dominissini, D., Dai, Q., Pan, T., & He, C. (2015). High-resolution N6-methyladenosine (m6A) map using photo-crosslinking-assisted m6A sequencing. *Angewandte Chemie - International Edition*, *54*(5). https://doi.org/10.1002/anie.201410647

Chen, Y. S., Yang, W. L., Zhao, Y. L., & Yang, Y. G. (2021). Dynamic transcriptomic m5C and its regulatory role in RNA processing. In *Wiley Interdisciplinary Reviews: RNA* (Vol. 12, Issue 4). https://doi.org/10.1002/wrna.1639

Coots, R. A., Liu, X. M., Mao, Y., Dong, L., Zhou, J., Wan, J., Zhang, X., & Qian, S. B. (2017). m6A Facilitates eIF4F-Independent mRNA Translation. *Molecular Cell*, *68*(3), 504-514.e7. https://doi.org/10.1016/j.molcel.2017.10.002

Cotsapas, C., Voight, B. F., Rossin, E., Lage, K., Neale, B. M., Wallace, C., AbecasisGonç, G. R., Barrett, J. C., Behrens, T., Cho, J., De Jager, P. L., Elder, J. T., Graham, R. R., Gregersen, P., Klareskog, L., Siminovitch, K. A., van Heel, D. A., Wijmenga, C., Worthington, J., … Daly, M. J. (2011).

Pervasive sharing of genetic effects in autoimmune disease. *PLoS Genetics*, *7*(8). https://doi.org/10.1371/journal.pgen.1002254

Cui, Q., Shi, H., Ye, P., Li, L., Qu, Q., Sun, G., Sun, G., Lu, Z., Huang, Y., Yang, C. G., Riggs, A. D., He, C., & Shi, Y. (2017). m6A RNA Methylation Regulates the Self-Renewal and Tumorigenesis of Glioblastoma Stem Cells. *Cell Reports*, *18*(11). https://doi.org/10.1016/j.celrep.2017.02.059

de Haas, E. C., Kumar, V., & Wijmenga, C. (2014). *Immunogenetics of Celiac Disease* (pp. 53–66). https://doi.org/10.1007/978-1-4614-8560-5_5

de Kauwe, A. L., Chen, Z., Anderson, R. P., Keech, C. L., Price, J. D., Wijburg, O., Jackson, D. C., Ladhams, J., Allison, J., & McCluskey, J. (2009). Resistance to Celiac Disease in Humanized HLA-DR3-DQ2-Transgenic Mice Expressing Specific Anti-Gliadin CD4 + T Cells . *The Journal of Immunology*, *182*(12), 7440–7450. https://doi.org/10.4049/jimmunol.0900233

Desrosiers, R., Friderici, K., & Rottman, F. (1974). Identification of methylated nucleosides in messenger RNA from Novikoff hepatoma cells. *Proceedings of the National Academy of Sciences of the United States of America*, *71*(10). https://doi.org/10.1073/pnas.71.10.3971

Dieli-Crimi, R., Cénit, M. C., & Núñez, C. (2015). The genetics of celiac disease: A comprehensive review of clinical implications. *Journal of Autoimmunity*, *64*, 26–41. https://doi.org/10.1016/j.jaut.2015.07.003

Diosdado, B., van Bakel, H., Strengman, E., Franke, L., van Oort, E., Mulder, C. J., Wijmenga, C., & Wapenaar, M. C. (2007). Neutrophil Recruitment and Barrier Impairment in Celiac Disease: A Genomic Study. *Clinical Gastroenterology and Hepatology*, *5*(5), 574–581. https://doi.org/10.1016/j.cgh.2006.11.014

Dominissini, D., Moshitch-Moshkovitz, S., Schwartz, S., Salmon-Divon, M., Ungar, L., Osenberg, S., Cesarkas, K., Jacob-Hirsch, J., Amariglio, N., Kupiec, M., Sorek, R., & Rechavi, G. (2012). Topology of the human and mouse m6A RNA methylomes revealed by m6A-seq. *Nature*, *485*(7397). https://doi.org/10.1038/nature11112

Dominissini, D., Nachtergaele, S., Moshitch-Moshkovitz, S., Peer, E., Kol, N., Ben-Haim, M. S., Dai, Q., Di Segni, A., Salmon-Divon, M., Clark, W. C., Zheng, G.,

Pan, T., Solomon, O., Eyal, E., Hershkovitz, V., Han, D., Doré, L. C., Amariglio, N., Rechavi, G., & He, C. (2016). The dynamic N1 - methyladenosine methylome in eukaryotic messenger RNA. *Nature*, *530*(7591). https://doi.org/10.1038/nature16998

Dubois, P. C. A., Trynka, G., Franke, L., Hunt, K. A., Romanos, J., Curtotti, A., Zhernakova, A., Heap, G. A. R., Ádány, R., Aromaa, A., Bardella, M. T., Van Den Berg, L. H., Bockett, N. A., De La Concha, E. G., Dema, B., Fehrmann, R. S. N., Fernández-Arquero, M., Fiatal, S., Grandone, E., … Van Heel, D. A. (2010). Multiple common variants for celiac disease influencing immune gene expression. *Nature Genetics*, *42*(4), 295–302. https://doi.org/10.1038/ng.543

Durbin, A. F., Wang, C., Marcotrigiano, J., & Gehrke, L. (2016). RNAs containing modified nucleotides fail to trigger RIG-I conformational changes for innate immune signaling. *MBio*, *7*(5). https://doi.org/10.1128/mBio.00833-16

Edupuganti, R. R., Geiger, S., Lindeboom, R. G. H., Shi, H., Hsu, P. J., Lu, Z., Wang, S. Y., Baltissen, M. P. A., Jansen, P. W. T. C., Rossa, M., Müller, M., Stunnenberg, H. G., He, C., Carell, T., & Vermeulen, M. (2017). N6-methyladenosine (m6A) recruits and repels proteins to regulate mRNA homeostasis. *Nature Structural and Molecular Biology*, *24*(10). https://doi.org/10.1038/nsmb.3462

Engel, M., Eggert, C., Kaplick, P. M., Eder, M., Röh, S., Tietze, L., Namendorf, C., Arloth, J., Weber, P., Rex-Haffner, M., Geula, S., Jakovcevski, M., Hanna, J. H., Leshkowitz, D., Uhr, M., Wotjak, C. T., Schmidt, M. V., Deussing, J. M., Binder, E. B., & Chen, A. (2018). The Role of m6A/m-RNA Methylation in Stress Response Regulation. *Neuron*, *99*(2), 389-403.e9. https://doi.org/10.1016/j.neuron.2018.07.009

Farh, K. K. H., Marson, A., Zhu, J., Kleinewietfeld, M., Housley, W. J., Beik, S., Shoresh, N., Whitton, H., Ryan, R. J. H., Shishkin, A. A., Hatan, M., Carrasco-Alfonso, M. J., Mayer, D., Luckey, C. J., Patsopoulos, N. A., De Jager, P. L., Kuchroo, V. K., Epstein, C. B., Daly, M. J., … Bernstein, B. E. (2015). Genetic and epigenetic fine mapping of causal autoimmune disease variants. *Nature*, *518*(7539). https://doi.org/10.1038/nature13835

Feighery, C. (1999). Fortnightly review: Coeliac disease. *BMJ*, *319*(7204). https://doi.org/10.1136/bmj.319.7204.236

Feng, Z., Li, Q., Meng, R., Yi, B., & Xu, Q. (2018). METTL3 regulates alternative splicing of MyD88 upon the lipopolysaccharide-induced inflammatory response in human dental pulp cells. *Journal of Cellular and Molecular Medicine*, *22*(5). https://doi.org/10.1111/jcmm.13491

Fernandez-jimenez, N., Castellanos-rubio, A., Plaza-izurieta, L., Irastorza, I., Elcoroaristizabal, X., Jauregi-miguel, A., Lopez-euba, T., Tutau, C., De pancorbo, M. M., Vitoria, J. C., & Bilbao, J. R. (2014). Coregulation and modulation of NFκB-related genes in celiac disease: Uncovered aspects of gut mucosal inflammation. *Human Molecular Genetics*. https://doi.org/10.1093/hmg/ddt520

Fernandez-Jimenez, N., Garcia-Etxebarria, K., Plaza-Izurieta, L., Romero-Garmendia, I., Jauregi-Miguel, A., Legarda, M., Ecsedi, S., Castellanos-Rubio, A., Cahais, V., Cuenin, C., Degli Esposti, D., Irastorza, I., Hernandez-Vargas, H., Herceg, Z., & Bilbao, J. R. (2019). The methylome of the celiac intestinal epithelium harbours genotype-independent alterations in the HLA region. *Scientific Reports*, *9*(1), 1–13. https://doi.org/10.1038/s41598-018-37746-6

Festen, E. A. M., Goyette, P., Green, T., Boucher, G., Beauchamp, C., Trynka, G., Dubois, P. C., Lagacé, C., Stokkers, P. C. F., Hommes, D. W., Barisani, D., Palmieri, O., Annese, V., van Heel, D. A., Weersma, R. K., Daly, M. J., Wijmenga, C., & Rioux, J. D. (2011). A meta-analysis of genome-wide association scans identifies IL18RAP, PTPN2, TAGAP, and PUS10 as shared risk loci for crohn's disease and celiac disease. *PLoS Genetics*, *7*(1). https://doi.org/10.1371/journal.pgen.1001283

Fusunyan, R. D., Quinn, J. J., Ohno, Y., MacDermott, R. P., & Sanderson, I. R. (1998). Butyrate enhances interleukin (IL)-8 secretion by intestinal epithelial cells in response to IL-1β and lipopolysaccharide. *Pediatric Research*, *43*(1). https://doi.org/10.1203/00006450-199801000-00013

Garcia-Campos, M. A., Edelheit, S., Toth, U., Safra, M., Shachar, R., Viukov, S., Winkler, R., Nir, R., Lasman, L., Brandis, A., Hanna, J. H., Rossmanith, W., &

Schwartz, S. (2019). Deciphering the “m6A Code” via Antibody-Independent Quantitative Profiling. *Cell*, *178*(3). https://doi.org/10.1016/j.cell.2019.06.013

Garcia-Etxebarria, K., Jauregi-Miguel, A., Romero-Garmendia, I., Plaza-Izurieta, L., Legarda, M., Irastorza, I., & Bilbao, J. R. (2016). Ancestry-based stratified analysis of Immunochip data identifies novel associations with celiac disease. *European Journal of Human Genetics*, *24*(12). https://doi.org/10.1038/ejhg.2016.120

Garrote, J. A., Gómez-González, E., Bernardo, D., Arranz, E., & Chirdo, F. (2008). Celiac Disease Pathogenesis: The Proinflammatory Cytokine Network. *Journal of Pediatric Gastroenterology and Nutrition*, *47*(Suppl 1), S27–S32. https://doi.org/10.1097/MPG.0b013e3181818fb9

Geula, S., Moshitch-Moshkovitz, S., Dominissini, D., Mansour, A. A. F., Kol, N., Salmon-Divon, M., Hershkovitz, V., Peer, E., Mor, N., Manor, Y. S., Ben-Haim, M. S., Eyal, E., Yunger, S., Pinto, Y., Jaitin, D. A., Viukov, S., Rais, Y., Krupalnik, V., Chomsky, E., … Hanna, J. H. (2015). m6A mRNA methylation facilitates resolution of naïve pluripotency toward differentiation. *Science*, *347*(6225), 1002–1006. https://doi.org/10.1126/science.1261417

Goel, G., Tye-Din, J. A., Qiao, S. W., Russell, A. K., Mayassi, T., Ciszewski, C., Sarna, V. K., Wang, S., Goldstein, K. E., Dzuris, J. L., Williams, L. J., Xavier, R. J., Lundin, K. E. A., Jabri, B., Sollid, L. M., & Anderson, R. P. (2019). Cytokine release and gastrointestinal symptoms after gluten challenge in celiac disease. *Science Advances*, *5*(8), eaaw7756. https://doi.org/10.1126/sciadv.aaw7756

Gonzalez-Moro, I., Olazagoitia-Garmendia, A., Colli, M. L., Cobo-Vuilleumier, N., Postler, T. S., Marselli, L., Marchetti, P., Ghosh, S., Gauthier, B. R., Eizirik, D. L., Castellanos-Rubio, A., & Santin, I. (2020). The T1D-associated lncRNA Lnc13 modulates human pancreatic β cell inflammation by allele-specific stabilization of STAT1 mRNA. *Proceedings of the National Academy of Sciences of the United States of America*, *117*(16). https://doi.org/10.1073/pnas.1914353117

Gravina, G. L., Senapedis, W., McCauley, D., Baloglu, E., Shacham, S., &

Festuccia, C. (2014). Nucleo-cytoplasmic transport as a therapeutic target of cancer. In *Journal of Hematology and Oncology* (Vol. 7, Issue 1). BioMed Central Ltd. https://doi.org/10.1186/s13045-014-0085-1

Greco, L., Romino, R., Coto, I., Di Cosmo, N., Percopo, S., Maglio, M., Paparo, F., Gasperi, V., Limongelli, M. G., Cotichini, R., D'Agate, C., Tinto, N., Sacchetti, L., Tosi, R., & Stazi, M. A. (2002). The first large population based twin study of coeliac disease. *Gut*, *50*(5). https://doi.org/10.1136/gut.50.5.624

Grilli, M., Chiu, J. J. S., & Lenardo, M. J. (1993). IMF-κB and Rel: Participants in a Multiform Transcriptional Regulatory System. *International Review of Cytology*, *143*(C). https://doi.org/10.1016/S0074-7696(08)61873-2

Gujral, N., Freeman, H. J., & Thomson, A. B. R. (2012). Celiac disease: Prevalence, diagnosis, pathogenesis and treatment. In *World Journal of Gastroenterology* (Vol. 18, Issue 42). https://doi.org/10.3748/wjg.v18.i42.6036

Gutierrez-Achury, J., Zhernakova, A., Pulit, S. L., Trynka, G., Hunt, K. A., Romanos, J., Raychaudhuri, S., Van Heel, D. A., Wijmenga, C., & De Bakker, P. I. W. (2015). Fine mapping in the MHC region accounts for 18% additional genetic risk for celiac disease. *Nature Genetics*, *47*(6), 577–578. https://doi.org/10.1038/ng.3268

Han, D., Liu, J., Chen, C., Dong, L., Liu, Y., Chang, R., Huang, X., Liu, Y., Wang, J., Dougherty, U., Bissonnette, M. B., Shen, B., Weichselbaum, R. R., Xu, M. M., & He, C. (2019). Anti-tumour immunity controlled through mRNA m6A methylation and YTHDF1 in dendritic cells. *Nature*, *566*(7743), 270–274. https://doi.org/10.1038/s41586-019-0916-x

Han, Y., Chen, W., Li, P., & Ye, J. (2015). Association between coeliac disease and risk of any malignancy and gastrointestinal malignancy: A meta-analysis. *Medicine (United States)*, *94*(38), 1–7. https://doi.org/10.1097/MD.0000000000001612

Harcourt, E. M., Ehrenschwender, T., Batista, P. J., Chang, H. Y., & Kool, E. T. (2013). Identification of a selective polymerase enables detection of N 6-methyladenosine in RNA. *Journal of the American Chemical Society*, *135*(51). https://doi.org/10.1021/ja4105792

Hofacker, I. L. (2003). Vienna RNA secondary structure server. *Nucleic Acids Research*. https://doi.org/10.1093/nar/gkg599

Hol, J., Wilhelmsen, L., & Haraldsen, G. (2010). The murine IL-8 homologues KC, MIP-2, and LIX are found in endothelial cytoplasmic granules but not in Weibel-Palade bodies. *Journal of Leukocyte Biology*, *87*(3), 501–508. https://doi.org/10.1189/jlb.0809532

Holmes, G. K. T., Prior, P., Lane, M. R., Pope, D., & Allan, R. N. (1989). Malignancy in coeliac disease - Effect of a gluten free diet. *Gut*, *30*(3), 333–338. https://doi.org/10.1136/gut.30.3.333

Hsu, P. J., Zhu, Y., Ma, H., Guo, Y., Shi, X., Liu, Y., Qi, M., Lu, Z., Shi, H., Wang, J., Cheng, Y., Luo, G., Dai, Q., Liu, M., Guo, X., Sha, J., Shen, B., & He, C. (2017). Ythdc2 is an N6 -methyladenosine binding protein that regulates mammalian spermatogenesis. *Cell Research*, *27*(9). https://doi.org/10.1038/cr.2017.99

Huang, H., Weng, H., & Chen, J. (2020). m6A Modification in Coding and Non-coding RNAs: Roles and Therapeutic Implications in Cancer. *Cancer Cell*, *37*(3), 270–288. https://doi.org/10.1016/j.ccell.2020.02.004

Huang, H., Weng, H., Sun, W., Qin, X., Shi, H., Wu, H., Zhao, B. S., Mesquita, A., Liu, C., Yuan, C. L., Hu, Y. C., Hüttelmaier, S., Skibbe, J. R., Su, R., Deng, X., Dong, L., Sun, M., Li, C., Nachtergaele, S., … Chen, J. (2018). Recognition of RNA N 6 -methyladenosine by IGF2BP proteins enhances mRNA stability and translation. *Nature Cell Biology*, *20*(3). https://doi.org/10.1038/s41556-018-0045-z

Imaeda, A., Tomoike, F., Hayakawa, M., Nakamoto, K., Kimura, Y., Abe, N., & Abe, H. (2019). N6-methyl adenosine in siRNA evades immune response without reducing RNAi activity. *Nucleosides, Nucleotides and Nucleic Acids*, *38*(12). https://doi.org/10.1080/15257770.2019.1641205

Jabri, B., & Sollid, L. M. (2006). Mechanisms of disease: Immunopathogenesis of celiac disease. In *Nature Clinical Practice Gastroenterology and Hepatology* (Vol. 3, Issue 9, pp. 516–525). Nature Publishing Group. https://doi.org/10.1038/ncpgasthep0582

Jabri, B., & Sollid, L. M. (2009). Tissue-mediated control of immunopathology in coeliac disease. In *Nature Reviews Immunology* (Vol. 9, Issue 12). https://doi.org/10.1038/nri2670

Jabs, S., Biton, A., Bécavin, C., Nahori, M. A., Ghozlane, A., Pagliuso, A., Spanò, G., Guérineau, V., Touboul, D., Giai Gianetto, Q., Chaze, T., Matondo, M., Dillies, M. A., & Cossart, P. (2020). Impact of the gut microbiota on the m6A epitranscriptome of mouse cecum and liver. *Nature Communications*, *11*(1), 1–16. https://doi.org/10.1038/s41467-020-15126-x

Jain, D., Puno, M. R., Meydan, C., Lailler, N., Mason, C. E., Lima, C. D., Anderson, K. V., & Keeney, S. (2018). Ketu mutant mice uncover an essential meiotic function for the ancient RNA helicase YTHDC2. *ELife*, *7*. https://doi.org/10.7554/eLife.30919

Jauregi-Miguel, A., Santin, I., Garcia-Etxebarria, K., Olazagoitia-Garmendia, A., Romero-Garmendia, I., Sebastian-delaCruz, M., Irastorza, I., Castellanos-Rubio, A., & Bilbao, J. R. (2019). MAGI2 Gene Region and Celiac Disease. *Frontiers in Nutrition*, *6*. https://doi.org/10.3389/fnut.2019.00187

Jelínková, L., Tučková, L., Cinová, J., Flegelová, Z., & Tlaskalová-Hogenová, H. (2004). Gliadin stimulates human monocytes to production of IL-8 and TNF-α through a mechanism involving NF-κB. *FEBS Letters*, *571*(1–3), 81–85. https://doi.org/10.1016/j.febslet.2004.06.057

Jia, G., Fu, Y., Zhao, X., Dai, Q., Zheng, G., Yang, Y., Yi, C., Lindahl, T., Pan, T., Yang, Y. G., & He, C. (2011). N6-Methyladenosine in nuclear RNA is a major substrate of the obesity-associated FTO. *Nature Chemical Biology*, *7*(12), 885–887. https://doi.org/10.1038/nchembio.687

Jiang, X., Liu, B., Nie, Z., Duan, L., Xiong, Q., Jin, Z., Yang, C., & Chen, Y. (2021). The role of m6A modification in the biological functions and diseases. In *Signal Transduction and Targeted Therapy* (Vol. 6, Issue 1). https://doi.org/10.1038/s41392-020-00450-x

Jonkhout, N., Tran, J., Smith, M. A., Schonrock, N., Mattick, J. S., & Novoa, E. M. (2017). The RNA modification landscape in human disease. In *RNA* (Vol. 23, Issue 12). https://doi.org/10.1261/rna.063503.117

Karikó, K., Buckstein, M., Ni, H., & Weissman, D. (2005). Suppression of RNA recognition by Toll-like receptors: The impact of nucleoside modification and the evolutionary origin of RNA. *Immunity*, *23*(2). https://doi.org/10.1016/j.immuni.2005.06.008

Kashyap, T., Argueta, C., Aboukameel, A., Unger, T. J., Klebanov, B., Mohammad, R. M., Muqbil, I., Azmi, A. S., Drolen, C., Senapedis, W., Lee, M., Kauffman, M., Shacham, S., & Landesman, Y. (2016). Selinexor, a Selective Inhibitor of Nuclear Export (SINE) compound, acts through NF-κB deactivation and combines with proteasome inhibitors to synergistically induce tumor cell death. *Oncotarget*, *7*(48). https://doi.org/10.18632/oncotarget.12428

Kasowitz, S. D., Ma, J., Anderson, S. J., Leu, N. A., Xu, Y., Gregory, B. D., Schultz, R. M., & Wang, P. J. (2018). Nuclear m6A reader YTHDC1 regulates alternative polyadenylation and splicing during mouse oocyte development. *PLoS Genetics*, *14*(5). https://doi.org/10.1371/journal.pgen.1007412

Ke, S., Alemu, E. A., Mertens, C., Gantman, E. C., Fak, J. J., Mele, A., Haripal, B., Zucker-Scharff, I., Moore, M. J., Park, C. Y., Vågbø, C. B., Kuśnierczyk, A., Klungland, A., Darnell, J. E., & Darnell, R. B. (2015). A majority of m6A residues are in the last exons, allowing the potential for 3' UTR regulation. *Genes and Development*, *29*(19). https://doi.org/10.1101/gad.269415.115

Kim, H., Lim, J. W., & Kim, K. H. (2001). Helicobacter pylori-induced expression of interleukin-8 and cyclooxygenase-2 in AGS gastric epithelial cells: Mediation by nuclear factor-κB. *Scandinavian Journal of Gastroenterology*, *36*(7). https://doi.org/10.1080/003655201300191969

Kim, S. M., Mayassi, T., & Jabri, B. (2015). Innate immunity: Actuating the gears of celiac disease pathogenesis. *Best Practice and Research: Clinical Gastroenterology*, *29*(3), 425–435. https://doi.org/10.1016/j.bpg.2015.05.001

König, J., Zarnack, K., Rot, G., Curk, T., Kayikci, M., Zupan, B., Turner, D. J., Luscombe, N. M., & Ule, J. (2010). ICLIP reveals the function of hnRNP particles in splicing at individual nucleotide resolution. *Nature Structural and Molecular Biology*, *17*(7). https://doi.org/10.1038/nsmb.1838

Koranda, J. L., Dore, L., Shi, H., Patel, M. J., Vaasjo, L. O., Rao, M. N., Chen, K.,

Lu, Z., Yi, Y., Chi, W., He, C., & Zhuang, X. (2018). Mettl14 Is Essential for Epitranscriptomic Regulation of Striatal Function and Learning. *Neuron*, *99*(2), 283-292.e5. https://doi.org/10.1016/j.neuron.2018.06.007

Kumar, V., Wijmenga, C., & Xavier, R. J. (2014). Genetics of immune-mediated disorders: From genome-wide association to molecular mechanism. In *Current Opinion in Immunology* (Vol. 31). https://doi.org/10.1016/j.coi.2014.09.007

Lammers, K. M., Khandelwal, S., Chaudhry, F., Kryszak, D., Puppa, E. L., Casolaro, V., & Fasano, A. (2011). Identification of a novel immunomodulatory gliadin peptide that causes interleukin-8 release in a chemokine receptor CXCR3-dependent manner only in patients with coeliac disease. *Immunology*, *132*(3), 432–440. https://doi.org/10.1111/j.1365-2567.2010.03378.x

Lee, C., & Huang, C. H. (2013). LASAGNA-search: An integrated web tool for transcription factor binding site search and visualization. *BioTechniques*. https://doi.org/10.2144/000113999

Lerner, A. (2010). New therapeutic strategies for celiac disease. In *Autoimmunity Reviews* (Vol. 9, Issue 3). https://doi.org/10.1016/j.autrev.2009.05.002

Li, F., Zhao, D., Wu, J., & Shi, Y. (2014). Structure of the YTH domain of human YTHDF2 in complex with an m6A mononucleotide reveals an aromatic cage for m6A recognition. In *Cell Research* (Vol. 24, Issue 12, pp. 1490–1492). Nature Publishing Group. https://doi.org/10.1038/cr.2014.153

Li, H. B., Tong, J., Zhu, S., Batista, P. J., Duffy, E. E., Zhao, J., Bailis, W., Cao, G., Kroehling, L., Chen, Y., Wang, G., Broughton, J. P., Chen, Y. G., Kluger, Y., Simon, M. D., Chang, H. Y., Yin, Z., & Flavell, R. A. (2017). M 6 A mRNA methylation controls T cell homeostasis by targeting the IL-7/STAT5/SOCS pathways. *Nature*, *548*(7667). https://doi.org/10.1038/nature23450

Li, X., Xiong, X., & Yi, C. (2016). Epitranscriptome sequencing technologies: Decoding RNA modifications. In *Nature Methods* (Vol. 14, Issue 1). https://doi.org/10.1038/nmeth.4110

Lichinchi, G., Gao, S., Saletore, Y., Gonzalez, G. M., Bansal, V., Wang, Y., Mason, C. E., & Rana, T. M. (2016). Dynamics of the human and viral m(6)A RNA methylomes during HIV-1 infection of T cells. *Nature Microbiology*, *1*.

https://doi.org/10.1038/nmicrobiol.2016.11

Linder, B., Grozhik, A. V., Olarerin-George, A. O., Meydan, C., Mason, C. E., & Jaffrey, S. R. (2015). Single-nucleotide-resolution mapping of m6A and m6Am throughout the transcriptome. *Nature Methods*, *12*(8). https://doi.org/10.1038/nmeth.3453

Lionetti, E., Castellaneta, S., Francavilla, R., Pulvirenti, A., Tonutti, E., Amarri, S., Barbato, M., Barbera, C., Barera, G., Bellantoni, A., Castellano, E., Guariso, G., Limongelli, M. G., Pellegrino, S., Polloni, C., Ughi, C., Zuin, G., Fasano, A., & Catassi, C. (2014). Introduction of Gluten, HLA Status, and the Risk of Celiac Disease in Children. *New England Journal of Medicine*, *371*(14). https://doi.org/10.1056/nejmoa1400697

Liu, H., Wang, H., Wei, Z., Zhang, S., Hua, G., Zhang, S. W., Zhang, L., Gao, S. J., Meng, J., Chen, X., & Huang, Y. (2018). MeT-DB V2.0: Elucidating context-specific functions of N 6 -methyl-adenosine methyltranscriptome. *Nucleic Acids Research*, *46*(D1), D281–D287. https://doi.org/10.1093/nar/gkx1080

Liu, J., Yue, Y., Han, D., Wang, X., Fu, Y., Zhang, L., Jia, G., Yu, M., Lu, Z., Deng, X., Dai, Q., Chen, W., & He, C. (2014). A METTL3-METTL14 complex mediates mammalian nuclear RNA N6-adenosine methylation. *Nature Chemical Biology*, *10*(2), 93–95. https://doi.org/10.1038/nchembio.1432

Liu, N., Dai, Q., Zheng, G., He, C., Parisien, M., & Pan, T. (2015). N6 -methyladenosine-dependent RNA structural switches regulate RNA-protein interactions. *Nature*, *518*(7540). https://doi.org/10.1038/nature14234

Liu, N., Parisien, M., Dai, Q., Zheng, G., He, C., & Pan, T. (2013). Probing N6-methyladenosine RNA modification status at single nucleotide resolution in mRNA and long noncoding RNA. *RNA*, *19*(12). https://doi.org/10.1261/rna.041178.113

Liu, N., Zhou, K. I., Parisien, M., Dai, Q., Diatchenko, L., & Pan, T. (2017). N6-methyladenosine alters RNA structure to regulate binding of a low-complexity protein. *Nucleic Acids Research*, *45*(10). https://doi.org/10.1093/nar/gkx141

Louka, A. S., & Sollid, L. M. (2003). HLA in coeliac disease: Unravelling the complex genetics of a complex disorder. In *Tissue Antigens* (Vol. 61, Issue 2).

https://doi.org/10.1034/j.1399-0039.2003.00017.x

Lu, T. X., Zheng, Z., Zhang, L., Sun, H.-L., Bissonnette, M., Huang, H., & He, C. (2020). A new model of spontaneous colitis in mice induced by deletion of an RNA m6A methyltransferase component METTL14 in T cells. *Cellular and Molecular Gastroenterology and Hepatology*. https://doi.org/10.1016/J.JCMGH.2020.07.001

M, C. (2016). The Selective Inhibitor of Nuclear Export Compound, Selinexor, Inhibits NF-κB and Induces Anti-Non-Small Cell Lung Cancer Activity Regardless of p53 Status. *International Journal of Cancer Research and Molecular Mechanisms*, *2*(2), 1–11. https://doi.org/10.16966/2381-3318.126

Ma, H., Wang, X., Cai, J., Dai, Q., Natchiar, S. K., Lv, R., Chen, K., Lu, Z., Chen, H., Shi, Y. G., Lan, F., Fan, J., Klaholz, B. P., Pan, T., Shi, Y., & He, C. (2019). Publisher Correction: N 6-Methyladenosine methyltransferase ZCCHC4 mediates ribosomal RNA methylation (Nature Chemical Biology, (2019), 15, 1, (88-94), 10.1038/s41589-018-0184-3). In *Nature Chemical Biology* (Vol. 15, Issue 5). https://doi.org/10.1038/s41589-019-0233-6

Machnicka, M. A., Milanowska, K., Oglou, O. O., Purta, E., Kurkowska, M., Olchowik, A., Januszewski, W., Kalinowski, S., Dunin-Horkawicz, S., Rother, K. M., Helm, M., Bujnicki, J. M., & Grosjean, H. (2013). MODOMICS: A database of RNA modification pathways - 2013 update. *Nucleic Acids Research*, *41*(D1). https://doi.org/10.1093/nar/gks1007

Maity, A., & Das, B. (2016). N6-methyladenosine modification in mRNA: Machinery, function and implications for health and diseases. In *FEBS Journal* (Vol. 283, Issue 9). https://doi.org/10.1111/febs.13614

Maiuri, M. C., De Stefano, D., Mele, G., Fecarotta, S., Greco, L., Troncone, R., & Carnuccio, R. (2003). Nuclear factor κB is activated in small intestinal mucosa of celiac patients. *Journal of Molecular Medicine*, *81*(6), 373–379. https://doi.org/10.1007/s00109-003-0440-0

Mäki, M., & Collin, P. (1997). Coeliac disease. In *Lancet* (Vol. 349, Issue 9067, pp. 1755–1759). Elsevier B.V. https://doi.org/10.1016/S0140-6736(96)70237-4

Manavalan, J. S., Hernandez, L., Shah, J. G., Konikkara, J., Naiyer, A. J., Lee, A.

R., Ciaccio, E., Minaya, M. T., Green, P. H. R., & Bhagat, G. (2010). Serum cytokine elevations in celiac disease: Association with disease presentation. *Human Immunology*, *71*(1), 50–57. https://doi.org/10.1016/j.humimm.2009.09.351

Mauer, J., Luo, X., Blanjoie, A., Jiao, X., Grozhik, A. V., Patil, D. P., Linder, B., Pickering, B. F., Vasseur, J. J., Chen, Q., Gross, S. S., Elemento, O., Debart, F., Kiledjian, M., & Jaffrey, S. R. (2017). Reversible methylation of m6 Am in the 5′ cap controls mRNA stability. *Nature*, *541*(7637). https://doi.org/10.1038/nature21022

Maynard, C. L., Elson, C. O., Hatton, R. D., & Weaver, C. T. (2012). Reciprocal interactions of the intestinal microbiota and immune system. In *Nature* (Vol. 489, Issue 7415). https://doi.org/10.1038/nature11551

McIntyre, A. B. R., Gokhale, N. S., Cerchietti, L., Jaffrey, S. R., Horner, S. M., & Mason, C. E. (2020). Limits in the detection of m6A changes using MeRIP/m6A-seq. *Scientific Reports*, *10*(1). https://doi.org/10.1038/s41598-020-63355-3

Meresse, B., Curran, S. A., Ciszewski, C., Orbelyan, G., Setty, M., Bhagat, G., Lee, L., Tretiakova, M., Semrad, C., Kistner, E., Winchester, R. J., Braud, V., Lanier, L. L., Geraghty, D. E., Green, P. H., Guandalini, S., & Jabri, B. (2006). Reprogramming of CTLs into natural killer-like cells in celiac disease. *Journal of Experimental Medicine*, *203*(5). https://doi.org/10.1084/jem.20060028

Meyer, K. D., Patil, D. P., Zhou, J., Zinoviev, A., Skabkin, M. A., Elemento, O., Pestova, T. V., Qian, S. B., & Jaffrey, S. R. (2015). 5′ UTR m6A Promotes Cap-Independent Translation. *Cell*, *163*(4), 999–1010. https://doi.org/10.1016/j.cell.2015.10.012

Meyer, K. D., Saletore, Y., Zumbo, P., Elemento, O., Mason, C. E., & Jaffrey, S. R. (2012). Comprehensive analysis of mRNA methylation reveals enrichment in 3′ UTRs and near stop codons. *Cell*, *149*(7). https://doi.org/10.1016/j.cell.2012.05.003

Molinie, B., Wang, J., Lim, K. S., Hillebrand, R., Lu, Z. X., Van Wittenberghe, N., Howard, B. D., Daneshvar, K., Mullen, A. C., Dedon, P., Xing, Y., &

Giallourakis, C. C. (2016). M6 A-LAIC-seq reveals the census and complexity of the m6 A epitranscriptome. *Nature Methods*, *13*(8). https://doi.org/10.1038/nmeth.3898

Mowel, W. K., Kotzin, J. J., McCright, S. J., Neal, V. D., & Henao-Mejia, J. (2018). Control of Immune Cell Homeostasis and Function by lncRNAs. In *Trends in Immunology* (Vol. 39, Issue 1, pp. 55–69). Elsevier Ltd. https://doi.org/10.1016/j.it.2017.08.009

Murray, J. A., Watson, T., Clearman, B., & Mitros, F. (2004). Effect of a gluten-free diet on gastrointestinal symptoms in celiac disease. *American Journal of Clinical Nutrition*, *79*(4). https://doi.org/10.1093/ajcn/79.4.669

Nayler, O., Hartmann, A. M., & Stamm, S. (2000). The ER repeat protein YT521-B localizes to a novel subnuclear compartment. *Journal of Cell Biology*, *150*(5). https://doi.org/10.1083/jcb.150.5.949

Nisticò, L., Fagnani, C., Coto, I., Percopo, S., Cotichini, R., Limongelli, M. G., Paparo, F., D'Alfonso, S., Giordano, M., Sferlazzas, C., Magazzù, G., Momigliano-Richiardi, P., Greco, L., & Stazi, M. A. (2006). Concordance, disease progression, and heritability of coeliac disease in Italian twins. *Gut*, *55*(6). https://doi.org/10.1136/gut.2005.083964

Olazagoitia-Garmendia, A., & Castellanos-Rubio, A. (2021). Relative Quantification of Residue-Specific m6A RNA Methylation Using m6A-RT-QPCR. In *Methods in Molecular Biology* (Vol. 2298). https://doi.org/10.1007/978-1-0716-1374-0_12

Olazagoitia-Garmendia, A., Sebastian-delaCruz, M., & Castellanos-Rubio, A. (2021). Involvement of lncRNAs in celiac disease pathogenesis. In *International Review of Cell and Molecular Biology* (Vol. 358). https://doi.org/10.1016/bs.ircmb.2020.10.004

Olivares, M., Benítez-Páez, A., de Palma, G., Capilla, A., Nova, E., Castillejo, G., Varea, V., Marcos, A., Garrote, J. A., Polanco, I., Donat, E., Ribes-Koninckx, C., Calvo, C., Ortigosa, L., Palau, F., & Sanz, Y. (2018). Increased prevalence of pathogenic bacteria in the gut microbiota of infants at risk of developing celiac disease: The PROFICEL study. *Gut Microbes*, *9*(6).

https://doi.org/10.1080/19490976.2018.1451276

Palmer, D. C., & Restifo, N. P. (2009). Suppressors of cytokine signaling (SOCS) in T cell differentiation, maturation, and function. In *Trends in Immunology* (Vol. 30, Issue 12). https://doi.org/10.1016/j.it.2009.09.009

Parkes, M., Cortes, A., Van Heel, D. A., & Brown, M. A. (2013). Genetic insights into common pathways and complex relationships among immune-mediated diseases. In *Nature Reviews Genetics* (Vol. 14, Issue 9). https://doi.org/10.1038/nrg3502

Parmar, A., Greco, D., Venäläinen, J., Gentile, M., Dukes, E., & Saavalainen, P. (2013). Gene Expression Profiling of Gliadin Effects on Intestinal Epithelial Cells Suggests Novel Non-Enzymatic Functions of Pepsin and Trypsin. *PLoS ONE*, *8*(6). https://doi.org/10.1371/journal.pone.0066307

Patil, D. P., Chen, C. K., Pickering, B. F., Chow, A., Jackson, C., Guttman, M., & Jaffrey, S. R. (2016). M6 A RNA methylation promotes XIST-mediated transcriptional repression. *Nature*, *537*(7620). https://doi.org/10.1038/nature19342

Patil, D. P., Pickering, B. F., & Jaffrey, S. R. (2018). Reading m6A in the Transcriptome: m6A-Binding Proteins. In *Trends in Cell Biology* (Vol. 28, Issue 2, pp. 113–127). Elsevier Ltd. https://doi.org/10.1016/j.tcb.2017.10.001

Pendleton, K. E., Chen, B., Liu, K., Hunter, O. V., Xie, Y., Tu, B. P., & Conrad, N. K. (2017). The U6 snRNA m6A Methyltransferase METTL16 Regulates SAM Synthetase Intron Retention. *Cell*, *169*(5). https://doi.org/10.1016/j.cell.2017.05.003

Picarelli, A., Di Tola, M., Sabbatella, L., Anania, M. C., Di Cello, T., Greco, R., Silano, M., & De Vincenzi, M. (1999). 31-43 Amino acid sequence of the α-gliadin induces anti-endomysial antibody production during in vitro challenge. *Scandinavian Journal of Gastroenterology*, *34*(11). https://doi.org/10.1080/003655299750024896

Ping, X. L., Sun, B. F., Wang, L., Xiao, W., Yang, X., Wang, W. J., Adhikari, S., Shi, Y., Lv, Y., Chen, Y. S., Zhao, X., Li, A., Yang, Y., Dahal, U., Lou, X. M., Liu, X., Huang, J., Yuan, W. P., Zhu, X. F., … Yang, Y. G. (2014). Mammalian

WTAP is a regulatory subunit of the RNA N6-methyladenosine methyltransferase. *Cell Research*, *24*(2). https://doi.org/10.1038/cr.2014.3

Plaza-Izurieta, L., Fernandez-Jimenez, N., Irastorza, I., Jauregi-Miguel, A., Romero-Garmendia, I., Vitoria, J. C., & Bilbao, J. R. (2015). Expression analysis in intestinal mucosa reveals complex relations among genes under the association peaks in celiac disease. *European Journal of Human Genetics*, *23*(8), 1100–1105. https://doi.org/10.1038/ejhg.2014.244

Ricaño-Ponce, I., Zhernakova, D. V., Deelen, P., Luo, O., Li, X., Isaacs, A., Karjalainen, J., Di Tommaso, J., Borek, Z. A., Zorro, M. M., Gutierrez-Achury, J., Uitterlinden, A. G., Hofman, A., van Meurs, J., Netea, M. G., Jonkers, I. H., Withoff, S., van Duijn, C. M., Li, Y., … BIOS consortium. (2016). Refined mapping of autoimmune disease associated genetic variants with gene expression suggests an important role for non-coding RNAs. *Journal of Autoimmunity*, *68*, 62–74. https://doi.org/10.1016/j.jaut.2016.01.002

Roadmap Epigenomics Consortium, Kundaje, A., Meuleman, W., Ernst, J., Bilenky, M., Yen, A., Heravi-Moussavi, A., Kheradpour, P., Zhang, Z., Wang, J., Ziller, M. J., Amin, V., Whitaker, J. W., Schultz, M. D., Ward, L. D., Sarkar, A., Quon, G., Sandstrom, R. S., Eaton, M. L., … Kellis, M. (2015). Integrative analysis of 111 reference human epigenomes. *Nature*, *518*(7539). https://doi.org/10.1038/nature14248

Robinson, E. K., Covarrubias, S., & Carpenter, S. (2020). The how and why of lncRNA function: An innate immune perspective. In *Biochimica et Biophysica Acta - Gene Regulatory Mechanisms* (Vol. 1863, Issue 4, p. 194419). Elsevier B.V. https://doi.org/10.1016/j.bbagrm.2019.194419

Rodríguez, J. A., & Henderson, B. R. (2000). Identification of a functional nuclear export sequence in BRCA1. *Journal of Biological Chemistry*, *275*(49), 38589–38596. https://doi.org/10.1074/jbc.M003851200

Roebuck, K. A. (1999). Regulation of interleukin-8 gene expression. In *Journal of Interferon and Cytokine Research* (Vol. 19, Issue 5). https://doi.org/10.1089/107999099313866

Roignant, J. Y., & Soller, M. (2017). m6A in mRNA: An Ancient Mechanism for

Fine-Tuning Gene Expression. In *Trends in Genetics* (Vol. 33, Issue 6). https://doi.org/10.1016/j.tig.2017.04.003

Romero-Garmendia, I., Jauregi-Miguel, A., Santin, I., Bilbao, J. R., & Castellanos-Rubio, A. (2018). Subcellular Fractionation from Fresh and Frozen Gastrointestinal Specimens. *J. Vis. Exp*, *137*, 57740. https://doi.org/10.3791/57740

Roundtree, I. A., Luo, G. Z., Zhang, Z., Wang, X., Zhou, T., Cui, Y., Sha, J., Huang, X., Guerrero, L., Xie, P., He, E., Shen, B., & He, C. (2017). YTHDC1 mediates nuclear export of N6-methyladenosine methylated mRNAs. *ELife*, *6*. https://doi.org/10.7554/eLife.31311

Rubio-Tapia, A., & Murray, J. A. (2010). Classification and management of refractory coeliac disease. In *Gut* (Vol. 59, Issue 4). https://doi.org/10.1136/gut.2009.195131

Samasca, G., Sur, G., Lupan, I., & Deleanu, D. (2014). Gluten-free diet and quality of life in celiac disease. In *Gastroenterology and Hepatology from Bed to Bench* (Vol. 7, Issue 3). https://doi.org/10.22037/ghfbb.v7i3.617

Schuppan, D., Junker, Y., & Barisani, D. (2009). Celiac Disease: From Pathogenesis to Novel Therapies. In *Gastroenterology* (Vol. 137, Issue 6). https://doi.org/10.1053/j.gastro.2009.09.008

Schwartz, S., Bernstein, D. A., Mumbach, M. R., Jovanovic, M., Herbst, R. H., León-Ricardo, B. X., Engreitz, J. M., Guttman, M., Satija, R., Lander, E. S., Fink, G., & Regev, A. (2014). Transcriptome-wide mapping reveals widespread dynamic-regulated pseudouridylation of ncRNA and mRNA. *Cell*, *159*(1). https://doi.org/10.1016/j.cell.2014.08.028

Schwartz, S., Mumbach, M. R., Jovanovic, M., Wang, T., Maciag, K., Bushkin, G. G., Mertins, P., Ter-Ovanesyan, D., Habib, N., Cacchiarelli, D., Sanjana, N. E., Freinkman, E., Pacold, M. E., Satija, R., Mikkelsen, T. S., Hacohen, N., Zhang, F., Carr, S. A., Lander, E. S., & Regev, A. (2014). Perturbation of m6A writers reveals two distinct classes of mRNA methylation at internal and 5' sites. *Cell Reports*, *8*(1). https://doi.org/10.1016/j.celrep.2014.05.048

Sendino, M., Omaetxebarria, M. J., & Rodríguez, J. A. (2018). Hitting a moving

target: inhibition of the nuclear export receptor XPO1/CRM1 as a therapeutic approach in cancer. *Cancer Drug Resistance*, *1*(3), 139–163. https://doi.org/10.20517/cdr.2018.09

Shafik, A., Schumann, U., Evers, M., Sibbritt, T., & Preiss, T. (2016). The emerging epitranscriptomics of long noncoding RNAs. In *Biochimica et Biophysica Acta - Gene Regulatory Mechanisms* (Vol. 1859, Issue 1). https://doi.org/10.1016/j.bbagrm.2015.10.019

Shan, L., Molberg, Ø., Parrot, I., Hausch, F., Filiz, F., Gray, G. M., Sollid, L. M., & Khosla, C. (2002). Structural basis for gluten intolerance in Celiac Sprue. *Science*, *297*(5590), 2275–2279. https://doi.org/10.1126/science.1074129

Shi, H., Wang, X., Lu, Z., Zhao, B. S., Ma, H., Hsu, P. J., Liu, C., & He, C. (2017). YTHDF3 facilitates translation and decay of N 6-methyladenosine-modified RNA. *Cell Research*, *27*(3). https://doi.org/10.1038/cr.2017.15

Shulman, Z., & Stern-Ginossar, N. (2020). The RNA modification N 6-methyladenosine as a novel regulator of the immune system. *Nature Immunology*, *21*(5), 501–512. https://doi.org/10.1038/s41590-020-0650-4

Silano, M., Vincentini, O., & De Vincenzi, M. (2009). Toxic, Immunostimulatory and Antagonist Gluten Peptides in Celiac Disease. *Current Medicinal Chemistry*, *16*(12). https://doi.org/10.2174/092986709787909613

Silvester, J. A., & Leffler, D. A. (2017). Is Autoimmunity Infectious? The Effect of Gastrointestinal Viral Infections and Vaccination on Risk of Celiac Disease Autoimmunity. In *Clinical Gastroenterology and Hepatology* (Vol. 15, Issue 5). https://doi.org/10.1016/j.cgh.2016.12.014

Slotkin, W., & Nishikura, K. (2013). Adenosine-to-inosine RNA editing and human disease. In *Genome Medicine* (Vol. 5, Issue 11). https://doi.org/10.1186/gm508

Smyth, D. J., Plagnol, V., Walker, N. M., Cooper, J. D., Downes, K., Yang, J. H. M., Howson, J. M. M., Stevens, H., McManus, R., Wijmenga, C., Heap, G. A., Dubois, P. C., Clayton, D. G., Hunt, K. A., van Heel, D. A., & Todd, J. A. (2008). Shared and Distinct Genetic Variants in Type 1 Diabetes and Celiac Disease. *New England Journal of Medicine*, *359*(26).

https://doi.org/10.1056/nejmoa0807917

Spitale, R. C., Flynn, R. A., Zhang, Q. C., Crisalli, P., Lee, B., Jung, J. W., Kuchelmeister, H. Y., Batista, P. J., Torre, E. A., Kool, E. T., & Chang, H. Y. (2015). Structural imprints in vivo decode RNA regulatory mechanisms. *Nature*, *519*(7544). https://doi.org/10.1038/nature14263

Squires, J. E., Patel, H. R., Nousch, M., Sibbritt, T., Humphreys, D. T., Parker, B. J., Suter, C. M., & Preiss, T. (2012). Widespread occurrence of 5-methylcytosine in human coding and non-coding RNA. *Nucleic Acids Research*, *40*(11). https://doi.org/10.1093/nar/gks144

Stene, L. C., Honeyman, M. C., Hoffenberg, E. J., Haas, J. E., Sokol, R. J., Emery, L., Taki, I., Norris, J. M., Erlich, H. A., Eisenbarth, G. S., & Rewers, M. (2006). Rotavirus infection frequency and risk of celiac disease autoimmunity in early childhood: A longitudinal study. *American Journal of Gastroenterology*, *101*(10). https://doi.org/10.1111/j.1572-0241.2006.00741.x

Struyf, S., Gouwy, M., Dillen, C., Proost, P., Opdenakker, G., & Van Damme, J. (2005). Chemokines synergize in the recruitment of circulating neutrophils into inflamed tissue. *European Journal of Immunology*, *35*(5). https://doi.org/10.1002/eji.200425753

Sun, H., Zhang, M., Li, K., Bai, D., & Yi, C. (2019). Cap-specific, terminal N 6-methylation by a mammalian m6Am methyltransferase. In *Cell Research* (Vol. 29, Issue 1). https://doi.org/10.1038/s41422-018-0117-4

Sun, S. C., Chang, J. H., & Jin, J. (2013). Regulation of nuclear factor-κB in autoimmunity. In *Trends in Immunology* (Vol. 34, Issue 6, pp. 282–289). Elsevier. https://doi.org/10.1016/j.it.2013.01.004

Sunil, Y., Ramadori, G., & Raddatz, D. (2010). Influence of NFκB inhibitors on IL-1β-induced chemokine CXCL8 and -10 expression levels in intestinal epithelial cell lines: Glucocorticoid ineffectiveness and paradoxical effect of PDTC. *International Journal of Colorectal Disease*, *25*(3). https://doi.org/10.1007/s00384-009-0847-3

Syed, Y. Y. (2019). Selinexor: First Global Approval. In *Drugs* (Vol. 79, Issue 13, pp. 1485–1494). Springer International Publishing.

https://doi.org/10.1007/s40265-019-01188-9

Tan, D. S. P., Bedard, P. L., Kuruvilla, J., Siu, L. L., & Razak, A. R. A. (2014). Promising SINEs for embargoing nuclear-cytoplasmic export as an anticancer strategy. In *Cancer Discovery* (Vol. 4, Issue 5, pp. 527–537). American Association for Cancer Research Inc. https://doi.org/10.1158/2159-8290.CD-13-1005

Trynka, G., Zhernakova, A., Romanos, J., Franke, L., Hunt, K. A., Turner, G., Bruinenberg, M., Heap, G. A., Platteel, M., Ryan, A. W., De Kovel, C., Holmes, G. K. T., Howdle, P. D., Walters, J. R. F., Sanders, D. S., Mulder, C. J. J., Mearin, M. L., Verbeek, W. H. M., Trimble, V., … Wijmenga, C. (2009). Coeliac disease-associated risk variants in TNFAIP3 and REL implicate altered NF-κB signalling. *Gut*, *58*(8). https://doi.org/10.1136/gut.2008.169052

Trynka, Gosia, Hunt, K. A., Bockett, N. A., Romanos, J., Mistry, V., Szperl, A., Bakker, S. F., Bardella, M. T., Bhaw-Rosun, L., Castillejo, G., De La Concha, E. G., De Almeida, R. C., Dias, K. R. M., Van Diemen, C. C., Dubois, P. C. A., Duerr, R. H., Edkins, S., Franke, L., Fransen, K., … Van Heel, D. A. (2011). Dense genotyping identifies and localizes multiple common and rare variant association signals in celiac disease. *Nature Genetics*, *43*(12), 1193–1201. https://doi.org/10.1038/ng.998

Tye-Din, J. A., Dzuris, J. L., Russell, A. K., Wang, S., Goldstein, K., Williams, L. J., & Anderson, R. P. (2017). Serum IL-2 and IL-8 are Elevated within 4 h after Gluten Ingestion in Celiac Disease (CED) Patients on Gluten-Free Diet (GFD) and Potential to Resolve Indeterminate Diagnoses for Patients on GFD. *Gastroenterology*, *152*(5), S114. https://doi.org/10.1016/s0016-5085(17)30720-5

Tye-Din, J. A., Skodje, G. I., Sarna, V. K., Dzuris, J. L., Russell, A. K., Goel, G., Wang, S., Goldstein, K. E., Williams, L. J., Sollid, L. M., Lundin, K. E. A., & Anderson, R. P. (2020). Cytokine release after gluten ingestion differentiates coeliac disease from self-reported gluten sensitivity. *United European Gastroenterology Journal*, *8*(1), 108–118. https://doi.org/10.1177/2050640619874173

Vader, W., Stepniak, D., Kooy, Y., Mearin, L., Thompson, A., Van Rood, J. J., Spaenij, L., & Koning, F. (2003). The HLA-DQ2 gene dose effect in celiac disease is directly related to the magnitude and breadth of gluten-specific T cell responses. *Proceedings of the National Academy of Sciences of the United States of America*, *100*(21). https://doi.org/10.1073/pnas.2135229100

Van Heel, D. A., Franke, L., Hunt, K. A., Gwilliam, R., Zhernakova, A., Inouye, M., Wapenaar, M. C., Barnardo, M. C. N. M., Bethel, G., Holmes, G. K. T., Feighery, C., Jewell, D., Kelleher, D., Kumar, P., Travis, S., Walters, J. R. F., Sanders, D. S., Howdle, P., Swift, J., … Wijmenga, C. (2007). A genome-wide association study for celiac disease identifies risk variants in the region harboring IL2 and IL21. *Nature Genetics*, *39*(7), 827–829. https://doi.org/10.1038/ng2058

van Heel, D. A., Hunt, K., Greco, L., & Wijmenga, C. (2005). Genetics in coeliac disease. In *Best Practice and Research: Clinical Gastroenterology* (Vol. 19, Issue 3 SPEC. ISS., pp. 323–339). Bailliere Tindall Ltd. https://doi.org/10.1016/j.bpg.2005.01.001

Van Tran, N., Ernst, F. G. M., Hawley, B. R., Zorbas, C., Ulryck, N., Hackert, P., Bohnsack, K. E., Bohnsack, M. T., Jaffrey, S. R., Graille, M., & Lafontaine, D. L. J. (2019). The human 18S rRNA m6A methyltransferase METTL5 is stabilized by TRMT112. *Nucleic Acids Research*, *47*(15). https://doi.org/10.1093/nar/gkz619

Viatour, P., Merville, M. P., Bours, V., & Chariot, A. (2005). Phosphorylation of NF-κB and IκB proteins: Implications in cancer and inflammation. In *Trends in Biochemical Sciences* (Vol. 30, Issue 1). https://doi.org/10.1016/j.tibs.2004.11.009

Vriezinga, S. L., Auricchio, R., Bravi, E., Castillejo, G., Chmielewska, A., Crespo Escobar, P., Kolaček, S., Koletzko, S., Korponay-Szabo, I. R., Mummert, E., Polanco, I., Putter, H., Ribes-Koninckx, C., Shamir, R., Szajewska, H., Werkstetter, K., Greco, L., Gyimesi, J., Hartman, C., … Mearin, M. L. (2014). Randomized Feeding Intervention in Infants at High Risk for Celiac Disease. *New England Journal of Medicine*, *371*(14).

https://doi.org/10.1056/nejmoa1404172

Wang, H., Hu, X., Huang, M., Liu, J., Gu, Y., Ma, L., Zhou, Q., & Cao, X. (2019). Mettl3-mediated mRNA m 6 A methylation promotes dendritic cell activation. *Nature Communications*, *10*(1). https://doi.org/10.1038/s41467-019-09903-6

Wang, P., Doxtader, K. A., & Nam, Y. (2016). Structural Basis for Cooperative Function of Mettl3 and Mettl14 Methyltransferases. *Molecular Cell*, *63*(2), 306–317. https://doi.org/10.1016/j.molcel.2016.05.041

Wang, Shaoru, Wang, J., Zhang, X., Fu, B., Song, Y., Ma, P., Gu, K., Zhou, X., Zhang, X., Tian, T., & Zhou, X. (2016). N6-Methyladenine hinders RNA- and DNA-directed DNA synthesis: Application in human rRNA methylation analysis of clinical specimens. *Chemical Science*, *7*(2). https://doi.org/10.1039/c5sc02902c

Wang, Siwei, Sun, C., Li, J., Zhang, E., Ma, Z., Xu, W., Li, H., Qiu, M., Xu, Y., Xia, W., Xu, L., & Yin, R. (2017). Roles of RNA methylation by means of N6-methyladenosine (m6A) in human cancers. In *Cancer Letters* (Vol. 408). https://doi.org/10.1016/j.canlet.2017.08.030

Wang, X., Lu, Z., Gomez, A., Hon, G. C., Yue, Y., Han, D., Fu, Y., Parisien, M., Dai, Q., Jia, G., Ren, B., Pan, T., & He, C. (2014). N 6-methyladenosine-dependent regulation of messenger RNA stability. *Nature*, *505*(7481), 117–120. https://doi.org/10.1038/nature12730

Wang, X., Zhao, B. S., Roundtree, I. A., Lu, Z., Han, D., Ma, H., Weng, X., Chen, K., Shi, H., & He, C. (2015). N6-methyladenosine modulates messenger RNA translation efficiency. *Cell*, *161*(6), 1388–1399. https://doi.org/10.1016/j.cell.2015.05.014

Wei, C. M., Gershowitz, A., & Moss, B. (1975). Methylated nucleotides block 5′ terminus of HeLa cell messenger RNA. *Cell*, *4*(4). https://doi.org/10.1016/0092-8674(75)90158-0

Wei, C. M., Gershowitz, A., & Moss, B. (1976). 5′-Terminal and Internal Methylated Nucleotide Sequences in Hela Cell mRNA. *Biochemistry*, *15*(2). https://doi.org/10.1021/bi00647a024

Wei, C. M., & Moss, B. (1977). Nucleotide Sequences at the N6-Methyladenosine

Sites of HeLa Cell Messenger Ribonucleic Acid. *Biochemistry*, *16*(8). https://doi.org/10.1021/bi00627a023

Wei, J., Liu, F., Lu, Z., Fei, Q., Ai, Y., He, P. C., Shi, H., Cui, X., Su, R., Klungland, A., Jia, G., Chen, J., & He, C. (2018). Differential m 6 A, m 6 A m , and m 1 A Demethylation Mediated by FTO in the Cell Nucleus and Cytoplasm. *Molecular Cell*, *71*(6), 973-985.e5. https://doi.org/10.1016/j.molcel.2018.08.011

Wei, W., Ji, X., Guo, X., & Ji, S. (2017). Regulatory Role of N6-methyladenosine (m6A) Methylation in RNA Processing and Human Diseases. *Journal of Cellular Biochemistry*, *118*(9). https://doi.org/10.1002/jcb.25967

Wen, J., Lv, R., Ma, H., Shen, H., He, C., Wang, J., Jiao, F., Liu, H., Yang, P., Tan, L., Lan, F., Shi, Y. G., He, C., Shi, Y., & Diao, J. (2018). Zc3h13 Regulates Nuclear RNA m6A Methylation and Mouse Embryonic Stem Cell Self-Renewal. *Molecular Cell*, *69*(6). https://doi.org/10.1016/j.molcel.2018.02.015

Winkler, R., Gillis, E., Lasman, L., Safra, M., Geula, S., Soyris, C., Nachshon, A., Tai-Schmiedel, J., Friedman, N., Le-Trilling, V. T. K., Trilling, M., Mandelboim, M., Hanna, J. H., Schwartz, S., & Stern-Ginossar, N. (2019). m 6 A modification controls the innate immune response to infection by targeting type I interferons. *Nature Immunology*, *20*(2), 173–182. https://doi.org/10.1038/s41590-018-0275-z

Wojtas, M. N., Pandey, R. R., Mendel, M., Homolka, D., Sachidanandam, R., & Pillai, R. S. (2017). Regulation of m6A Transcripts by the 3'→5' RNA Helicase YTHDC2 Is Essential for a Successful Meiotic Program in the Mammalian Germline. *Molecular Cell*, *68*(2). https://doi.org/10.1016/j.molcel.2017.09.021

Xiao, W., Adhikari, S., Dahal, U., Chen, Y. S., Hao, Y. J., Sun, B. F., Sun, H. Y., Li, A., Ping, X. L., Lai, W. Y., Wang, X., Ma, H. L., Huang, C. M., Yang, Y., Huang, N., Jiang, G. Bin, Wang, H. L., Zhou, Q., Wang, X. J., … Yang, Y. G. (2016). Nuclear m6A Reader YTHDC1 Regulates mRNA Splicing. *Molecular Cell*, *61*(4). https://doi.org/10.1016/j.molcel.2016.01.012

Xu, C., Liu, K., Ahmed, H., Loppnau, P., Schapira, M., & Min, J. (2015). Structural basis for the discriminative recognition of N6-Methyladenosine RNA by the

human YT521-B homology domain family of proteins. *Journal of Biological Chemistry*, *290*(41). https://doi.org/10.1074/jbc.M115.680389

Xu, C., Wang, X., Liu, K., Roundtree, I. A., Tempel, W., Li, Y., Lu, Z., He, C., & Min, J. (2014). Structural basis for selective binding of m6A RNA by the YTHDC1 YTH domain. *Nature Chemical Biology*, *10*(11), 927–929. https://doi.org/10.1038/nchembio.1654

Yang, C., Hu, Y., Zhou, B., Bao, Y., Li, Z., Gong, C., Yang, H., Wang, S., & Xiao, Y. (2020). The role of m6A modification in physiology and disease. In *Cell Death and Disease* (Vol. 11, Issue 11). https://doi.org/10.1038/s41419-020-03143-z

Yang, Y., Fan, X., Mao, M., Song, X., Wu, P., Zhang, Y., Jin, Y., Yang, Y., Chen, L. L., Wang, Y., Wong, C. C. L., Xiao, X., & Wang, Z. (2017). Extensive translation of circular RNAs driven by N 6 -methyladenosine. *Cell Research*, *27*(5). https://doi.org/10.1038/cr.2017.31

Yeruva, S., Ramadori, G., & Raddatz, D. (2008). NF-κB-dependent synergistic regulation of CXCL10 gene expression by IL-1β and IFN-γ in human intestinal epithelial cell lines. *International Journal of Colorectal Disease*, *23*(3). https://doi.org/10.1007/s00384-007-0396-6

Zaccara, S., Ries, R. J., & Jaffrey, S. R. (2019). Reading, writing and erasing mRNA methylation. In *Nature Reviews Molecular Cell Biology* (Vol. 20, Issue 10). https://doi.org/10.1038/s41580-019-0168-5

Zhang, C., & Darnell, R. B. (2011). Mapping in vivo protein-RNA interactions at single-nucleotide resolution from HITS-CLIP data. *Nature Biotechnology*, *29*(7). https://doi.org/10.1038/nbt.1873

Zhang, Zhang, Chen, L. Q., Zhao, Y. L., Yang, C. G., Roundtree, I. A., Zhang, Z., Ren, J., Xie, W., He, C., & Luo, G. Z. (2019). Single-base mapping of m6A by an antibody-independent method. *Science Advances*, *5*(7). https://doi.org/10.1126/sciadv.aax0250

Zhang, Zijie, Luo, K., Zou, Z., Qiu, M., Tian, J., Sieh, L., Shi, H., Zou, Y., Wang, G., Morrison, J., Zhu, A. C., Qiao, M., Li, Z., Stephens, M., He, X., & He, C. (2020). Genetic analyses support the contribution of mRNA N6-

methyladenosine (m6A) modification to human disease heritability. *Nature Genetics*, 1–11. https://doi.org/10.1038/s41588-020-0644-z

Zheng, G., Dahl, J. A., Niu, Y., Fedorcsak, P., Huang, C. M., Li, C. J., Vågbø, C. B., Shi, Y., Wang, W. L., Song, S. H., Lu, Z., Bosmans, R. P. G., Dai, Q., Hao, Y. J., Yang, X., Zhao, W. M., Tong, W. M., Wang, X. J., Bogdan, F., … He, C. (2013). ALKBH5 Is a Mammalian RNA Demethylase that Impacts RNA Metabolism and Mouse Fertility. *Molecular Cell*, *49*(1), 18–29. https://doi.org/10.1016/j.molcel.2012.10.015

Zhou, J., Wan, J., Gao, X., Zhang, X., Jaffrey, S. R., & Qian, S. B. (2015). Dynamic m6 A mRNA methylation directs translational control of heat shock response. *Nature*, *526*(7574), 591–594. https://doi.org/10.1038/nature15377

Zhu, T., Roundtree, I. A., Wang, P., Wang, X., Wang, L., Sun, C., Tian, Y., Li, J., He, C., & Xu, Y. (2014). Crystal structure of the YTH domain of YTHDF2 reveals mechanism for recognition of N6-methyladenosine. In *Cell Research* (Vol. 24, Issue 12, pp. 1493–1496). Nature Publishing Group. https://doi.org/10.1038/cr.2014.152